STRUCTURAL, THERMAL, CORROSION INHIBITION AND ELECTRICAL CONDUCTIVITY STUDIES ON SOME SCHIFF BASES AND THEIR TRANSITION METAL COMPLEXES

Thesis submitted to the University of Calicut
in partial fulfilment of the requirements
for the award of the degree of

Doctor of Philosophy
in
Chemistry

By

K. STANLY JACOB

DEPARTMENT OF CHEMISTRY
UNIVERSITY OF CALICUT
KERALA - 673 635

APRIL – 2008

Dr. Geetha Parameswaran
Professor (Retd.)
Department of Chemistry
University of Calicut

Calicut University P. O
Kerala - 673 635

CERTIFICATE

This is to certify that the thesis entitled, **"Structural, Thermal, Corrosion inhibition and Electrical conductivity Studies on some Schiff bases and their Transition Metal Complexes"**, is an authentic record of the research work carried out by **Mr. K. Stanly Jacob** under my supervision in partial fulfilment of the requirements for the degree of Doctor of Philosophy in Chemistry of the University of Calicut and further that no part thereof has been presented before for any other degree.

C. U. Campus

Dr. Geetha Parameswaran

(Supervising Teacher)

DECLARATION

I hereby declare that this thesis entitled, "**Structural, Thermal, Corrosion inhibition and Electrical conductivity Studies on some Schiff bases and their Transition Metal Complexes"**, submitted to the University of Calicut in partial fulfilment of the requirements for the Doctoral Degree in Chemistry is a bonafide research work done by me under the supervision and guidance of **Dr.Geetha Parameswaran**, Professor (Retd), Department of Chemistry, University of Calicut.

I further declare that this thesis has not previously formed the basis of any degree, diploma or other similar title.

C. U. Campus

K. Stanly Jacob

ACKNOWLEDGEMENT

I wish to express my deep sense of gratitude and respect to Dr. Geetha Parameswaran, Professor (Retd), Department of Chemistry, University of Calicut for her constant encouragement, inspiring guidance and support throughout this work. I am indebted to her for giving me considerable freedom of thought and expression which I enjoyed during my research tenure. I also thank family members of Dr. Geetha Parameswaran for their support and care extended to me.

I wish to acknowledge my heartfelt thanks to Dr. P. Mohamed Shafi, Professor and Head, Department of Chemistry, University of Calicut for providing me necessary facilities. My sincere thanks to all the teachers, technical staff, non-teaching staff and research scholars of the Department of Chemistry, University of Calicut for their help extended during my research work.

I take this opportunity to thank Dr. Krishna Kumar, Executive Director C-MET and Dr. K. R. Dayas, Director, CMET Thrissur for their encouragement and motivation rendered throughout the entire period of my research work. I express my heartfelt thanks to all members of C-MET Thrissur, for their co-operation and fruitful discussions which helped me to complete my research work.

I am very happy to record my grateful regards to Dr. M. K. Jayaraj, Reader, Department of Physics, CUSAT Cochin; Dr. A. C. Hegde, Professor, Department of Chemistry, NIT Surathkal and the Director and staff of Sophisticated Analytical Instrumentation Facility (SAIF), Cochin University for the characterisation and evaluation of my research samples

It would not have been possible to realise this work without the immense support and advice of (Late) Dr. P. Sasidharan, former Director, Dr. R. Ratheesh, Scientist, Dr. S. Sankaranarayanan Potty, Scientist, Mr. P. A. Abraham, Technical staff and Mr. S. Rajesh, Research Fellow of C-MET Thrissur; Mr. Satheesan, Technical Staff, Department of Chemistry, Calicut University and Mr. M. Jayashankar of RRL Trivandrum.

I am deeply indebted to faculty members Dr. Joby Kakkassery and Dr. Francy Kakkassery, ST. Thomas' College, Trichur; Mrs. K. P. Rema, S. N College, Nattika; Dr. G. Indiradevi, Z. G. College Calicut; Mr. P. K. Sreekumar, N. S. S. College Panthalam; Mrs. Soosanna Seth, M.C. College, Calicut; Dr. Jacob John, Govt. College, Pattambi for their timely help and suggestions which helped me to complete this research work.

I sincerely remember and acknowledge the moral support and help extended by my wife Jolly, daughter Sniya, parents and family members. Above all I thank the Almighty for the blessings showered upon me.

K. Stanly Jacob

DEDICATED TO MY PARENTS

PREFACE

Transition metal complexes with Schiff bases as ligands have been amongst the widely studied coordination compounds and find remarkable applications in different fields. The chelating characters of Schiff bases towards transition metals are very interesting. Schiff bases coordinate to the metal ion through nitrogen atom of azomethine group. The presence of functional group with replaceable hydrogen atom near enough to >C=N renders extra stability to metal complexes through chelation.

In the present course of studies the complexation of four new Schiff bases furoin-2-aminothiophenol (FATP), furoin-2-aminophenol (FAP), furoin thiosemicarbazone (FTSC) and furoin semicarbazone (FSC) have been studied extensively. Co(II), Ni(II), Cu(II) and Zn(II) metal ions are used for complexation. Characterisation of metal complexes has been done based on the physicochemical studies. These results are presented in Part I.

Thermal studies of selected Schiff base complexes are carried out using Thermogravimetry. Order of reaction, activation energy and entropy of activation are evaluated using the Coats–Redfern equation. The results of these studies are given in Part II

Based on the X-ray powder diffraction pattern the crystal lattice and cell dimensions of eight newly synthesised Schiff base complexes are determined and reported in Part III

Part IV explores the application of newly synthesised Schiff bases as corrosion inhibitors on mild steel in hydrochloric acid media.

Another potential application of the synthesised ligands and complexes as semiconductor materials is envisaged by studying the solid state D.C electrical conductivity and their temperature dependence. The results are summarised in Part V.

Detailed lists of references have been arranged in serial order and are given at the end of each part. The thesis concludes with a brief summary.

The research work presented in this thesis has partly been published/under publication as indicated

1. "Synthesis, Spectral and DC electrical conductivity studies of Copper complex of Schiff base furoin thiosemicarbazone", Stanly Jacob.K and Geetha Parameswaran, Proceeding of National Seminar on Emerging Trends and New Vistas in Chemistry, (EMTIC 2005), Department of Chemistry, University of Calicut, Kerala, November (2005) 120-123.
2. Synthesis and characterisation of Co(II), Ni(II), Cu(II) and Zn(II) complexes of Schiff bases furoin-2-aminothiophenol, furoin-2-amino

phenol, furoin thiosemicarbazone and furoin semicarbazone. (To be communicated to Transition Metal Chemistry)

3. Thermal decomposition and kinetic studies of transition metal complexes derived from Schiff bases furoin-2-aminothiophenol, furoin-2-aminophenol, furoin thiosemicarbazone and furoin semi-carbazone. (To be communicated to Thermochemica Acta)
4. Powder X-ray diffraction studies of transition metal complexes of furoin based Schiff bases. (To be communicated to Bulletin of Material Science)
5. Corrosion inhibition studies of four new Schiff bases on mild steel in 1M HCl. (To be communicated to Electrochemica Acta)
6. Electrical conductivity of metal complexes derived from furoin based Schiff base ligands. (To be communicated to Material Chemistry and Physics).

ABBREVIATIONS USED IN THIS THESIS

FATP	-	Furoin-2-aminothiophenol
FAP	-	Furoin-2-aminophenol
FTSC	-	Furoin thiosemicarbazone
FSC	-	Furoin semicarbazone
M	-	Central metal ion in the complex
L	-	Ligand moiety in a complex
B. M.	-	Bohr Magneton
DMSO	-	Dimethyl sulphoxide
MS	-	Mild Steel
EIS	-	Electrochemical Impedance Spectroscopy

CONTENTS

TITLE **PAGE NO**

PART I

SYNTHESIS AND CHARACTERISATION

PART II

THERMOGRAVIMETRIC ANALYSIS

PART III

X-RAY DIFFRACTION STUDIES

PART IV

CORROSION INHIBITION STUDIES OF SCHIFF BASES ON MILD STEEL

PART V

ELECTRICAL CONDUCTIVITY STUDIES OF SCHIFF BASES AND THEIR TRANSITION METAL COMPLEXES

PART I

SYNTHESIS AND CHARACTERISATION

CHAPTER 1
INTRODUCTION

Coordination chemistry, the chemistry of metal complexes, is one of the most active research areas in inorganic chemistry. The study of coordination chemistry in the modern day context began with two notable scientists Alfred Werner and Sorphus Mads Jorgenson. The pioneering contribution of Werner to the study of coordination chemistry fetched him the Nobel Prize in Chemistry in 1913. Werner's basic ideas on the stereo-chemistry of metal complexes, mechanism of isomerisation etc. remain unchallenged even today despite all the advanced technical developments which have taken place since his days. However the advent of sophisticated physicochemical techniques of high precision and capability has considerably enriched our understanding of the nature of the metal-ligand bond, the structure and stereochemistry of metal complexes, their stability and other properties. Research has come long way from the time of Werner and Jorgenson, in terms of the growth that the coordination chemistry has experienced over the last few decades. Their work was a stepping stone for the development of modern inorganic chemistry which is truly a multidisciplinary one in the present day context.

Coordination chemistry encompasses such diverse fields as dyes, colour photography, mineral extraction, nuclear fuels, toxicology,

bioinorganic chemistry, medicine, catalysis, material science, ceramics, microelectronics, photonics etc. Industries dealing with organic chemicals, pharmaceuticals, petrochemicals and plastics owe a lot to the findings in the field of coordination chemistry. Nature makes extensive use of coordination compounds and their study is becoming increasingly important in biology as well as in chemistry. Many of the biologically active compounds are complexes and even the simpler types of complexes have served as model compounds in investigating bodily process. The living system is partially supported by coordination compounds. Hemoglobin, an iron complex, carries oxygen to animal cells. Myoglobin, chlorophyll and cytochromes are some of the other important complex compounds in living systems. Inorganic compounds particularly metallic ions and complexes are essential cofactors in a variety of enzymes and proteins.

The elegance and the variety of the coordination compounds and the intriguing range of concepts that are required to interpret their behaviour have attracted many researchers to the study of their synthesis and to seek an understanding of their chemical reactions. The study of complexes has enabled the inorganic chemists to make significant progress in refining the concept of chemical bonding and to explain the influence that bonding has, on the various properties of the compounds.

Schiff base ligands

Schiff bases, named after Hugo Schiff (1834-1915), and their transition metal complexes continue to be of interest even after over hundred years of study. The condensation products of primary amines with carbonyl compounds were first reported by Schiff in 1864 and the products are often referred to as Schiff bases[1-4]. Schiff bases are compounds containing azomethine group (>C=N) and have the general structure R-N=C-R' where R and R' are aryl, alkyl, cycloalkyl or heterocyclic groups which may be variously substituted. Often they are referred to as anils, imines or azomethines. The synthesis and properties of Schiff bases have been widely reviewed[5-11]. The availability of different types of amines and carbonyl compounds enabled the synthesis of Schiff bases with diverse structural features. Nevertheless, most of the studies are on metal complexes derived from salicylaldehyde[12]. The presence of phenolic -OH group sufficiently near to the azomethine group of salicylaldimines makes them versatile multidendate ligands complexing with almost all metal ions. In order to understand the chemistry of metal chelates, awareness about the formation and stability of complexes is of great help.

The bonding ability of the ligands depends on the nature of atoms that act as coordination site, their electro negativity and steric factors. By virtue of the presence of lone pair of electrons on the nitrogen atom, electron donating character of the double bond and low electro negativity of nitrogen,

N of the azomethine group (>C=N) act as good donor site and Schiff base as active ligands. The formation of chelates gives extra stability to the complexes especially when the ring is five or six membered. Hence the presence of a functional group with replaceable hydrogen atom near to >C=N will be additional factor of stability.

Applications of Schiff bases and transition Metal Complexes

The transition metal complexes find extensive application in technology, industry and medicine. There has been an upsurge of research in the area of catalysis by transition metal complexes since 1940's. The demand for cheaper and more efficient process in the industry resulted in the rapid development of newer process technologies relevant to industrial scale reactions for the production of organic compounds using transition metal complexes as catalysts. A great number of soluble metal complexes are now being employed in industry as catalyst for preparation of variety of useful compounds. Platinum complexes containing diphosphine and other chelating agent containing asymmetric carbon atoms have found a place in the chemical industry as stereo specific catalysts. Some of them give products with high degree of specificity. This is important in the manufacture of some drugs. For example, laevodihydroxy phenyl alanine is used in the treatment of Parkinson's disease. It is known that the Zeigler catalyst, a complex

aluminium and titanium is used for the low pressure polymerization of ethylene, which makes thousands of polythene articles.

The chelate metal complexes are a strong candidate as organic electroluminescent materials. The chelate metal complexes such as tris (8-hydroxy quinolinate) aluminium have excellent electroluminescent properties and used in the fabrication of electroluminescent devices[13]. Transition metal complexes with low lying excited states are finding increasing use as photo sensitizers. Major work horse is those derived from poly pyridine complexes and metallo porphyrins. With help of suitable molecular engineering, the metal complexes readily attached to the surface of mesoporous membranes type films. These films with anchored complexes are finding increasing use in energy conversion devices such as dye sensitized photo electrochemical solar cells, intercalation batteries, optical display and optical sensors[14].

Recently much interest has been paid to the rapid thermal decomposition of metal complexes based molecular precursors to create metals and metal oxides[15]. Metal complexes with pyruvic acid oxime were studied as precursors to variety of nano metal oxides[16-18]. Saravanan et al. had synthesised nano crystal of ZnO and ZnS by the thermal decomposition of cupferon complex[19].

Acid solutions are extensively used in the industries for manufacturing processes and other applications like acid pickling, acid cleaning, acid de-scaling and oil well acidifying. The use of acids leads the industrial pipe

lines and metal vessels to corrode and there by reducing the production and causing economical loss. Compounds containing functional groups with hetero atoms, which can donate lone pair of electrons, are found to be very efficient as inhibitors against metal corrosion in many environments. Many N-heterocyclic compounds with polar groups and or π electrons also act as efficient corrosion inhibitor in acidic solutions. Schiff base, an organic compound which has both these features combined in one molecule, will be potential inhibitor. Several Schiff bases have been previously reported as effective corrosion inhibitors for steel, copper and aluminum in acid mediums like hydrochloric acid, sulphuric acid, acetic acid, formic acid etc.[20-31]

Epoxy resins are of considerable technological importance, as they form continuous phase that binds together many light weight, tough composite materials. In order to convert epoxy resins from liquid or semi-solid monomers into hard, infusible thermoset networks it is necessary to use cross-linking agents. Epoxy resins once cured, are thermoset polymers and tend to be both stiff and brittle and require some degree of modification to achieve acceptable physical properties in the processed resins. Use of metal containing epoxy polymers allow the possibility of producing epoxy polymers with good mechanical properties and high thermal stability as well as achieving low processing temperatures. Extensive work has been carried out, over the last thirty years, into the use of metals and their salts in the formulation of epoxy resin systems. Organo–transition metal complexes have

also been added to improve physical properties such as adhesion, flexural strength, fracture toughness, water adsorption and heat resistance. Hamerton in his review publication demonstrates the use of transition metal complexes for improving physical properties such as viscosity or fracture toughness and electrical, thermal and chemical properties of epoxy resins[32]. Transition metal complexes containing acetyl acetonate ligands have been extensively used for the modification of different type of epoxy resins[33-35]. Several reports have been published in which coordination compounds containing acraylate[36], imidazole[37,38] and thalocyanine ligands[39] were extensively used as catalysts or epoxy modifiers for resins to improve their final properties. Coordination compounds containing Schiff base ligands were also used for the curing of the epoxy resins. Chantarasiri and co-workers have developed tetradendate and hexadendate Schiff base having bisphenol structure and used their metal complexes as cross linking agents for BADGE-type epoxy resins. It was observed that the introduction of the Schiff base metal complexes into the BADGE network gave good thermal stability[40,41].

Considerable interest has been shown in the synthesis and study of molecular complexes which may behave like semiconducting materials. Intense work has been done to prepare and develop new inorganic complexes which show semiconducting properties. Several reports published in which the electrical conductivities of the metal complexes and ligands and their

temperature dependence were studied. It was found that many of the complexes shown typical semiconductor property[42-46].

A number of cobalt complexes are used as driers for the conversion of liquids to solids and in inks, paints, varnishes and other surface coatings. The most important among them are cobalt soaps, which are complexes of carboxylate anions such as oleate, stearate, naphthenate, octanoate etc. Cobalt octanoates and naphthenates have been investigated as driers for linseed oil on paper[47]. Both bis(acetylacetonato)cobalt(II) and tris(acetyl-acetonato)cobalt(III) have been found to posses fungicidal activity[48]. Besides, bis(salicyladehyde)diimine complexes of cobalt take up and release molecular oxygen and are used in the purification of oxygen[49]. Cobalt complexes find various applications as additives for polymers. Thus cobalt phthalocyanines act as smoke retardants for styrene polymers. Bis(acetylacetonato)cobalt(II) in the presence of triphenyl phosphate has been found to act as an antioxidant for polyenes. Azides of cobaltamines have been suggested as detonators.

Nickel complexes are used in heterogeneous catalysis, electroplating, and in making pigments and ceramics. The Ni(II) complex of benzoic acid derivative acts as a stabilizer against oxidation of polybutadiene[50]. A number of nickel complexes of Schiff bases have been seen to possess fungicidal and bacterial activity. Nickel complex of N-benzoyl-N'-(2-amino phenyl) thiocarbamide has been shown to exhibit antifungal activity. The organisms *'Pyricularia oryzae'* which cause rice blast and *'Helmithosporium oryzae'*

which cause brown leaf spot can be controlled with Ni(II) complexes of 1-phenyl-3-methyl-4-nitroso-2-pyrozolin-5-one and 3-methyl-4-nitroso-2-pyrazo-lin-5-one[51].

The applications of copper complexes are extremely varied and of great importance. Copper complexes are widely used as polymer additives, fungicides and crop protectors. They are also used in antifouling paints and as fungicides for textiles[52]. Bis(acetylacetonato)copper(II) has been used as a source of copper in copper–vapour[53] lasers and it has also been investigated as a substitute for silver iodide as an ice–nucleating agent for the initiation of rainfall[54]. Copper phathalocyanine is more effective as smoke retardant for polystyrene than such complexes of other first row transition metals. Bis(acetylacetonato)copper(II) is employed in the protection of fabrics against fungicidal attack. Copper complexes of ligand N-benzoyl-N'-(2-aminophenyl)thiocarbamide are found to be effective fungicides for *Aspergillus niger*, *Fusarium oxysporium* and *Helminthosporium oryzae*[51]. Copper complexes are reported to be more active fungicides than similar iron, cobalt and nickel complexes. The complexes were found to be more effective than the free ligands[55].

Coordination compounds are widely used for the estimation and separation of metal ions. Dimethylglyoxime, 8-hydroxyl quinoline, oxidation-reduction indicators such as ferroin, volumetric reagent EDTA etc. are examples for such compounds. The role of coordination compounds in

colorimetric, spectrophotometric and polarographic analysis is also significant.

Complexes of alkali, alkaline earth and noble metals have found use in the treatment of diseases. For example, gold compounds are used in the treatment of arthritis and platinum compounds for some cancer. Complexes of alkali and alkaline earth metals with crown ethers and other cyclic ligands play important biological roles. Chelating agents in connection with cation exchange resin and solvent extraction have been particularly useful in the separation of radioactive metal. One of the general methods used for water softening is the effective removal of ions from solution by the formation of soluble complexes. Chemotherapy and chelation therapy using metals have now drawn attention as additional outlet for coordination chemistry. The classical example is the use of D-Pencillamine to treat Wilson's disease, which is caused by the inability of body to metabolize copper in the normal way. Another example is the use of desferrioxamine for the iron overload in Cooley's anemia, which is caused by the fault in hemoglobin synthesis. Heavy metal poisons can be removed from the body by the use of complexing, chelating or sequestering agents. In various imaging techniques, coordination complexes are used so that they transport metal to specific sites in the body. For example technetium complexes are used in radio imaging. In nmr imaging, paramagnetic complexes are used so that they go to specific sites in the body and improve the contrast[56,57]. Biological significance of the

azomethine group has never been doubt. Major biochemical interest in Schiff base compounds stems from their ability in designing metal containing model systems, which mimic biologically active systems[58].

Metal chelates of Schiff bases hold exciting possibilities for the future, particularly in designing novel corrosion inhibitors, epoxy curing agents, semi conducting materials, catalytic systems, in formulating new synthetic routes and in developing new analytical, antifungal and antibacterial agents. Hopefully results of this investigation would attract increased interest in these fields.

Review of metal complexes of Schiff bases derived from 2-amino phenol

Schiff bases are an important class of ligands in coordination chemistry and find extensive applications in different spheres[59,60]. Synthesis and characterisation of number of metal complexes of Schiff bases derived from aminophenols have been reported[61,62]. Syamal et al.[63] have characterised Fe(III) complexes of tridendate Schiff bases derived from simple or substituted salicylaldehyde and 2-aminophenol. Tez Can[64] has prepared and characterised the complexes of transition metals, rare earth metals and main group metals with Schiff base salicylidene-2-aminophenol and salicylidene-2-hydroxy-1-naphthyl amine. Salam[65] have synthesised Cu(II) and Ni(II) complexes of some dibasic tridendate Schiff bases prepared by condensation

of 2-aminophenol with 5-X-salicyladehyde and 2-hydroxyl-1-naphthaldehyde. Syamal and Singh have carried out the synthesis and characterisation of Cu(II), Ni(II), Fe(III), Zn(II) and Cd(II) complexes of polystyrene supported resin containing Schiff base derived from 3-formyl salicylic acid and 2-aminophenol[66]. Complexes of some metal ions with Schiff base ligands derived from isatin and 2-amino- phenol were synthesised and characterised via elemental analysis, IR, electronic spectral data,^{1}H NMR spectra, conductance and magnetic measurements[67].

Zelentsov[68] reported the synthesis of new high spin Co(II) chelates with tetradendate Schiff base ligand obtained by condensing 2-aminophenol or 4-nitro-2-aminophenol with glyoxal or glutaricaldehyde. The complexes were characterised by spectral and other techniques. The synthesis and characterisation of Schiff bases from 2-aminophenol and crocetindialdehyde, 2, 7-dimethyloctatrienedial or terephthaldehyde were carried out by Fehn et al.[69] Mayadevi[70] synthesised and characterised new transition metal complexes of Schiff base quinoxaline-2-carboxalidene-2-aminophenol. A tetrahedral structure was assigned for the Mn(II), Co(II), Ni(II) and Cu(II) complexes. For the Fe(III) complex, an octahedral dimeric structure was suggested.

Schiff bases[71] derived from salicylaldehyde and 2–aminophenol were synthesised and characterised by Naik and co-workers. Magnetic electronic spectral studies provide the evidence of the existence of octahedral geometry

for the complexes. Chae et al.[72] have prepared Schiff base ligands by the reaction of salicylaldehyde and 2-hydroxy-1-naphthaldehyde with 2-amino phenol and 2-amino-p-cresol respectively. The structures and properties of ligands and their Co(II) complexes were studied by elemental analysis, ^{1}H NMR, IR, UV-Visible spectra and TGA. The molar ratio of Schiff base to the metal of complexes is 1:1. Co(II) complexes have a hexacoordinated octahedral configuration. The redox process of ligands and complexes in DMSO solution were studied by cyclic voltammetry.

Mehta[73] have synthesised Schiff bases derived from condensation of 2-hydroxy-1-naphthaldehyde and 2-amino phenol. The copper complex was characterised by elemental analysis, molar conductance, electronic absorption spectra, IR and ESR spectral data and magnetic susceptibility data. The application of ligands and copper complexes as antibacterial agents were carried out.

The synthesis of new coordination compounds of Cu(II), Ni(II), Co(II), Sn(II), Hg(II) etc. with Schiff bases derived from 7-formyl-8-hydroxy quinoline(oxine) and 2-aminophenol have been reported by Sonbati and Bindary[74]. The ligands and the complexes were characterised by elemental analysis, IR, UV, EPR and NMR spectra together with magnetic susceptibility measurements. Infrared and NMR studies show that Schiff bases behave as monobasic and tridendate ligand, coordinating through the oxygen atom of

the deprotonated phenolic group, the nitrogen atom of the azomethine group and pyridine.

Saidul Islam[75] reported the synthesis of mixed ligand transition metal complexes of Cu, Ni and Co ions with Schiff base ligands derived from the condensation of o-hydroxy benzaldehyde with amino phenols and nitrogen donor amine bases, like ethylenediamine, 2-aminopyridine, and o-phenylene diamine or thiocyanate. These complexes were characterised and their anti-bacterial, anti-fungal and toxicological activity have been evaluated.

Neutral complexes of Cu(II), Ni(II), Co(II), Mn(II), VO(IV) and Zn(II) have been synthesised from the Schiff bases derived from salicylidene-4-aminoantipyrine[76] and 2-aminophenol and acetoacetanilido-4-amino anti-pyrine[77] and 2-aminophenol. Complexes of Cu(II), Ni(II), Co(II), Mn(II), Zn (II) and VO(II) have been prepared in ethanol using Schiff bases derived from acetoacetanilido-4-aminoantipyrine and 2-amino phenol .

Minu and co-workers reported the synthesis of ruthenium and lanthanide complexes of Schiff base N-(2-pyrrolymethylene)-2-amino-phenol[78]. All complexes were characterised by analytical and spectroscopic method. Three new Schiff base complexes $[Ni(HL)(L)]\cdot(ClO_4)\cdot 0.16(H_2O)$(1), $[ZnLZn(OOCCH_3)_4ZnL]$ (2) and $[Cd_2(L)_2(OCH_3CO)_2(H_2O)_2]$ (3) have been synthesised using the Schiff base ligand and the corresponding metal ions[79]. The Schiff base has been prepared by mixing pyridine-2-carboxaldehyde and 2-aminophenol and was isolated prior to the reaction with metal ions.

Complex 1 is mononuclear, 2 is trinuclear and 3 is diphenoxo-bridged dimer. 3 forms infinite 1D chains through hydrogen bonding interactions. Only 2 and 3 exhibit strong fluorescence emission bands at 635 and 630 nm, respectively.

Review of metal complexes of Schiff bases derived from 2-aminothio phenol

The NS donor systems incorporating into the Schiff base skeleton have attracted the interest of the researchers due to their pharmacological and physicochemical activities and have been widely studied. Schiff bases derived from o-aminothiophenol and various aldehydes, ketones, and their complexes have been extensively reviewed[61,62]. Characterisation of transition metal complexes of Schiff base derived from 2-aminothiophenol and pyridine-2 aldehyde have been reported by Mehta et al[80]. The spectral data and magnetic measurements suggest that these complexes have planar configuration. Cu(II), Ni(II), Cu(II) and Zn(II) complexes of the Schiff bases derived from 2-formyl cyclohexanone and 2-aminothiphenol were reported [81]. IR and ^{1}H NMR data show that while the free ligands exist in the ketamine form, in the complexes, they exist in the enamine form. The subnormal magnetic moments of Cu(II) complexes were ascribed to antiferromagnetic interaction arising from dimerization. Metal complexes of heterocyclic Schiff bases derived from 2-acetyl thiophene and 2-aminothiophenol were prepared

by Varsheny and Ambwani[82]. Serial dilution method was used to evaluate antimicrobial activity against two bacteria, *staphylococcus aureus* and *E. Coli* and two fungi, *Aspergillus niger* and *Candida albicans*.

Synthesis, characterisation and antimicrobial activities of some Pd(II) complexes of ethylidine aminothiophenol having NS donor sets are reported by Nighat and Singh[83]. Ruthenium(II) and oxovanadium(IV) complexes of highly conjugated Schiff base derived from diketones and 2-aminothiophenol were reported[84]. The subnormal magnetic moments and hyperfine splitting of these complexes were ascribed to an antiferromagnetic exchange interaction arising from dimerization.

Bouwman et al.[85] synthesised and characterised nickel complexes of 2-aminothiophenol and 2-tert-butyl thiobenzaldehyde. The benzathiozolidine ring opens upon reaction with nickel acetate in ethanol to form a mononuclear complex. Soliman[86] synthesised new transition metal chelate of 3-methoxy salicylidene-2-aminothiophenol Schiff base and found that Schiff base coordinated as a tridendate ligand with ONS donors derived from the phenolic O, azomethine N and thiophenolic S. The thermal decomposition of the complexes was found to follow first order kinetics. The preparation and characterisation of complexes of Schiff base salicylidene-2-amino thiophenol and some neutral ligand with manganese, cobalt and zinc(II) have been reported[87]. All the complexes except the complexes of Zn(II) are paramagnetic.

Neutral complexes of Cu(II), Ni(II), Co(II), Mn(II), VO(IV) and Zn(II) have been synthesised from the Schiff bases derived from salicylidene-4-aminoantipyrine and 2-aminothiophenol[76]. All of the complexes exhibit square-planar geometry except the Mn(II) and VO(IV) complexes. The Mn(II) chelates show an octahedral environment and the VO(IV) chelates exist in a square-pyramidal geometry. The reactivity studies of $[Rh_2(\mu\text{-}O_2CCH_3)(phen)_2\text{-}(CH_3CN)_2][PF_6]_2$ with the model ligand 2-aminothiophenol were reported[88]. The main finding of this study is that $[Rh_2(\mu O_2CCH_3)(phen)_2]^{2+}$ reacts with 2-aminothiophenol to form a stable Rh(III) compound in the presence of O_2. The ligand 2-aminothiophenol was used as a model for the chemistry of reactive thiol groups such as those found in amino acids and glutathione**.** Eikey[89] have been carried out a detailed review of the synthesis and reactivities of Groups 6, 7, and 8 metal complexes of 2-aminothiophenol until august 2002. In this report general description of the bonding and reactivity of transition metal nitrido and imido complexes followed by a discussion of the common synthetic routes were done.

Complexes of Cu(II), Ni(II), Co(II), Mn(II), Zn(II) and VO(II) have been prepared in ethanol using Schiff bases derived from acetoacetanilido-4-aminoantipyrine and 2-aminothiophenol[77]. Micro analytical data, magnetic susceptibility, spectral techniques were used to confirm the structures of the chelates. The *in vitro* antimicrobial activity of the investigated compounds was tested against the micro organisms. A bis(phenol-armed) acyclic Schiff

base ligand H_2L has been synthesised from 3,6-diformylpyridazine and two equivalents of o-aminothiophenol. The ligand H_2L has been structurally characterised and is shown to be close to planar with both intramolecular and intermolecular hydrogen bonding interactions present. Three complexes of Co, Ni, and Cu with the ligand have been prepared and characterised[90].

The ternary complexes of Cu(II) with salicylidene-2-amino thiophenol and glycine, alanine, valine and histidene amino acids have been studied in solution and in solid state by Soliman[91]. The complexes were found to have the formula [M(L)(AA)] and five coordinated square bi-pyramidal distorted trigonal bipyramidal geometry. The thermal stability of the complexes was studied and the weight losses were correlated with the mass fragmentation pattern.

Ruthenium complexes of Schiff base salicylideneimine-2-thiophenol were reported by Khalill and co-workers[92]. UV-VIS spectra of the two complexes in different solvents exhibited visible bands due to metal-to-ligand charge transfer. Electrochemical investigation of the free ligand and complexes showed some cathodic and anodic irreversible peaks due to inter conversions through electron transfer. Oxovanadium(IV) complexes with Schiff base ligand, salicylidene-o–aminothiophenol, have been synthesised and characterised by Pragnesh et al.[93] Spectral studies indicate that the oxovanadium(IV) complexes assume a six-coordinate octahedral geometry. The antibacterial activities of the complexes against *Salmonella typhi*,

Escherichia coli and *Serratia mercescens* are higher as compared to the free ligands.

Spectroscopic and electrochemical studies of transition metal complexes of Schiff base derived from 1,7-bis(2-formylphenyl)-1,4,7-tri oxaheptane and 2-aminothiophenol were reported[94]. It was found that the ligand can effectively be used in solvent extraction of Cu(II) and Ni(II) from the aqueous phase to the organic phase.

Review of metal complexes of Schiff bases of semicarbazone

The chemistry of transition metal complexes of semicarbazones has been receiving considerable attention largely because of their special properties. According to the IUPAC recommendations[95] for the nomenclature of organic compounds, derivatives of semicarbazide of the types R-CH=N-NH-CO-NH_2 and R^1R^2C=N-NH-CO-NH_2, which are usually obtained by condensation of semicarbazide with suitable aldehydes and ketones, may be named by adding the class name 'semicarbazone' after the name of the condensed aldehydes RCHO or ketone $RR'C$=O. It is usual also to include in this class derivatives with substituents on the amide or thio amide nitrogen, R^1R^2C=N-NH-CX-NR^3R^4, on the X atom, R^1R^2C=N-N=CX R^3-NH_2 or on the 'hydrazinic' nitrogen R^1R^2C=N-NR^3-CX-NH_2 .

These classes of compounds usually react with metallic cations giving complexes in which semicarbazones behave as chelating ligands. Research

on the coordination chemistry[96], analytical applications[97] and biological activities[98] of these complexes has increased steadily for many years. Cambridge structural database reveals that a thousand papers related to semicarbazones were published in the last decade[99].

Casas[100] have conducted a detailed review of the structural aspects of the complexes formed by semicarbazones with metallic elements of group 12, 13, 14 and 15 up to year 1998. This paper elaborately explains about the nature of the metal-to-ligand bonds and the coordination behaviour of the ligand.

Potent cytotoxic Cu(II) complexes of furannic semicarbazones like 2-furfuralsemicarbazone,5-methyl-2-furfuralsemicarbazone, 2-furfural-4-phenyl semicarbazone and 3-(2-furyl)prop-2-enalsemicarbazone were prepared by Ibrahim et al[101]. The stability constants were calculated and a relation between stability and molecular weight of the ligands were proposed. Kasuga[102] synthesised and structurally characterised 4-and 6-coordinate Ni(II) complexes of three semicarbazone ligands. Their antimicrobial activities were evaluated by the MIC against four bacteria (*B. subtilis, S. aureus, E. coli and P. aeruginosa*), two yeasts (*C. albicans* and *S. cerevisiae*) and two molds (*A. niger* and *P. citrinum*). The structure–activity correlation in this series of Ni(II) complexes was discussed based on their ligand-replacement abilities. The Cu(II) complexes of the Schiff base salicylaldehyde semicarbazone have been prepared and structurally characterised by Patole[103]. They proposed that

compound shows a distorted square planar geometry where the metal atom lies slightly below the ligand donor atom plane and exhibits a longer Cu–Cl bond distance (2.226 A°). It was observed that the superoxide dismutase activity of the compound can be synergistically enhanced by the addition of heterocyclic bases. Complexes of semicarbazone of starch dialdehyde with Ca(II), Cd(II), Co(II), Cu(II), Fe(II), Mg(II), Mn(II), Ni(II), Pb(II) and Zn(II) were reported[104]. The spectral characterisation showed that the carbonyl oxygen atoms and the C=N nitrogen atoms of the semicarbazone are involved in chelation of the metal atoms.

Lee[105] investigated Cu(II) complexes containing a series of salicylaldehyde semicarbazone ligands using physicochemical techniques. The X-ray structure of copper complex of salicylaldehyde-N,N-dibenzyl semicarbazone shows that the complex is monomeric and the copper atom is four coordinated in a distorted square planar geometry. Twelve Zn(II) complexes with semicarbazone ligands were reported[106]. Seven three-dimensional structures of Zn(II) complexes were determined by single-crystal X-ray analysis. Their antimicrobial activities were evaluated by MIC against four bacteria, two yeasts and two molds.

Cu(II) and Ni(II) complexes of new Schiff base ligand 2-acetyl-2-thiazoline semicarbazone were synthesised and characterised by physical measurements and crystal structures determined with help of X-ray technique[107]. The geometry around the metallic atoms is described as a

distorted square-pyramid for the copper complex and as a distorted octahedron for the nickel complex. 2-benzoylpyridine semicarbazone and its Cu(II) and Zn(II) complexes were reported by Rebolledo[108]. In both cases, the neutral semicarbazone acts as a tridentate ligand which coordinates the metal through the pyridine and imine nitrogen atoms and the carbonyl oxygen.

Leovac[109] carried out the synthesis and physicochemical characterisation of Ni(II) complexes of pyridoxal semicarbazone. Spectral studies on Co(II), Ni(II) and Cu(II) high-spin type complexes with semicarbazone derived from 2-acetylfuran were conducted by Chandra et al.[110] and different geometries were assigned to each complex. Cu(II) complexes of 2-hydroxyacetophenone-N(4)-phenyl semicarbazone were studied by Kala[111].

Review of metal complexes of Schiff bases of thiosemicarbazone

Thiosemicarbazones which comprise a well known group of NS donors have been extensively used for complex formation in the recent past and are widely employed in medical science[112]. A number of reviews on various aspects of the thiosemicarbazones have been published[100,113-115]. In this section, emphasis is given for the synthetic, physicochemical and structural aspects of the metal complexes of thiosemicarbazones.

Thiosemicarbazone are prepared through the condensation, between aliphatic, aromatic or heterocyclic carbonyl compounds and thiosemicarbazide[116,117]. Neutral cationic or anionic complexes can be formed from thiosemicarbazones because of its existence in two tautomeric forms such as thione (I) and thiol (II) forms.

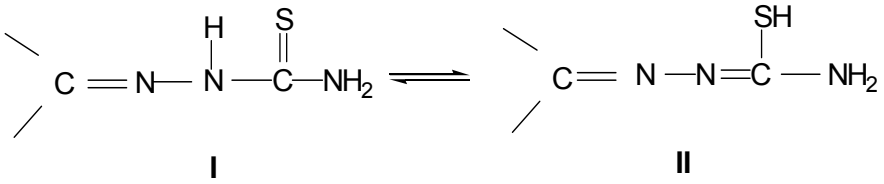

I II

When the thiosemicarbazone exist in cis-configuration, it forms stable five membered rings with metal ion during the complex formation, by coordinating through the azomethine nitrogen and thioketosulpur atoms. Some times they exist in trans configuration and the bonding is through sulphur atom alone i.e. it acts as a monodendate.

Ferrari reported synthesis and characterisation of several new transition metal complexes with novel ligands like pyridoxal thiosemicarbazone[118], 5-formyluracil thiosemicarbazone[119,120], p-fluorobenzaldehyde thiosemicarbazones[121,122], methyl pyruvate thiosemicarbazone[123], α-keto glutaricacid thiosemicarbazone[123] and 1-methylisatin-3-thiosemicarbazone[124].

Duran and co-workers[125] electrochemically synthesised and structurally characterised the binuclear complex bis(1-phenylglyoxalbis(3-

piperidyl thiosemicarbazone)zinc(II). Diaz et al.[126] carried out EPR characterisation of Cu(II) complexes of acetaldehyde thiosemicarbazone, pyruvic acid thiosemicarbazone and ribose bis-thiosemicarbazone at room temperature and low temperature. Computer simulation of the EPR spectra has revealed differences in the magnetic parameters of the compound. Mn(II), Co(II), Ni(II), Cu(II) and Zn(II) complexes with a new Schiff base vitamin K_3-thiosemicarbazone was synthesised, characterised and antibacterial activity determined by Li[127]. In all the complexes, the ligand coordinates through sulfur and oxygen atoms, and the geometry around metal atom is best described as octahedral.

West and his co-workers have been reported numerous new ligands and their transition metal complexes. The newly synthesised ligands were 2-pyridineformamide-N(4)-methylthiosemicarbazone[128], 2-pyridineformamide-3-piperidyl thiosemicarbazone[129], acetone-3-hexamethyleneiminyl thiosemicarbazone[130], pyrazineformamide-N(4)-methyl thiosemicarbazone[131] and 5-methyl-2-hydroxyacetophenone N(4)-substituted thiosemicarbazones[132]. The ligands and complexes were characterised by molar conductivities, magnetic susceptibilities and spectroscopic and X-ray techniques.

The synthesis of three bis(thiosemicarbazone) compounds formed by the reaction of benzil with either thiosemicarbazide, 4-methyl-3-thiosemicarbazide or 4-phenyl-3-thiosemicarbazide were reported by Alsop et al[133]. Sharma prepared novel complexes of Cu(II) derived from 5-

nitrofuran-2-carboxaldehyde thiosemicarbazones and characterised using spectroscopic techniques[134]. These copper complexes are bidentate and possess octahedral geometry around Cu(II) ion. Ni(II) complexes of ortho-naphthaquinone thiosemicarbazone were synthesised and spectroscopically characterised by Afrasiabi[135]. The X-ray crystal structure and *in vitro* anticancer studies were also carried out.

A variety of thiosemicarbazones 2-benzoylpyridine N(4), N(4)-(butane-1,4-diyl)thiosemicarbazone[136], di-2-pyridylketone N(4), N(4)-(butane-1,4-diyl)thiosemicarbazone[137], 2-benzoylpyridineN(4)-phenylthio-semicarbazone[138], N(4)-phenylthiosemicarbazone[139] and salicylaldehyde N(4)-cyclohexyl thiosemicarbazone[139] were synthesised and their transition metal complexes were reported by Kurup et al. The metal complexes were characterised using conventional techniques. The antibacterial properties of some of them were investigated.

Zn(II) complexes derived from pyridine-2-carbaldehyde thiosemicar-bazone and (1E)-1-pyridin-2-ylethan-1-onethiosemicarbazone were synthesised and characterised using spectral and XRD techniques by Demertzi[140]. The antiproliferative activity of Zn(II) complexes were also studied. Leovac[141] describes the synthesis of Ni(II) complexes with Schiff base pyridoxal semicarbazone and proposed that Schiff bases are coordinated as tridentate ligands with an ONX set of donor atoms. Ni(II) complexes of picolinaldehyde N-oxide thiosemicarbazone were synthesised and

characterised by single crystal X-ray diffraction, IR, and thermal analysis by Yu-Qing[142]. The antimicrobial activities of complex were also evaluated. Ni(II) complexes of 5-methyl-2-furfuraldehyde thiosemicarbazone were prepared and structural and biological activities were determined by Jouad[143].

Chandra reported Co(II), Mn(II), Co(II) and Ni(II) complexes with new ligands like indoxyl thiosemicarbazone[144,145], 2-methylcyclohexanone thiosemicarbazone and 2-methylcyclohexanone-4N-methyl-3-thiosemicarbazone[146]. A new macrocyclic Schiff base (1,2,5,6,8,11-hexaazacyclododeca-7,12-dithione-2,4,8,10-tetraene) containing thiosemicarbazone moiety was also synthesised and its Cu(II) and Ni(II) complexes were reported[147]. The complexes were characterised on the basis of elemental analysis, molar conductance, magnetic susceptibility, IR, electronic, ^{1}H NMR, mass and EPR spectral studies. The geometry of the complexes was also described.

Very few reports are available for the metal complexes of furoin based ligands. Mehta[148] has reported the synthesis and characterisation of transition metal complexes of 2-furoinoxime. A new Schiff base formed by the condensation of the S-benzyldithiocarbazate and furoin was reported by Mahmoud[149]. Cu, Ni, Cd, Co and Pd complexes of the above Schiff base were prepared and characterised by conventional methods. Daoud[150] prepared silicon and organosilicon derivatives of furoin, benzoin and pyridine. They have proposed a chelating structures for the resulting derivatives in which ligands acted as bidendate.

Scope of present investigation

It becomes evident from the above review that much systematic investigation has already been on metal complexes of Schiff bases derived from 2-aminophenol, 2-aminothiophenol, semicarbazone and thiosemi-carbazone on various aldehydes and ketones. However no work has been reported on metal complexes of furoin-2-aminothiophenol, furoin-2-aminophenol, and furoin thiosemicarbazone and furoin semicarbazone. The observation is that many such ligands and their metal complexes have ample applications and demand detailed investigation. In the present investigation, the focus is mainly on the metal complexes of Schiff bases mentioned above. The metal complexes of these Schiff bases with transition metal ions like Co(II), Ni(II), Cu(II) and Zn(II) have been synthesised and characterised by various physicochemical methods. The thermal decomposition of the representative complexes have been studied by thermogravimetric technique so as to understand the thermal stabilities and their decomposition pattern. Crystalline states of selected complexes were established by indexing its X-ray powder diffraction pattern. To find out some potential application of the new ligands and complexes, the corrosion inhibition efficiency of the four new Schiff base ligands as well as the solid state electrical conductivity were also envisaged.

CHAPTER 2
MATERIALS, METHODS AND INSTRUMENTS

In this chapter, a brief description of the general reagents employed for the present study and purification procedures adopted wherever necessary are described. It also gives details of the analytical and physical methods used for the characterisation of ligands and complexes synthesised.

.

Materials

Analar grade metal acetates were used as source of metal for synthesis of the complexes. For preparation of ligands, analar grade samples of furoin from Sigma Aldrich and other chemicals 2-aminothiophenol, 2-aminophenol, and thiosemicarbazide and semicarbazide hydrochloride from E-Merck were used. The solvents were purified by standard procedures[151]. All the reagents such as perchloric acid, nitric acid, hydrochloric acid, sulphuric acid, ammonia and sodium acetate used in the present investigation were of analar grade. The procedure for the preparation of ligands and complexes are given in the following chapters of part I of this thesis.

Analytical methods

C H N S analysis

Carbon, hydrogen nitrogen and sulphur content of the ligands and their metal complexes were determined by microanalysis using Elementar make Vario EL III model CHNS analyzer.

Estimation of metals

The standard methods[152] were adopted for the estimation of metal content in the complexes. The metal content of the complex was estimated volumetrically after decomposing the complexes with a mixture of nitric, hydrochloric and perchloric acids. For this a known amount of complex (0.2-0.3g) was digested with concentrated nitric acid perchloric acid mixture followed by concentrated HCl. The digestion process was repeated three times by adding fresh amounts of hydrochloric acid. The resultant solution was then quantitatively made up to 100 ml. The metal content in the complex was estimated using a definite volume of this solution.

Amount of copper was determined iodometrically by the addition of KI and subsequent titration of liberated iodine by standard sodium thiosulphate. Cobalt and Zinc was estimated volumetrically by complexometric titration using standard EDTA with Eriochromeblack–T as indicator. Gravimetrically, nickel was estimated by precipitating as dimethyl glyoxymate.

Metal content in the metal complexes were also estimated by pyrolysis method. About 0.2g complex was weighed out in a silica crucible and heated strongly. During heating, all the organic particles in the chelate were burnt off and the metal oxide left behind was weighed. From the weight of the metal oxide, the metal percentage was calculated.

Experimental Techniques

Physicochemical techniques such as solution conductance, magnetic susceptibility measurements and spectral studies like UV-Visible and IR have been used to elucidate the structure and geometry of the complexes. Thermogravimetric and X-ray diffraction studies have also been carried out.

Molar conductance measurements

Molar conductance of the approximately 10^{-3}M solutions of the complexes was carried out using a Philips conductivity bridge at 28 ± 2°C.

Magnetic measurements

Magnetic susceptibilities of the complexes were determined at room temperature by Gouy method using $Hg[Co(NCS)_4]$ as calibrant[153]. Diamagnetic corrections were applied using Pascal constants taking into consideration the magnetic contribution of various atoms and structural units[154,155]. The effective magnetic moments were calculated from the corrected susceptibilities using the equation.

$$\mu_{eff} = 2.84\sqrt{\Psi'_M}.T \quad (1)$$

where ψ'_M is the molar susceptibility corrected diamagnetism and T is the absolute temperature. The theoretical magnetic moments were calculated using the formula

$$\mu_{eff} = g\sqrt{S(S+1)} \quad (2)$$

Infrared Spectra

The infrared spectra of the ligands and metal complexes were recorded using KBr disc technique in the range 4000-400cm^{-1} on a Thermonicolet Avatar make 370 DTGS model FT-IR Spectrophotometer. The importance of IR spectroscopy lies in the fact that characteristic infrared absorption of a group occurs at about the same frequency irrespective of the molecule in which the group is present.

Electronic spectra

The UV-Visible spectra of the ligands and complexes were recorded on a Carry UV-Visible Spectrophotometer using DMSO as solvent. Electronic spectral studies were carried out mainly in a structural diagnostic perspective so as to supplement any information obtained from magnetic studies.

Thermo gravimetric analysis

Thermograms of the complexes were recorded on a Perkin Elmer make Pyris diamond model thermal analyzer in air or oxygen atmosphere at a heating rate of 10 or 15°C/ m. Each mass loss consideration from the TG plot can be assigned to the decomposition or volatilization of a particular group.

Powder X-ray diffraction technique

The X-ray powder diffraction pattern of the complexes and ligands was recorded on AXS Bruker Germany make D 5005 model powder X-ray diffractometer with copper Kα radiation.

Instruments

The following instruments have been used for the present investigation

1. Elementar make Vario EL III model CHNS analyzer
2. Philips make conductivity bridge
3. Gouy Type magnetic balance
4. Thermonicolet Avatar make 370 DTGS model FT-IR Spectrophotometer
5. Carry make UV-VIS Spectrophotometer
6. Perkin Elmer make Pyris diamond model thermal analyzer
7. AXS Bruker make D 5005 model powder X-ray diffractometer.

CHAPTER 3
STUDIES ON Co(II), Ni(II), Cu(II) AND Zn(II) COMPLEXES OF FUROIN-2-AMINOTHIOPHENOL (FATP)

Furoin-2-aminothiophenol (FATP) a potential tridendate Schiff base ligand has been synthesised for the first time. This ligand forms a variety of complexes with various transition metals. Detailed investigation on synthetic and structural aspects of metal complexes derived from furoin and 2-aminothiophenol are rare. In this chapter, therefore, the results of a brief study of the coordination compounds of Schiff base derived from furoin and 2-aminothiophenol are discussed.

Preparation of furoin-2-aminothiophenol

An ethanolic solution of furoin (2.88g**,** 0.015mol) was mixed with a solution of 2-aminothiophenol (1.87g, 0.015 mol) in hot ethanol and refluxed for four hours on a water bath. The resulting solution was concentrated and cooled in an ice bath. The precipitate formed was collected through filtration using a vacuum pump and washed with ethanol and dried over anhydrous $CaCl_2$. The melting point of FATP was found to be 115°C.

Characterisation of the ligand

The ligand FATP was characterised on the basis of elemental analysis and spectral data. The analytical data obtained are shown in the table 1.3.1 and were found to be in agreement with the empirical formula for FATP. The UV and IR spectra of the ligand showed the characteristic bands. Based on the above results, the structure of the ligand FATP was confirmed and shown in the figure 1.3.1.

Table 1.3.1 Analytical data for the ligand FATP

FATP	C %	H %	N %	S %
Found	63.85	4.30	4.32	9.85
Calculated	64.14	5.01	4.68	10.71

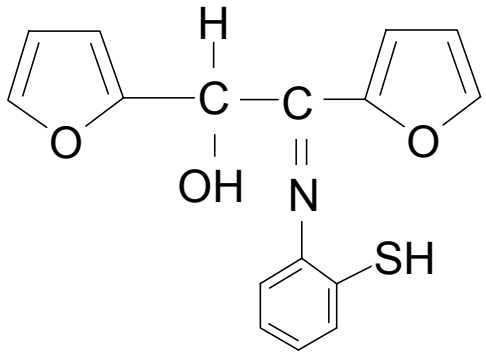

Figure 1. 3. 1 Structure of Schiff base furoin-2-aminothiophenol

Synthesis of complexes

Co(II), Ni(II), Cu(II) and Zn(II) complexes of FATP were prepared by mixing ethanolic solutions of metal acetate (0.005mol), 2-amino thiophenol (0.005mol) and furoin (0.005mol) in the presence of sodium acetate (1g). The resulting solution was refluxed for about 3-4 hours, concentrated and kept overnight in an ice bath. The complex formed was filtered using a vacuum pump and washed with ethanol, chloroform and ether, dried in a desiccator over anhydrous calcium chloride. In the preparation of Cu(II) complex, sodium acetate was not added.

Characterisation of the complexes

The complexes were characterised on the basis of elemental analysis, magnetic measurements, electronic and infrared spectral data, conductance measurements, thermal analysis and X-ray diffraction data.

Results and discussion

The complexes are coloured, non hygroscopic solids and are air and photo stable. They are insoluble in water but slightly soluble in organic solvents like ethanol, methanol and completely soluble in DMSO.

Elemental analysis

The complexes were analyzed for metal and sulphur content by standard methods[152]. Percentage of carbon, hydrogen and nitrogen was

determined by microanalytical methods**.** The results are summerised in table 1.3.2.

Molar conductance

It is observed that the molar conductance values of the complexes in DMSO at a concentration of 10^{-3}M at room temperature are in the range of 4-12 $ohm^{-1}cm^2$ mol^{-1}. The very low values indicate that these complexes behave as non electrolytes in DMSO and are neutral in nature[156].

Magnetic measurements

The values of the magnetic moments of the complexes are tabulated in table 1.3.2. The Co(II) complex possess magnetic moment of 4.90 BM. It is reported that an octahedral geometry can be assigned to Co(II) complexes, if the measured μ_{eff} value is in the range of 4.3-5.2 BM[157]. Ni(II) complex exhibited magnetic moment values of 3.20 BM which suggests an octahedral arrangement around the metal ion. The magnetic moment values of Cu(II) complex is 1.84 BM as expected for an octahedral geometry which corresponds to a d^9configuration with one unpaired electron[158,159]. Zn(II) complex was found to be diamagnetic.

Table 1. 3. 2 Microanalytical, magnetic and conductance data of transition metal complexes of furoin-2-aminothiophenol

Complex	Colour	M%	C%	H%	N%	S%	μ_{eff} (BM)	Ω^{-1}
[Co(FATP) $(H_2O)_3$]	Purple	14.69 (14.36)	46.88 (46.80)	4.91 (5.12)	3.48 (3.41)	8.15 (7.80)	4.90	12.63
[Ni(FATP) $(H_2O)_3$]	Greenish yellow	13.95 (14.19)	45.90 (46.82)	3.77 (3.65)	3.85 (3.41)	8.02 (7.80)	3.20	8.84
[Cu(FATP) $(H_2O)_3$]	Black	16.25 (15.40)	47.75 (46.27)	4.75 (5.06)	3.41 (3.35)	7.82 (7.68)	1.84	4.31
[Zn(FATP) $(H_2O)_3$]	Greenish yellow	15.38 (15.75)	47.48 (46.07)	4.00 (4.56)	3.36 (3.36)	7.93 (7.68)	D	8.8

D- Diamagnetic, M- Metal, Ω^{-1}- Molar conductance in $ohm^{-1}cm^2mol^{-1}$. Calculated values are given in parenthesis

Infrared spectral studies

The infrared spectroscopic results provide support for the molecular constitution of these complexes. The assignments are made on the basis of comparison with the spectra of similar type of compounds. A representative IR spectrum of the ligand FATP and its Cu(II) complex are given as figures 1.3.2 and 1.3.3 respectively. The selected infrared absorption frequencies of the ligand and complexes are given in the table 1.3.3

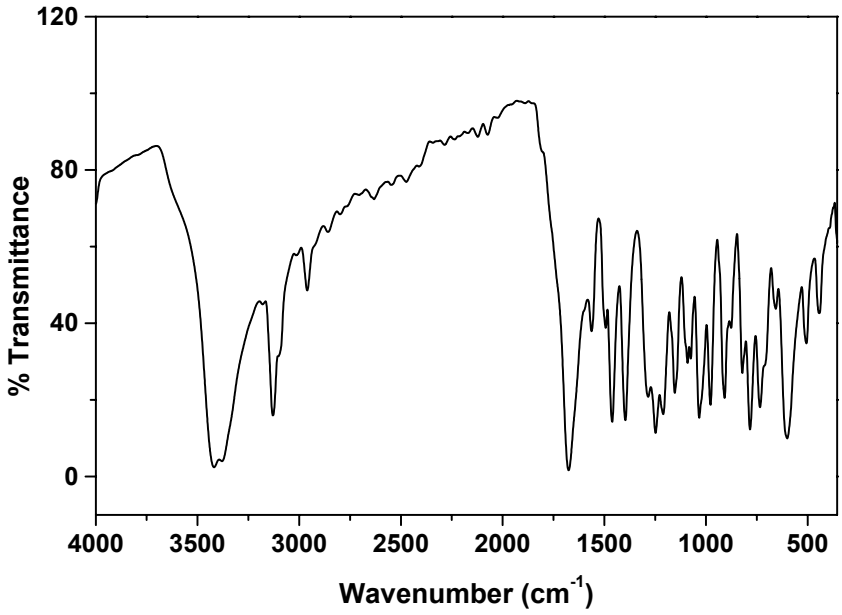

Figure 1. 3. 2 IR spectrum of the ligand FATP

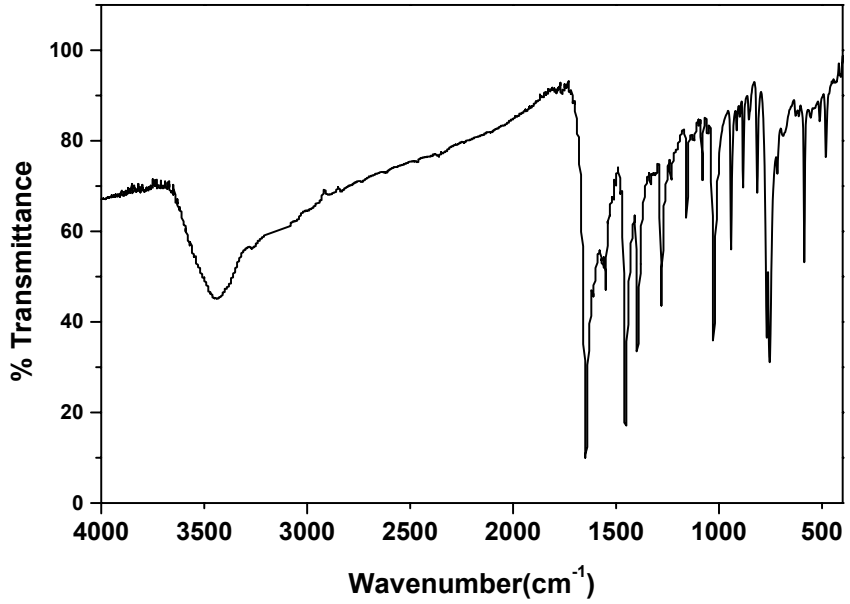

Figure 1. 3. 3 IR spectrum of Cu(II) complex of FATP

On complex formation most of the bands in the IR spectrum of the ligand FATP undergo frequency shift and in many cases intensity changes. A strong intense band approximately at 1676cm^{-1} in the spectrum of the ligand may be assigned to νC=N stretch. This band shows a downward shift by about 25-35cm^{-1} in the spectra of all the metal complexes, indicating the participation of the azomethine nitrogen in coordination with metals[160]. The depression in stretching frequency may tentatively attributed to a lowering of the C=N bond order as a result of the M-N bond formation in the complexes[161]. The shifted band in many cases is coincident with the C=C band, which then shows greater intensity or broadening. Further evidence for

bonding by nitrogen and oxygen atoms is provided by far IR spectra of complexes. Due to interference of skeletal vibrations of ligands with M-N and M-O vibrations, definite assignments of bands are difficult. Therefore only tentative assignments are made on the basis of information available in literature. Spectra of all complexes showed bands at 586-579cm^{-1} and 483-478cm^{-1} which may be assigned to the νM-N and νM-O stretching vibrations[162-164].

It was observed that the symmetric vibrations of C-S, which appeared as a band near 701cm^{-1} in the ligand spectrum, has been shifted to lower frequencies after complexation. Similarly a weak band of S-H, which appeared at 2650cm^{-1} in the case of ligand, has been disappeared in the spectrum of all complexes[165]**.** This suggests that the –SH group is involved in coordination. A broad band at 3450-3400cm^{-1} in the spectra of several complexes is attributed to the hydroxyl stretching mode of water molecule [166,167]. In addition a medium band approximately at 870-950cm^{-1} suggests that water molecules are coordinated.

Table 1. 3. 3 Characteristic Infrared absorption frequencies (cm^{-1}) of metal complexes of furoin-2-aminothiophenol

Substance	ν H_2O	ν C=N	ν M-N	ν M-O
Ligand FATP	_	1676	_	_
Co(FATP) $(H_2O)_3$	3405	1646	586	481
Ni(FATP) $(H_2O)_3$	3410	1646	586	481
Cu(FATP) $(H_2O)_3$	3443	1647	586	483
Zn(FATP) $(H_2O)_3$	3430	1645	579	478

Electronic spectra

The electronic spectrum depends on the energy of metal d orbital, their degeneracy and the number of electrons distributed**.** These features are in turn controlled by the oxidation state of the metal, number and kind of the ligand and the geometry of the complex[168]. The electronic spectral data obtained were found to agree with conclusions arrived from magnetic susceptibility measurements.

The expected octahedral transitions of Co(II) are $^4T_{1g}(F) \rightarrow {}^4T_{2g}(F)$, $^4T_{1g}(F) \rightarrow {}^4A_{2g}(F)$ and $^4T_{1g}(F) \rightarrow {}^4T_{1g}(P)$ [169,170]. The middle band is due to a transition of two electron which is forbidden and give a weak band and $^4A_{2g}$ (F) and $^4T_{1g}$(P) are very close in octahedral geometry. Due to these

factors detection of middle band is very difficult. The electronic spectrum of Co(II) gives two peaks at 1075nm and 442nm due to $^4T_{1g}(F) \rightarrow {}^4T_{2g}(F)$ and $^4T_{1g}(F) \rightarrow {}^4T_{1g}(P)$ transitions corresponding to octahedral geometry**.** The purple colour of Co(II) complex is also suggestive of octahedral geometry.

Ni(II) complex of FATP exhibit two d-d transitions in the electronic spectra at about 544nm and 978nm due to $^3A_{2g}(F) \rightarrow {}^3T_{1g}(F)$ and $^3A_{2g}(F) \rightarrow {}^3T_{2g}(F)$ transitions of octahedral geometry[171]. The distorted octahedral geometry for Cu(II) complex is indicated by a peak at 666nm[171]. The Zn(II) complexes do not show any characteristic d-d transition bands.

Thermal analysis

The prepared complexes were subjected to thermal analysis. Mass loss considerations of the decomposition indicate that the complexes have been converted to corresponding metal oxides. Detailed kinetic analysis of the TG traces of selected complexes is described in Part II.

X-ray diffraction

The powder X-ray diffraction pattern of the ligand and complexes are shown in the figure 1.3.4. The XRD patterns indicate that the ligand and its complexes are crystalline, with various degrees of crystallinity. Some of the extra peaks present in the complexes compared to ligand prove the coordination of metal ion[172]**.** The residue obtained after the thermal treatment of metal complexes was subject to X-ray diffraction analysis and patterns

obtained are given in the figure 1.3.5. It was found that the diffraction patterns obtained matches with the corresponding metal oxide diffraction patterns. The detailed X-ray diffraction studies of the selected complexes are described in part III.

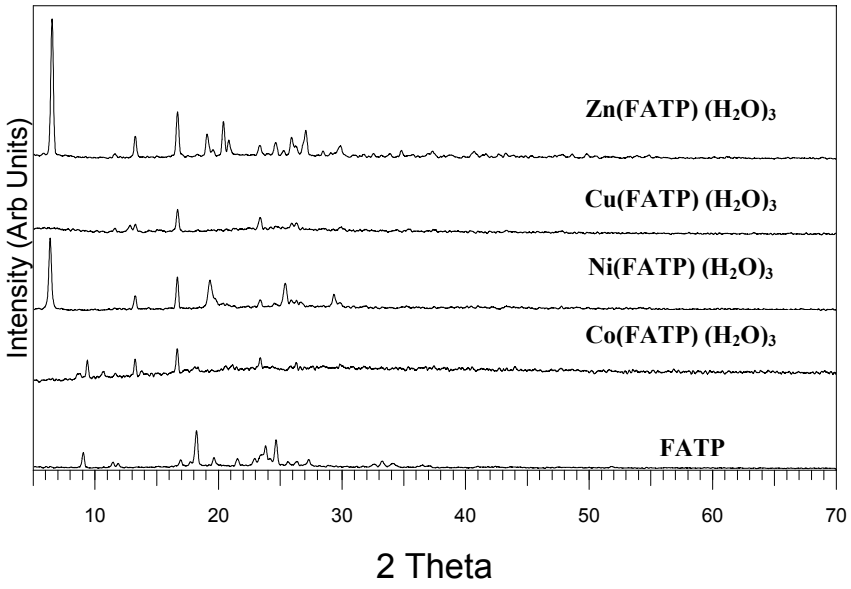

Figure 1. 3. 4 X-ray diffraction patterns of the ligand FATP and its metal complexes

Based on these observations, the structure of the Co(II), Ni(II), Cu(II) and Zn(II) complexes of FATP can be confirmed to be octahedral. From all these studies, it is clear that the ligand acts as dianionic tridentate towards metal ion. Above discussion suggest the following structure (figure 1.3.6) for these complexes.

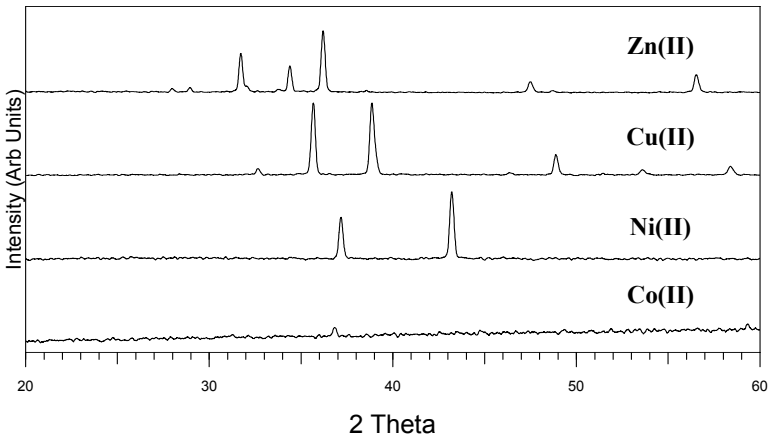

Figure 1. 3. 5 X-ray diffraction patterns of the residues of complexes of FATP

.

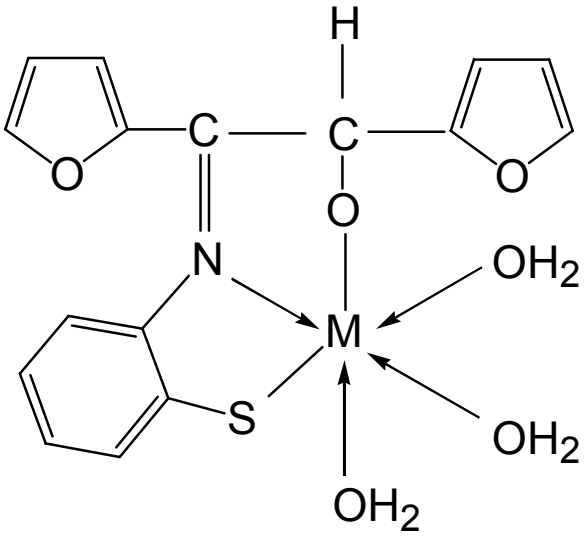

M= Co(II), Ni(II), Cu(II) and Zn(II)

Figure 1. 3. 6 Structure of metal complexes of ligand FATP

CHAPTER 4

STUDIES ON Co(II), Ni(II), Cu(II) AND Zn(II) COMPLEXES OF FUROIN-2-AMINOPHENOL (FAP)

Schiff bases are an important class of ligands in coordination chemistry and find extensive applications in different spheres. Much attention has been given to metal complexes of aminophenol. But Schiff base, furoin-2-aminophenol and its metal complexes were not reported yet. FAP a potential tridentate Schiff base ligand, has been synthesised for the first time. This ligand forms a variety of complexes with various transition metals. In this chapter, therefore, the results of a brief study of the coordination compounds of Schiff base derived from furoin and 2-amino phenol are discussed.

Preparation of the ligand furoin-2-aminophenol

Hot ethanolic solutions of furoin (2.88g, 0.015mol) and 2-amino phenol (1.64g, 0.015 mol) were mixed and refluxed for 3 hours on a water bath. The resulting solution was concentrated and cooled in an ice bath. The separated precipitate was collected through filtration using a vacuum pump and washed with ethanol, dried over anhydrous $CaCl_2$. The melting point of FAP was determined and found to be 173°C. The ligand was soluble in a mixture of ethanol and DMSO.

Characterisation of the ligand

Elemental analysis and spectral techniques were adopted for the characterisation of the ligand. The obtained analytical results are given in the table 1.4.1 and found to be in good agreement with the empirical formula.

Table 1. 4. 1 Analytical data for the ligand FAP

FAP	C %	H %	N %
Found	67.42	4.16	3.94
Calculated	67.77	4.58	3.38

The UV and IR spectra of the ligand showed characteristic bands. Based on the above results, the structure of the ligand was confirmed and is shown in the figure 1.4.1.

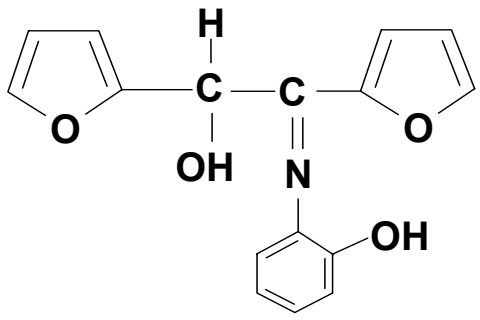

Figure 1. 4. 1 Structure of Schiff base furoin-2-aminophenol

Synthesis of complexes

The hot ethanolic solutions of corresponding metal acetate (0.005mol), 2-amino phenol (0.005mol) and furoin (0.005mol) were mixed and refluxed for about 3-4 hours in the presence of sodium acetate (0.5-1.0g) to get the Co(II), Ni(II), Cu(II) and Zn(II) metal complexes of FAP. The refluxed solution was concentrated, cooled in an ice bath for overnight and filtered. The obtained metal complexes dried in a desiccator over anhydrous calcium chloride.

Characterisation of the complexes

The metal complexes were subjected to magnetic and conductance measurements, elemental, electronic, IR, thermal and X-ray diffraction analysis.

Results and discussion

The complexes are coloured and non hygroscopic in nature. They are insoluble in water but slightly soluble in organic solvents like ethanol, methanol and completely soluble in DMSO.

Elemental analysis

Percentage of carbon, hydrogen and nitrogen was determined by micro analytical methods. The complexes were analyzed for metal by standard

methods[152]. The analytical data and physical appearance are summerised in table 1.4.2.

Molar conductance

The molar conductance values of the complexes in DMSO at a concentration of 10^{-3}M at room temperature were indicative of their non electrolytic nature[156].

Magnetic measurements

The values of the magnetic moments of the complexes are tabulated in table 1.4.2. The Co(II) complex has a magnetic moment value of 4.8 BM. An octahedral geometry is suggested around the metal ion[157]. Ni(II) complex has a magnetic moment value of 3.3 BM which is suggestive of octahedral configuration. Cu(II) complex give a magnetic moment value of 1.74 BM, which is expected for one unpaired electron of the d^9 configuration indicating the octahedral geometry[158,159]. Zn(II) complex was diamagnetic as expected.

Table 1. 4. 2 Microanalytical, magnetic and conductance data of transition metal complexes of furoin-2-aminophenol

Complex	Colour	M%	C%	H%	N%	μ_{eff} (BM)	Ω^{-1}
[Co(FAP) $(H_2O)_3$]	Black	14.20 (15.02)	49.25 (48.71)	3.68 (4.31)	3.40 (3.50)	4.8	7.77
[Ni(FAP) $(H_2O)_3$]	Greenish black	14.35 (14.97)	50.58 (48.72)	4. 03 (4.31)	3.17 (3.54)	3.3	7.66
[Cu(FAP) $(H_2O)_3$]	Greenish black	15.92 (16.01)	50.99 (48.26)	4.20 (4.27)	3.99 (3.52)	1.74	7.98
[Zn(FAP) $(H_2O)_3$]	Greenish black	15.35 (16.39)	50.61 (48.19)	4.23 (4.27)	3.86 (3.51)	D	1.90

D- Diamagnetic M- Metal, Ω^{-1} - Molar conductance in $ohm^{-1}cm^2mol^{-1}$. Calculated values are given in the parenthesis

Infrared spectral studies

The characteristic IR absorption bands of the ligands and the complexes are summerised in table 1.4.3. The comparison of the infrared spectra of the chelates and the ligand reveal that the spectra of chelates differ from that of the ligand in some characteristic frequencies. A strong intense band appears at 1676cm^{-1} in the spectrum of the ligand due to νC=N vibrations, has undergone a frequency shift of about 25-35cm^{-1} in all metal complexes. This shift indicates the coordination of nitrogen to metal ion[160]. The band at 1240cm^{-1} is characteristic of the C-O in the free ligand[86]. The shifting of this band to lower frequencies in the complexes indicates O-H group is ionised and coordinated. The presence of the -OH group in the ligand is indicated by a broad band approximately at 3300 cm^{-1}. In metal chelates this band is absent which suggests that, the -OH group is involved in the coordination[165]. The aromatic out of plane vibration is seen near 870 cm^{-1} and in plane vibration at 770cm^{-1} and 725 cm^{-1}.

Conclusive evidence of bonding of the ligand to the central metal ion is provided by the appearance of bands at ~586 cm^{-1} and~ 481 cm^{-1}, which can be assigned to M-N and M-O bands respectively[161]. The presence of coordinated water molecules in the complexes is confirmed by the appearance of band between 3250-3415 cm^{-1} and is followed by a sharp rocking mode of vibration between 840-850 cm^{-1} [166].

Table 1. 4. 3 Characteristic Infrared absorption frequencies (cm^{-1}) of metal complexes of furoin-2-aminophenol

Substance	νH_2O	νC=N	νM-N	M-O
Ligand FAP	_	1676	_	_
[Co(FAP) $(H_2O)_3$]	3382	1646	586	481
[Ni(FAP) $(H_2O)_3$]	3413	1647	586	481
[Cu(FAP) $(H_2O)_3$]	3398	1649	586	481
[Zn(FAP) $(H_2O)_3$]	3251	1647	579	470

Electronic spectra

The electronic spectral data were found to be in agreement with the conclusions arrived from magnetic susceptibility measurements. The electronic spectra of Co(II) complexes are characterised by two peaks at 1080nm and 450nm due to $^4T_{1g}$ (F) → $^4T_{2g}$ (F) and $^4T_{1g}$ (F) → $^4T_{1g}$(P) respectively[169,170]. Ni(II) complexes also exhibit two d-d transitions in the region at about 550nm and 370nm due to $^3A_{2g}$(F) → $^3T_{1g}$(F) and $^3A_{2g}$(F) → $^3T_{1g}$(P) transitions of octahedral geometry [171]. The electronic spectrum of Cu(II) complexes showed peak at 650nm which support a distorted octahedral geometry[171].

Thermal analysis

The prepared complexes were subjected to thermal analysis. Mass loss considerations of the decomposition indicate that the complexes have been converted to corresponding metal oxides. Detailed kinetic analysis of the TG traces of the selected complexes is described in Part II.

X-ray diffraction

The powder X-ray diffraction pattern of the ligand and complexes are shown in the figure 1.4.2.

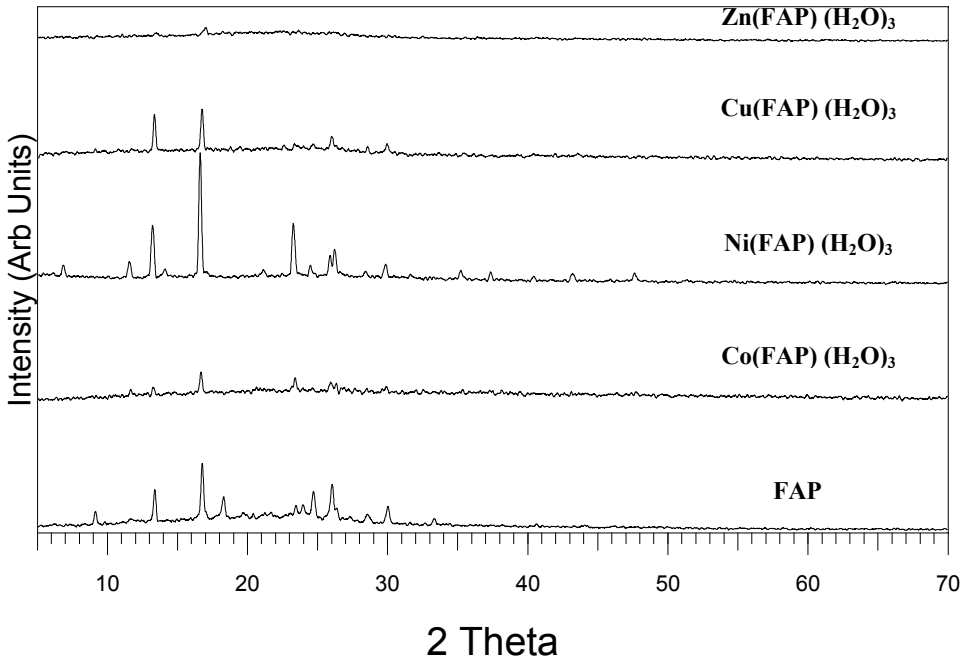

Figure 1. 4. 2 X-ray diffraction patterns of the FAP and its metal complexes

The well defined diffraction patterns were observed in the case of Ni(II) and Cu(II) of complexes of FAP. Very less number of peaks were observed in the case of Co(II) and Zn(II) complexes. The X-ray diffraction patterns of the residues obtained after thermal decomposition of metal complexes in air atmosphere confirms the presence of pure oxides of metal. The detailed X-ray diffraction studies of the selected complexes are described in part III.

Based on these observations, the structure of the Co(II), Ni(II), Cu(II) and Zn(II) complexes of FAP can be confirmed to octahedral. From all these studies, it is clear that the ligand acts as dianionic tridentate ligand towards metal ion. Above discussion suggest the following structure for these complexes (figure 1.4.3).

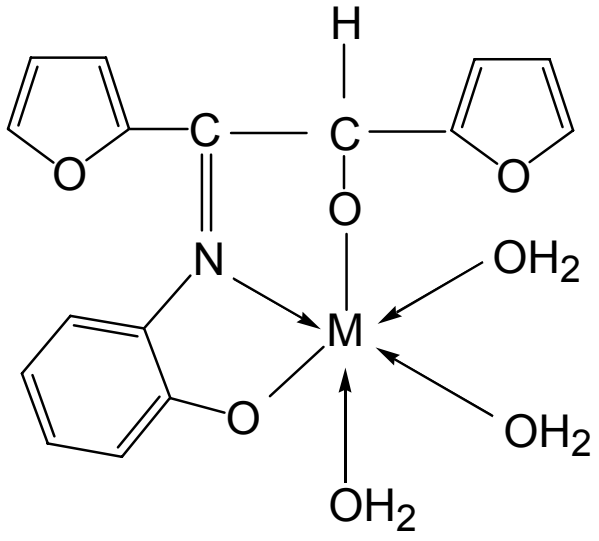

M= Co(II), Ni(II), Cu(II) and Zn(II)

Figure 1. 4. 3 Structure of metal complexes of FAP

CHAPTER 5
STUDIES ON Co(II), Ni(II), Cu(II) AND Zn(II) COMPLEXES OF FUROIN THIOSEMICARBAZONE (FTSC)

Transition metal complexes with Schiff bases as ligands have been amongst the most widely studied coordination compounds. The chemistry of transition metal complexes of thiosemicarbazones has been receiving considerable attention largely because of their pharmacological and other properties. The literature review reveals that detailed investigation on synthetic and structural aspects of metal complexes derived from furoin and thiosemicarbazide are rare. So furoin thiosemicarbazone (FTSC) a potential tridendate Schiff base ligand, have been synthesised from furoin and thiosemicarbazide. This ligand forms a variety of complexes with various transition metals. In this chapter, therefore, the results of a brief study of the coordination compounds of Schiff base furoin thiosemicarbazone are discussed.

Preparation of the furoin thiosemicarbazone

The ligand FTSC was prepared by refluxing the ethanolic solution containing equal moles of furoin and thiosemicarbazide for three hours on a water bath. The refluxed solution was concentrated and cooled in an ice bath. The ligand formed was separated by filtration and washed with ethanol and

dried over calcium chloride in a desiccator. The melting point of FTSC was found to be 96°C and it was soluble in ethanol and DMSO mixture.

Characterisation of the ligand

The C, H, N, and S content of the ligand were determined using micro analytical technique. The ligand FTSC was further characterised using spectral techniques like electronic and IR spectroscopy. The analytical data obtained are given in table 1.5.1 and were found to be in good agreement with the empirical formula for FTSC.

Table 1. 5. 1 Analytical data for the ligand FTSC

FTSC	C %	H %	N %	S %
Found	49.02	3.80	14.86	11.12
Calculated	49.80	4.15	15.85	12.10

The UV and IR spectra of the ligand showed the characteristic bands. Based on the above results, the structure of the ligand FTSC was confirmed as shown in the figure 1.5.1.

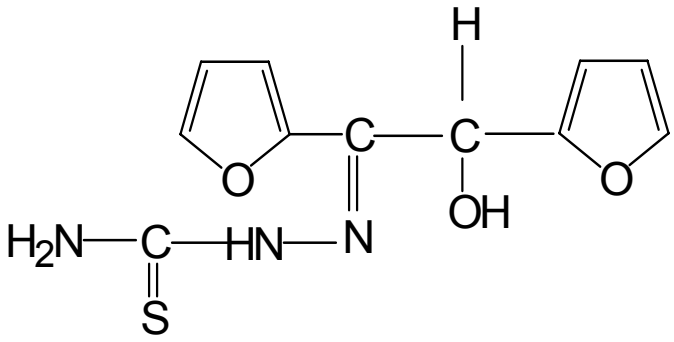

Figure 1. 5. 1 Structure of Schiff base furoin thiosemicarbazone

Synthesis of complexes

To prepare the Co(II), Ni(II), Cu(II) and Zn(II) complexes of FTSC, 0.005mol of the FTSC was first dissolved in a mixture of ethanol and DMSO by boiling. To this clear solution, 0.005mol of hot ethanolic solution of corresponding metal acetates were added slowly along with 0.5-1g of sodium acetate. The above solution was refluxed for 3-4 hours, then concentrated, cooled and filtered. The obtained complexes were dried in a desiccator over anhydrous calcium chloride.

Characterisation of the complexes

The complexes were characterised on the basis of elemental analysis, magnetic measurements, electronic and infrared spectral data, conductance measurements, thermal data and X-ray diffraction technique.

Results and discussion

The complexes are coloured, stable and non hygroscopic solids. They are insoluble in water but slightly soluble in organic solvents like ethanol, methanol and completely soluble in DMSO. The properties, structure and bonding of the complexes have been explained on the basis of information obtained from analytical, physicochemical and spectral investigations.

Elemental analysis

The complexes were analyzed for metal and sulphur content by standard methods[152]. C, H, N and S content were estimated by micro analytical methods. The results of above analysis are summerised in table 1.5.2.

Magnetic measurements

The Co(II) complexes possess magnetic moment values of 4.8 BM as expected for the octahedral Co(II) complexes[157]. The complex of Ni(II) have magnetic moment value of 3.3 BM which are in accordance with octahedral complex[153]. The magnetic moment values of Cu(II) possess normal values of 1.9 BM as expected for octahedral Cu(II)[158]. The magnetic susceptibility measurements support the diamagnetic nature of the Zn(II) complex.

Table 1. 5. 2 Microanalytical, magnetic and conductance data of metal complexes of furoin thiosemicarbazone

Complex	Colour	M%	C%	H%	N%	S%	μ_{eff} (BM)	Ω^{-1}
[Co(FTSC) $(H_2O)_3$]	Greenish black	15.32 (15.48)	36.05 (35.01)	3.91 (4.51)	10.95 (11.14)	8.15 (8.51)	4.8	17.39
[Ni(FTSC) $(H_2O)_3$]	Greenish black	15.61 (15.42)	36.15 (35.03)	3.85 (4.24)	10.02 (11.14)	9.20 (8.51)	3.3	17.60
[Cu(FTSC) $(H_2O)_3$]	Greenish black	16.83 (16.69)	35.02 (34.56)	3.98 (4.19)	10.85 (11.02)	8.02 (8.40)	1.9	6.55
[Zn(FTSC) $(H_2O)_3$]	Greenish black	16.53 (17.09)	35.02 (34.42)	3.38 (4.17)	10.05 (10.95)	7.79 (8.36)	D	5.89

D- Diamagnetic M- Metal, Ω^{-1} - Molar conductance in $ohm^{-1}cm^2mol^{-1}$.Calculated values are given in parenthesis

Molar conductance

Molar conductance of 10^{-3} M solutions of Co(II), Ni(II), Cu(II) and Zn(II) complexes in DMSO were found to be in the range of 5-18 $ohm^{-1}cm^2mol^{-1}$, indicating their non electrolytic nature[156].

Infrared spectral studies

The important infrared absorption frequencies obtained for the ligand FTSC and its complexes are given in the table 1.5.3. IR spectra of the ligand FTSC show bands at 1650 and 760cm^{-1} corresponding to C=N and C=S stretching respectively[166]. FTSC exists in thioketo form in the solid state as evidence from the IR spectral data. However, in solution, the ligand can exists in the thioketo (I) and thioenol (II) forms.

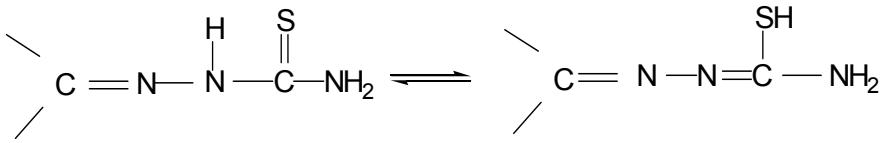

I II

In the deprotonated form it is potentially a tridendate ligand coordinating through N and the thiolate S forming five membered chelate ring.

The band at 850cm^{-1} is attributed to νC=S in the ligand. But in the case of complexes this band disappears and new band in the region 700-600cm^{-1} due to νC-S would be taken as evidence of the ligand coordinating via thioenol[167]. The appearance of bands near 500cm^{-1}and 481cm^{-1} due to M-N and M-O vibrations indicate the bonding of the ligand to central metal atom[162]. A broad feature at 3455-3310cm^{-1} in the spectra of complexes attributed to the hydroxyl stretching mode of water molecule. In addition a medium band approximately at 870-950cm^{-1} suggests that water molecules are coordinated[161].

Table 1. 5. 3 Characteristic Infrared absorption frequencies (cm^{-1}) of metal complexes of furoin thiosemicarbazone

Substance	νH$_2$O	νC=N	νM-N	νM-O
Ligand FTSC	-	1650	-	-
[Co(FTSC) (H$_2$O)$_3$]	3299	1644	501	481
[Ni(FTSC) (H$_2$O)$_3$]	3310	1641	510	476
[Cu(FTSC) (H$_2$O)$_3$]	3453	1646	512	481
[Zn(FTSC) (H$_2$O)$_3$]	3418	1644	508	481

Electronic spectra

The electronic spectra of Co(II) complex exhibited a peak at 570nm, which was taken as evidence to support the presence of Co(II) in octahedral geometry[169,170]. Ni(II) complexes also characterised by two peaks one at 564nm and other 390nm. These two peaks are due to the $^3A_{2g}(F) \rightarrow {}^3T_{1g}(F)$ and $^3A_{2g}(F) \rightarrow {}^3T_{1g}(P)$ transitions of octahedral geometry[171]. The octahedral geometry of Cu(II) complex is clear from the absorption peak at 619nm.

Thermal analysis

Thermal analysis of the prepared complexes was carried out and the mass loss considerations of the decomposition indicate that the complexes have been converted to corresponding metal oxides. Detailed kinetic analysis of these complexes is described in Part II.

X-ray diffraction

The copper and zinc complexes have well defined crystalline patterns as seen in the X-ray diffraction pattern as shown in the figure 1.5.2. But Co(II) and Ni(II) complexes does not have characteristic peaks indicating the amorphous nature of the complexes. The thermal decomposition products of the complexes were subjected to X-ray analysis and found that the residues are corresponding metal oxides. The detailed X-ray diffraction studies of the selected complexes are described in part III.

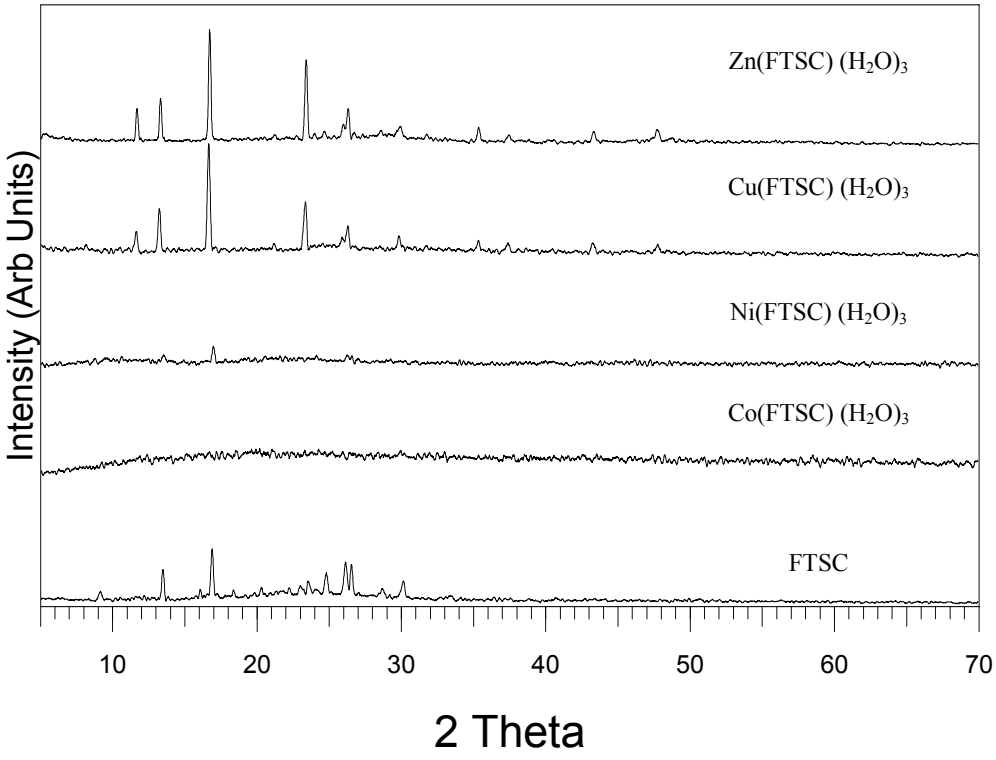

Figure 1. 5. 2 X-ray diffraction patterns of the ligand FTSC and its Co(II), Ni(II), Cu(II)and Zn(II) complexes

Based on these observations, the structure of the Co(II), Ni(II), Cu(II) and Zn(II) complexes of FTSC can be confirmed to be octahedral. From all these studies, it is clear that the ligand acts as dianionic tridentate ligand towards metal ion. The proposed structure of the complexes is shown in the figure 1.5.3.

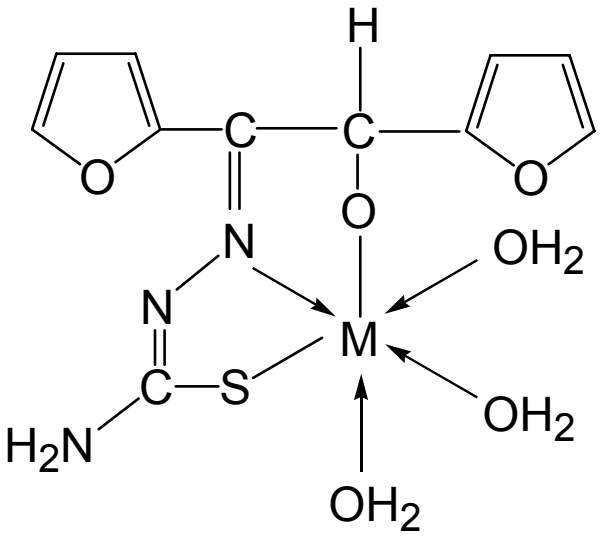

M = Co(II), Ni(II), Cu(II) and Zn(II)

Figure 1. 5. 3 Structure of metal complexes of ligand FTSC

CHAPTER 6
STUDIES ON Co(II), Ni(II), Cu(II) AND Zn(II) COMPLEXES OF FUROIN SEMICARBAZONE (FSC)

Semicarbazone is the one of the widely studied nitrogen and oxygen donor ligand like thiosemicarbazone. They are capable of acting as neutral or charged ligand moieties. Detailed survey of literature indicates that no reports were published about metal complexes containing the Schiff base, furoin semicarbazone. So a potential tridendate Schiff base ligand, furoin semicarbazone, derived from furoin and semicarbazide hydrochloride and its transition metal complexes have been synthesised and studied for the first time.

Preparation of the furoin semicarbazone

Equal moles of hot ethanolic solutions of furoin and semicarbazide hydrochloride were mixed and refluxed for three hours on a water bath. The ligand was separated out from the refluxed solution after concentration, cooling and filtration. The ligand FSC was soluble in ethanol, DMSO mixture.

Characterisation of the ligand

The ligand FSC was characterised on the basis of elemental analysis and spectral data. The analytical data is given in the table 1.6.1 and were found to be in agreement with the empirical formula for FSC.

Table 1. 6. 1 Analytical data for the ligand FSC

FSC	C %	H %	N %
Found	53.87	5.04	15.56
Calculated	53.0	4.42	16.87

The UV and IR spectra of the ligand showed the characteristic bands. Based on the above results, the structure of the ligands FSC was confirmed and shown in the figure 1.6.1

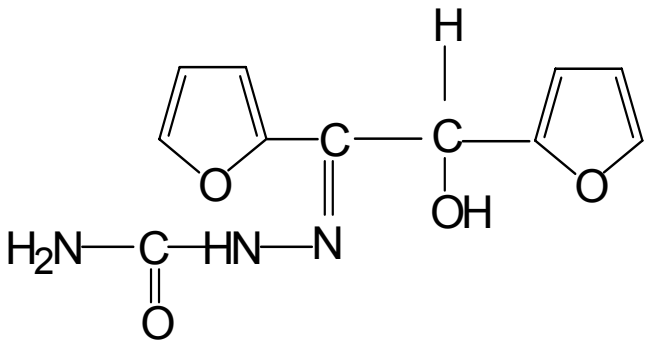

Figure 1. 6. 1 Structure of Schiff base furoin semicarbazone

Synthesis of complexes

Co(II), Ni(II), Cu(II) and Zn(II) complexes were prepared by mixing ethanolic solutions of metal acetate (0.005mol), semicarbazide hydrochloride (0.005mol) and furoin (0.005mol) in the presence of sodium acetate (0.5-1.0 gm). The resulting solution was refluxed for about 3-4 hours, concentrated and kept overnight in an ice bath. The complex formed was filtered using a vacuum pump and washed with ethanol, dried in a desiccator over anhydrous calcium chloride.

Characterisation of the complexes

The complexes were characterised on the basis of elemental analysis, magnetic measurements, electronic and infrared spectral data, conductance measurements, thermal data and X-ray diffraction technique.

Results and discussion

The complexes were insoluble in water but slightly soluble in organic solvents like ethanol, methanol and completely soluble in DMSO. The complexes were coloured and non hygroscopic solid.

Elemental analysis

The complexes were analysied for metal and sulphur by standard methods[152]. C, H, N content of the complexes were determined by micro

analytical methods**.** The results of analysis are tabulated in and given in the table 1.6.2.

Molar conductance

The low molar conductance values obtained for the four complexes i.e. 5-15 $ohm^{-1}cm^2\ mol^{-1}$, for 10^{-3} M solutions in DMSO at room temperature indicate the non electrolytic nature of complexes.

Magnetic measurements

The magnetic moment values obtained for the complexes are tabulated in table 1.6.2. The octahedral geometry of the Co(II) complex was confirmed from the measured magnetic moment value of 4.5 BM[157]. The magnetic moment value of Ni(II) complex was 2.9 BM which is in agreement with its octahedral geometry. Cu(II) complex of FSC registered magnetic moment value of 2.0 BM, therefore octahedral structure can be assigned to Cu(II) complex[158]. As expected the Zn(II) complex was found to be diamagnetic.

Table 1. 6. 2 Micro analytical, magnetic and conductance data of metal complexes of furoin semicarbazone

Complex	Colour	M%	C%	H%	N%	μ_{eff} (BM)	Ω^{-1}
[Co(FSC)$(H_2O)_3$]	Greenish black	16.95 (16.16)	35.06 (36.55)	4.9 (4.70)	11.05 (11.63)	4.5	10.00
[Ni(FSC)$(H_2O)_3$]	Greenish black	16.85 (16.10)	35.96 (36.57)	4.80 (4.71)	12.01 (11.64)	2.9	8.06
[Cu(FSC)$(H_2O)_3$]	Greenish black	16.57 (17.20)	36.85 (36.11)	4.93 (4.65)	11.20 (11.48)	2.0	15.23
[Zn(FSC)$(H_2O)_3$]	Greenish black	18.04 (17.62)	36.01 (35.90)	4.72 (4.62)	10.90 (11.42)	D	5.63

D- Diamagnetic M- Metal, Ω^{-1}- Molar conductance in $ohm^{-1}cm^2mol^{-1}$. Calculated values are given in the parenthesis.

Infrared spectral studies

The characteristic IR absorption bands of ligand FSC and its complexes are summerised in table 1.6.3.

Table 1. 6. 3 Characteristic Infrared absorption frequencies (cm^{-1}) of metal complexes of furoin semicarbazone

Substance	νH_2O	νC=N	νM-N	νM-O
Ligand FSC	_	1672	_	_
[Co(FSC) $(H_2O)_3$]	3390	1654	515	482
[Ni(FSC) $(H_2O)_3$]	3436	1639	505	487
[Cu(FSC) $(H_2O)_3$]	3448	1647	511	489
[Zn(FSC) $(H_2O)_3$]	3390	1645	508	481

The infrared spectroscopic results provide support for the molecular constitution of these complexes. Most of the bands in the spectrum of the ligands undergo frequency shifts and intensity changes during complex formation. In the case of ligand FSC, the band which appeared at 1672 cm^{-1} may be due to the presence of C=N band and there may be overlapping of C=O band in the same region. In all complexes new band appears around 1000cm^{-1} due to νC-O. This may be due to enolisation and subsequent coordination of carbonyl group[167]. The participation of azomethine nitrogen in complex formation has been indicated by the shift of band at 1672cm^{-1}

towards lower frequencies for about 25-35 cm^{-1} during complex formation[160]. The appearance of bands near 500cm^{-1} and 480cm^{-1} due to M-N and M-O vibrations indicates the bonding of the ligand to central metal atom[163]. The broad bands at 3450-3390cm^{-1} along with medium band at 870-950cm^{-1} suggest that water molecules are coordinated to central metal atom[166].

Electronic spectra

The octahedral geometry of the Co(II) complex was shown by the exhibited peaks at 1077nm and 544nm[169,170]. Ni(II) complex also characterised by two peaks, one at 972nm and other at 561nm. These two peaks are due to the $^3A_{2g}(F) \rightarrow {}^3T_{2g}(F)$ and $^3A_{2g}(F) \rightarrow {}^3T_{1g}(F)$ transitions of octahedral geometry[171]**.** The electronic spectrum of Cu(II) complexes showed peaks at 636 nm which support a distorted octahedral geometry.

Thermal analysis

The metal complexes were investigated for their thermal behavior during non isothermal heating. The mass residue obtained was corresponding to mass of metal oxides. Detailed kinetic analysis of the TG traces of selected complexes is described in Part II

X-ray diffraction

The X-ray diffraction patterns obtained for the ligand and complexes are given in figure 1.6.2. Cu(II) and Ni(II) complexes only showed

crystalline nature. Zn(II), Co(II) complexes and FSC are amorphous in nature. The analysis of thermal decomposition residues confirms the formation of oxides. The detailed x-ray diffraction analysis of selected complexes is described in part III.

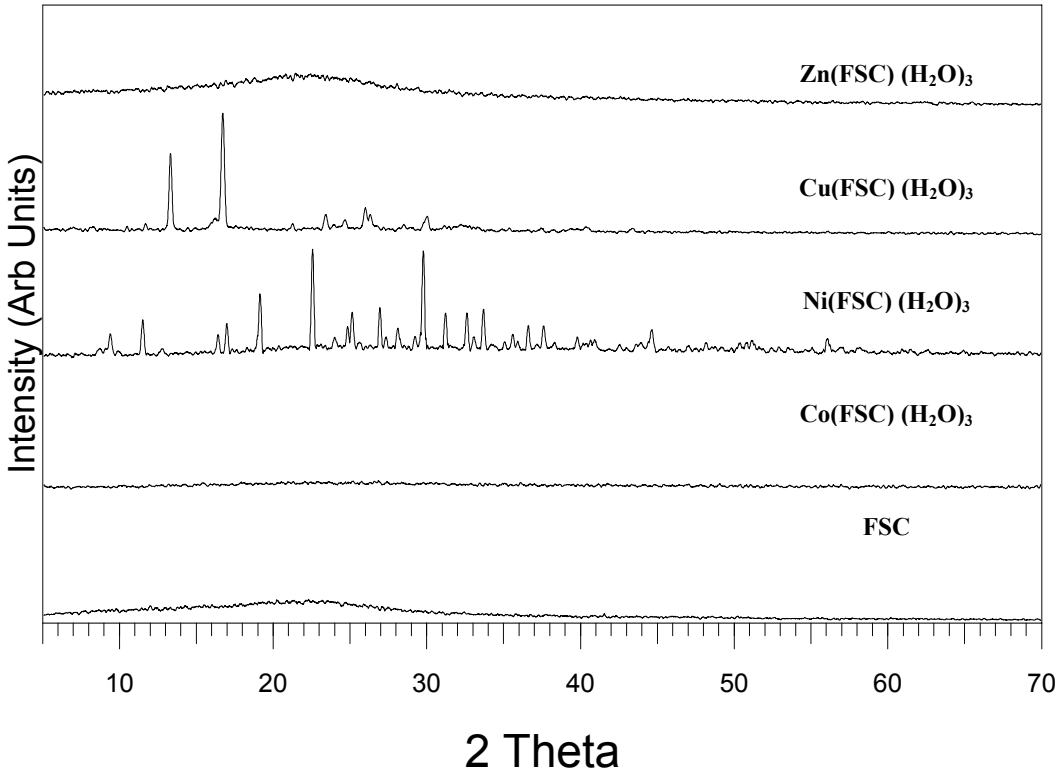

Figure 1. 6. 2 X-ray diffraction patterns of the ligand FSC and its metal complexes.

Based on these observations, the structure of the Co(II), Ni(II), Cu(II) and Zn(II) complexes of FSC can be confirmed to be octahedral. From all these studies, it is clear that the ligand acts as dianionic tridentate towards metal ion. Above discussion suggest the following structure for the complexes (figure 1.6.3).

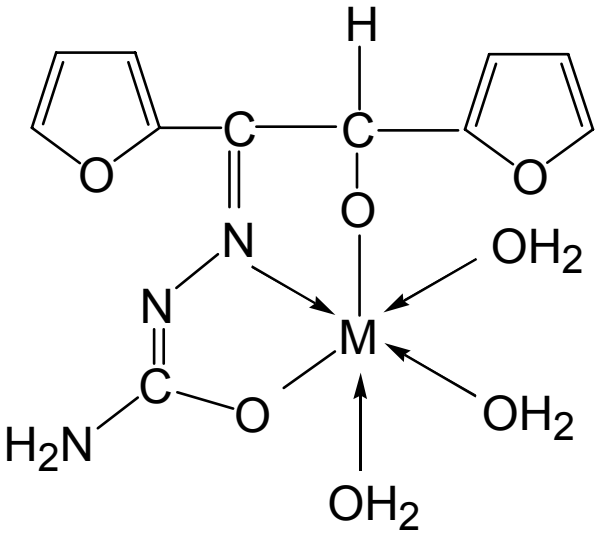

M= Co(II),Ni(II), Cu(II) and Zn(II)

Figure 1. 6. 3 Structure of metal complexes of FSC

REFERENCES

1. H. Schiff, Ann. Chem., 131 (1864) 118.
2. H. Schiff, Ann. Chem. Suppl., 3 (1864) 343.
3. H. Schiff, Ann. Chem., 150 (1869) 193.
4. H. Schiff, Ann. Chem., 151 (1869) 186.
5. A. F. Hotzclan Jr., J. P. Collman and R. M. Alire, J. Am. Chem. Soc., 80 (1958) 1100.
6. F. Lion and K. V. Martin, J. Inorg. Nucl. Chem., 26 (1964) 1577.
7. E. J. Olszewski, J. Inorg. Chem., 2 (1963) 661.
8. R. H. Holm, J. Am. Chem. Soc., 82 (1960) 5632.
9. P. J. M. C. Carthy, R. J. Hovey, K. Ueno and A.E Martell, J. Am. Chem. Soc., 77 (1955) 5820.
10. E. J. Olszewski and D. F. Martin, J. Inorg. Nucl. Chem., 26 (1964) 1577.
11. J. W. Smith, "The Chemistry of the Carbon Nitrogen Double bond", Interscience, New York (1970) 239.
12. R. H. Holm, G. W. Everett Jr and A. Chakravorthy, "Progress in Inorganic Chemistry", Ed. F. A. Cotton, Vol. 7, Interscience, NewYork (1966).
13. Y. Hamada, IEEE Trans. Electron Devices, 44, 8 (1997) 1208.
14. K. Kalyanasundaram and M. Gratzel, Coord. Chem. Rev., 77 (1998) 347-414.
15. C. B. Murray, D. J. Norris and M. G. Bawendi, J. Am. Chem. Soc., (1993) 8706.
16. A. W. Apblelf, G. D. Georgieva and J. T. Mague, Mat. Soc. Symp. Proc., 294 (1993) 123-128.

17. A. W. Apblelf, G. D.Georgieva, J.T. Mague and L. E. Reinardt, Ceram. Trans., 73 (1997) 105-112.
18. Z. Zhang, R. Liu, Mingzhao and Y. Qian, Mater. Chem. Phys., 71 (2001) 161-164.
19. P. Saravanan, S. Alam and G. N. Mathur, Mater. Lett., 58, 27-28 (2004) 3528-3531.
20. K. C. Emregul and O. Atakol, Mater. Chem. Phys., 83 (2004) 373–379.
21. H. A. Sorkhabi, B. Shaabani and D. Seifzadeh, Electrochemi. Acta, 50 (2005) 3446 -3452.
22. H. Shokry, M.Yuasa, I. Sekine, R. M. Issa, H. Y. El-baradie and G. K. Gomma, Corros. Sci., 40, 12 (1998) 2173-2186.
23. A. Dadgarnezhad, I. Sheikhoaie and F. Baghaei, Anti-Corros. Methods M, 51, 4(2004), 266-271.
24. K.C. Emregul, A. A. Akay and O. Atakol, Mater. Chem. Phys., 93 (2005) 325–329.
25. H. A. Sorkhabi, B. Shaabani and D. Seifzadeh, Appl. Surf. Sci., 239 (2005) 154-164.
26. A. Yurt, A. Balaban, S. U. Kandemir, G. Bereket and B. Erk, Mater. Chem. Phys., 85 (2004) 420-426.
27. M. N. Desai, M.B. Desai, C. B. Shah and S. M. Desai, Corros. Sci.**,** 26, 10 (1986) 827-837.
28. M. A. Quraishi, D. Jamal and M. Luqman, Indian J. Chem. Techn., 9 (2002) 479-483.
29. A. Aytac¸ U. Ozmen and M. Kabasakaloglu, Mater. Chem. Phys., 89 (2005) 176–181.
30. A. Bansiwal, P. Anthony and S. P. Mathur, British Corrosion Journal, 35, 4 (2000) 301-303.
31. M. N. Desai, M. M. Pandya, and G. V. Shah, Indian J. Techn., 19 (1981) 292-294.

32. I. Hamerton, B. J. Howlin and Peter Jepson, Coord. Chem. Rev., 224 (2002) 67-85.
33. Markovitz, U.S. Patent, 3812214 (1974).
34. P. V. Reddy and N. M. N. Gowda, J. Appl. Polym. Sci., 53 (1994) 1307.
35. J. D. B.Smith, J. Appl. Polym. Sci., 26,3 (1981) 979-986.
36. M. Anand and A. K. Srivastava, High Perf. Polym., 4 (1992) 97.
37. R. Dowbenko, C. C. Anderson and W. H. Chang, Ind. Eng. Chem. Prod. Res. Dev., 10 (1971) 344.
38. J. M. Barton, G. J. Buist, H. Hamerton, B. J. Howlin, J. R. Jones and S. Liu, J. Mater. Chem., 4 (1994) 379.
39. H. L. Parry, U S. Patent, 3301814 (1967).
40. N. Chantarisiri, T. Tuntulani, P. Tongraung, R. S. P. Magee and W. Wannarong, Eur. Polym. J., 36 (2000) 695.
41. N. Chantarasiri, T. Tuntulani, P. Tongraung and N. Chanma, Eur. Polym. J. 36(2000) 889.
42. Y. Aydogdu, F. Yakuphanoglu, A. Aydogdu, M. Sekerci, C. Alkan and I Aksoy, Mater. Lett**.,** 54 (2002) 352-358.
43. M. G. A. E. Wahed, A. M. Hassan and S. A. Hassan, J. of Mater. Sci. Lett., 12 (1993) 453- 454.
44. S. Sarkar, Y. Aydogdu, F. Dagdelen, B. B. Bhaumik and K. Dey, Mater. Chem. Phys., 88 (2004) 357–363.
45. M. G. A. E. Wahed, H. A. Bayoumi and M. I. Mohammed, Bull. Korean Chem. Soc., 24, 9 (2003) 1313-1318.
46. F. Yakuphanoglu, Y. Aydogdu, M. Gomleksiz, M. Sekerci, S. Agan and C. Alkan, Mater. Lett., 57 (2003) 2219– 2224.

47. H. Rakoff, W. F. Kwolek and L. E. Gast, J. Coating. Technol., (1978) 50-51.
48. J. H. Stoner, N. S. Baer and N. Indicator, J. Paint Technology, 47 (1975) 611.
49. F. R. Morral, "Kirk-Othmer Encyclopedia of Chemical Technology", Vol.6, Wiley, Newyork (1979) 495.
50. D. W. Locklin, Combustion, 51 (1980) 26.
51. K. C. Satpathy, H. P. Mishra and G. C. Prahgha, J. Indian Chem. Soc., 58 (1981) 844.
52. R. N. Kust, "Kirk-Othmer Encyclopedia of Chemical Technology", Vol.7, Wiley, New York (1979) 97.
53. M. C. Gokay, M. Soltanoalkotabi and L. A. Cross, J. Appl. Phys., 49 (1978) 4357.
54. A. M. Baklanov and B. Z. Gorbunov, J. Aerosol. Sci., 11 (1980) 495.
55. D. S. Rao and M. C. Ganorkar, J. Indian. Chem. Soc., 58 (1981) 217.
56. M. Kato and M.T. Hazu, J. Nucl. Med., 19 (1978) 397.
57. J. G. H. Du Preez, J. Coord. Chem., 13 (1984) 173.
58. R. H. Holm in "Inorganic Biochemistry", Editor G. L. Eichhom, Vol (II), Elsevier, Amsterdam (1973) 1137.
59. S. N. Dubey and B. K. Vaid, Synth. React. Inorg. Met. Org. Chem., 21, (1991) 1299.
60. A. M. Hendawy, E. G. Kourashy and M. M. Shanab, Polyhedron, 11 (1992) 523.
61. P. V. Marikutty, Ph. D Thesis, Calicut University, Kerala (2002).
62. U. C. Abdul Jaleel, Ph. D Thesis, Calicut University, Kerala (2005).
63. A. Syamal and K. S. Kala, Indian. J. Chem., 19A, 5 (1980) 488.
64. Tez Can, Chim. Acta. Turk., 12 (2) (1984) 376.

65. M. A. Salam, J. Bangladesh. Acad. Sci. (1992).

66. A. Syamal and M. M. Singh, Indian J. Chem. Sect. A, 32 (1993) 42-48.

67. M. A. Hassan, A. M. Khalifa and K. A. Shehata, Bull. Soc. Chim. Belg., 104 (3) (1995) 121-124.

68. V. V. Zelentsov, Russian J. Coord. Chem., 22, 9 (1996) 674-675.

69. A. Fehn, O. Briel and W. Beck, Chem. Ber. Recl., 130 (10) (1997) 1467-1473.

70. S. Mayadevi, K. K. Yusuff and Mohammed, Synth. React. Inorg. Met. Org. Chem., 27 (2) (1997) 319-330.

71. S. Naik, J. Indian. Coun. Chem. 15 (1) &(2) (1998) 7-9.

72. Chae Hee-Nam and C. Yong-Kook, J. Korean Chem. Soc., 42 (4) (1998) 422-431.

73. B. H. Mehta, Desai and Yogita, Orient. J. Chem., 15(1) (1999) 139-142.

74. A. Z. Sonbati and A. A. Bindary, Pol. J. Chem. 74 (5) (2000) 621-630.

75. M. Saidul Islam, M. A. Farooque, M. A. K. Bodruddoza, M. A. Mosaddik and M. S. Alam, J. Biol. Sci., 1 (8) (2001) 711-713.

76. N. Raman, A. Kulandaisamy and K. Jeyasubramanian, Synth. React. Inorg. Met. Org. Chem., Nano. Met. Chem., 31, 7 (2001) 1249–1270.

77. N. Raman, A. Kulandaisamy, C. Thangaraja and K. Jeyasubramanian, Trans. Meta. Chem., 28, 1 (2003) 29-36.

78. G. B. Minu, L. K.Wah, A. Dosieah, M. Ridana, O. Ramalingam and D. Lacour, Syn. Reac. Inorg. Met. Org. Chem., 34 (2004) 1-16.

79. A. Majumder, G. M. Rosair, A. Mallick, N. Chattopadhyay and S. Mitra, Polyhedron, 25, 8 (2006) 1753-1762.

80. B. H. Mehta and Rodrigues, Natl. Acad. Sci. Lett., 13, 9 (1990) 337-339.

81. C. Natarajan and C. D. Sheela, Indian. J. Chem., Sect. A, 30A (4) (1991) 357-362.

82. V. K. Varshney and Ambwani, J. Inst. Chem., 63 (6) (1991) 221-222.

83. F. Nighat and R. V. Singh, Phosphorous, Sulphur, Silicon, Relat. Elem.,104 (1-4) (1995) 53-62.

84. A. Periakaruppan, Transition Met. Chem., 22 (2) (1997) 167-171.

85. Bouwman, Elisabeth and Henderson, J. Chem. Soc., Dalton Trans., 20 (1998) 3495-3500.

86. A. A. Soliman and W. Linert, Thermochim. Acta., 338 (1-2) (1999) 67-75.

87. R. K. Parihari, R. K. Patel and R. N. Patel, J. Indian Chem. Soc., 76, 5 (1999) 258-259.

88. K. Sorasaenee, J. R.G. Mascaros, and K. R. Dunbar, Inorg. Chem., 41, 2 (2002) 433-436.

89. R. A. Eikey and M. M. Abu-Omar, Coord. Chem. Rev., 243, 1 (2003) 83-124.

90. S. Brooker, S. Iremonger and P. G. Plieger, Polyhedron, 22, 5 (2003) 665-671.

91. A. A. Soliman and G. G. Mohamed, Thermochim. Acta, 421, 1 (2004) 151-159.

92. M. M. H. Khalill, M. M. Aboaly and R. M. Ramadan, Spectrochim. Acta., Part A, 61 (2005) 157–161.

93. P. K. Pragnesh, P. M. Hitesh, P.B. Pramod and P. N. Mohan, J. Enym. Inhib. Med. Ch., 21, 2 (2006) 203-209.

94. H. Temel, H. Alp, S. Ilhan, B. Ziyadanogulları and I. Yılmaz, Monatsh. Chem., 138, 12 (2007) 1199-1209.

95. R. Panico, W. H. Powell and J. C. Richer (Eds.), IUPAC Nomenclature of Organic Compounds, Blackwell, London (1993) 105.

96. D. X. West, S. B. Padhye and P. B. Sonawane, Struct. Bond., 76 (1991)1

.

97. R. B. Singh and H. Ishii, Crit. Rev. Anal. Chem., 22 (1991) 381.

98. S. N. Pandeya and J. R. Dimmock, Pharmazie., 48 (1993) 659.

99. F. H. Allen, O. Kennard and R. Taylor, Acc. Chem. Res. 16 (1983) 146.

100. J. S. Casas, M. S. Garcia-Tasende and J. Sordo. Coord. Chem. Rev., 290 (2000) 197-261.

101. G. Ibrahim, G. M. Bouet, I. H. Hall and M. A. Khan, J. Inorg. Biochem., 81, 1-2 (2000) 29.

102. N. C. Kasuga, K. Sekino, C. Koumo, N. Shimada, M. Ishikawa and K. Nomiya, J. Inorg. Biochem., 84, 1 (2001) 55-65.

103. J. Patole, S. Dutta, S. Padhye and E. Sinn, Inorg. Chim. Acta., 318,1-2 (2001) 207-211.

104. A. Para and S. Awa, Carbohydrate Polym., 48, 1 (2002) 55-60.

105. P. F. Lee, C. T. Yang, D. Fan, J. J. Vittal and J. D. Ranford, Polyhedron, 22, 20 (2003) 2781-2786.

106. N. C. Kasuga, K. Sekino, M. Ishikawa, A. Honda, M. Yokoyama, S. Nakano, N. Shimada, C. Koumo and K. Nomiya, J. Inorg. Biochem. 96, 2-3 (2003) 298-310.

107. F. J. Barros-Garcia, F. Luna-Giles, M. A. Maldonado-Rogado and E. Vinuelas-Zahinos, Polyhedron 24, 18 (2005) 2972-2980.

108. A. P. Rebolledo, O. E. Piro, E. E. Castellano, L. R. Teixeira, A. A. Batista and H. Beraldo, J. Mole. Stru., 794, 1 (2006) 18-23.

109. V. M. Leovac, L. S. Jovanovic, V. S. Jevtovic, G. Pelosi and F. Isceglie, Polyhedron, 26, 13 (2007) 2971-2978.

110. S. Chandra and A. Kumar, Spectrochimica Acta. A, 66, 4-5 (2007) 1347-1351.

111. U. L. Kala, S. Suma, M. R. P. Kurup, S. Krishnan and R. P. John, Polyhedron, 26, 7 (2007) 1427-1435.

112. M. J. M. Campbell, Coord. Chem. Rev., 15 (1975) 279.

113. K. Joby Thomas, Ph. D Thesis, Calicut University, Kerala (1995).

114. M. Akbar Ali and S. E. Livingstone, Coord. Chem. Rev., 13 (1974) 101.

115. S. E. Livingstone, Q. Rev. Chem. Soc., 19 (1965) 386.

116. J. V. Martinez, C. L. Cabrera and J. G. Lara, Afinidad, 42 (399) (1985) 487.

117. R. K. S. Sharma and S. K. Sindhwani, Indian J. Chem., 26A (1987) 82.

118. M. B. Ferrari, G. G. Fava, C. Pelizzi, G. Pelosi and P. Tarasconi, Inorg. Chim. Acta., 269, 2 (1998) 297-301.

119. M. B. Ferrari, G. G. Fava, E. Leporati, G. Pelosi, R. Rossi, P. Tarasconi, R. Albertini, A. Bonati, P. Lunghi and S. Pinelli, J. Inorg. Biochem., 70, 2 (1998) 145-154.

120. M. B. Ferrari, F. Bisceglie, G. P. Pelosi, P. Tarasconi, R. Albertini, A. Bonati, P. Lunghi and S. Pinelli, J. Inorg. Biochem., 83, 2 (2001)169-179.

121. M. B. Ferrari, S. Capacchi, G. Reffo, G. Pelosi, P. Tarasconi, R. Albertini, S. Pinelli and P. Lunghi, J. Inorg. Biochem., 81,1 (2000) 89-97.

122. M. B. Ferrari, S. Capacchi, F. Bisceglie, G. Pelosi and P. Tarasconi Inorg. Chimi., 312, 1-2 (2001) 81-87.

123. M. B. Ferrari, G. G. Fava, G. Pelosi and P. Tarasconi, Polyhedron, 19, 16 (2000) 1895-1901.

124. M. B. Ferrari, C. Pelizzi, G. Pelosi and M. C. R. Arguelles, Polyhedron, 21, 25-26 (2002) 2593-2599.

125. M. L. Duran, A. Sousa, J. Romero, A. Castineiras, E. Bermejo and D. X. West, Inorg. Chim. Acta., 294, 1-2 (1999) 79-82.

126. A. Diaz, R. Pogni, R. Cao and R. Basosi, Inorg. Chimi. Acta., 275-276 (1998) 552-556.

127. Q. X. Li, H. A Tang, Y. Z. Li, M. Wang, L. F. Wang and C. G. Xia, J. Inorg. Biochem., 78, 2 (2000) 167-174.

128. D. X. West, J. K. Swearingen, J. V. Martinez, S. H. Ortega, A. K. El-Sawaf, F.V. Meurs, A. Castineiras, I. Garcia and E. Bermejo, Polyhedron, 18, 22-24 (1999) 2919-2929.

129. K. A. Ketcham, I. Garcia, J. K. Swearingen, A. K. El-Sawaf, E. Bermejo, A. Castineiras and D. X. West, Polyhedron, 21,15 (2002) 859-865.

130. A. Castineiras and D. X. West, J. of Molecular Structure, 604, 2-3 (2002) 113-118.

131. E. Labisbal, A. Sousa-Pedrares, A. Castineiras, J. K. Swearingen and D. X. West, Polyhedron, 21, 16 (2002) 1553-1559.

132. E. Labisbal, K. D. Haslow, A. Sousa-Pedrares, J. V. Martinez, S. H. Ortega and D. X. West, Polyhedron, 22, 20 (2003) 2831-2837.

133. L. Alsop, A. R. Cowley, J. R. Dilworth, P. S. Donnelly, J. M. Peach and J. T. Rider, Inorg. Chimi. Acta., 358, 9 (2005) 2770-2780.

134. S. Sharma, F. Athar, M. R. Maurya, F. Naqvi and A. Azam, European J. Medicinal Chem. 40, 6 (2005) 557-562.

135. Z. Afrasiabi, E. Sinn, W. Lin, Y. Ma, C. Campana and S. Padhye, J. Inorg. Biochem., 99, 7 (2005) 1526-1531.

136. A. Sreekanth and M. R. P. Kurup, Polyhedron, 22, 25-26 (2003) 3321-3332.

137. V. Philip, V. Suni, M. R. P. Kurup and M. Nethaji, Polyhedron, 23, 7 (2004) 1225-1233.

138. M. Joseph, M. Kuriakose, M. R. P. Kurup, E. Suresh, A. Kishore and S. G. Bhat, Polyhedron, 25, 1 (2006) 61-70.

139. E. B. Seena and M. R. P. Kurup, Polyhedron, 26, 4 (2007) 829-836.

140. D. K. Demertzi, P. N. Yadav, J. Wiecek, S. Skoulika, T. Varadinova and M. A. Demertzis, J. Inorg. Biochem., 100, 9 (2006) 1558-1567.

141. V. M. Leovac, L. S. Jovanovic, V. Divjakovic, A. Pevec, I. Leban and T. Armbruster, Polyhedron, 26, 1 (2007) 49-58.
142. Yu-Qing, D. J. Hua, Z. L. Gang, Z. X. Qing, B. H. Dong and L. Hong, J. Molecular Structure, 794, 1-3 (2006) 71-76.
143. E. M. Jouad, G. Larcher, M. Allain, A. Riou, G. M. Bouet, M. A. Khan and X. D. Thanh, J. Inorg. Biochem., 86, 2-3 (2001) 565-571.
144. S. Chandra and U. Kumar, Spectrochimica Acta Part A, 62, 4-5 (2005) 940-944.
145. S. Chandra and U. Kumar, Spectrochimica Acta Part A, 60, 12 (2004) 2825-2829.
146. S.Chandra and U. Kumar, Spectrochimica Acta Part A, 61, 1-2 (2005) 219-224.
147. S. Chandra and X. Sangeetika, Spectrochimica Acta Part A, 60, 1-2 (2004) 147-153.
148. B. H. Mehta and B. S. Nagarkoti, Asian. J. Chem., 12, 3 (2000) 853-856.
149. A. S. M. Mahmoud, J. King Soud University, Science, 9 (2) (1997) 189-199.
150. K. M. Daoud, M. A. Mohammed and M. A. Fattah, J. Indian Chem. Soc., 67 (1990) 896-870.
151. A. Weissberger, D. S. Proskauer, J. A. Riddick and E.Troops, "Organic solvents", Interscience, New York, 2 (1956).
152. A. I. Vogel, "A Text Book of Quantitative Inorganic Analysis", ELBS and Longman, London (1962).
153. B. N. Figgis and J. Lewis, "Progress in Inorganic Chemistry", Vol.6, Inter Science, New York (1964).
154. A. Earnshaw, E. A. King and L. K. Larkworthy, J. Chem. Soc., Sect. A, (1968) 1048.
155. B. N. Figgis and R. S. Nyholm, J. Chem. Soc., (1959) 388.
156. W. J. Geory, Coord. Chem. Rev., 7 (1971) 81.

157. J. Lewis and R. G. Wilkins, “The Magneto Chemistry of Complex Compounds in Coordination Chemistry”, Interscience, NewYork (1969).
158. A. Earnshow, “Introduction to Magneto Chemistry”, Academic Press, London, 1968.
159. B. N. Figgis and R.S. Nyholm, J. Amer. Chem. Soc., (1958) 4190.
160. R. K. Mahapatra, B. K. Mahapatra and S. Guru, J. Inorg. Nucl. Chem., 39 (1997) 2281.
161. N. B. Colthup, L. H. Daly and S. EWiberly, “Introduction to Infrared and Raman Spectroscopy”, Academic Press, New York, 2nd Ed., (1975).
162. R. Ferrare, “Low Frequency Vibrations of Inorganic and Coordination Compounds”, Plenum Press, New York (1971).
163. N.S. Biradar and V. H. Kulkurni,Z. Inorg. Ally. Chem., 387 (1972) 275.
164. R. C. Sharma and C. C. Patel, Indian J. Chem., 8 (1970) 747.
165. Koji Nakanishi, Infrared Absorption Spectroscopy”, Holden Day Inc. SanFrancisco, 1962.
166. K. Nakamato, “Infrared Spectra of Inorganic and Coordination Compounds”, John Wiley, New York (1966).
167. L. J. Bellamy, “The Infrared Spectra of Complex Molecule”, Chapman and Hall, London (1978).
168. Sutton, “Electronic Spectra of Metal Complexes”, McGraw Hill, London (1968).
169. K. Jorgensen, Acta. Chem. Scand., 10 (1956) 887.
170. A. Saaco, F. A. Cotton, J. Am. Soc., 84 (1962) 2043.
171. B. P. Lever, “Inorganic Electronic Spectroscopy”, Elsevier, London (1968).
172. O. Turkoglu, M. Soylak and I. Belenli, Collect. Czech. Chem. Commun., 68 (2003) 1233-1242.

PART II

THERMOGRAVIMETRIC ANALYSIS

CHAPTER 1
INTRODUCTION

Nowadays the thermal analysis techniques like TGA, DTA, DSC etc. play an important role in studying the structure and properties of metal complexes[1-7]. Liptay reports[8] about the frequency of thermal analytical investigation during the period 1975-1987. The compounds studied are most often inorganic and coordination compounds. Between 15-20% of the contributions in the Journal of Thermal analysis in the last decade referred to the thermal behavior of coordination compounds. Numerous transition metal complexes are of special interest in industry, medicine and biology. Up till now a number of solid-state reactions of coordination compounds such as thermal summarization, conformational changes, polymeric transformations, thermal phase transitions, thermochromism were studied and increasingly enter into the scientific basis of coordination chemistry[9-13]. The above uses and reactions are related to room temperature structures of the compounds as well as their thermal stability.

Thermal analysis is a group of techniques in which a physical property of a substance or its reaction products is measured as a function of temperature, whilst the substance is subjected to controlled temperature program[14]. Depending upon the properties measured and temperature

programs, more than a dozen thermal methods can be recognized. We shall confine our discussion to thermogravimetric method, which provide primarily chemical rather than physical information about samples. This technique can be used to study the kinetics of chemical reaction and determine basic kinetic constants such as the rate constant, activation energy, order of reaction, frequency factor etc.

Thermogravimetry

Thermogravimetry is a technique in which the mass of the substance, in an environment heated or cooled at a controlled rate, is recorded as a function of temperature[15]. The resulting mass change versus temperature curve give information concerning the thermal stability and composition of the initial sample, the thermal stability and composition of any intermediate compounds that may be formed and the composition of the initial sample and the compositions of the residue, if any. The analytical instrument used is a thermobalance with a furnace programmed for a linear rise of temperature with time. The books by Duval[16], Smoothers and Yao Chiang[17], Mackenzic[14], Schulze[18] and Garn[19] describes in detail the principle, instrumentation and application of thermal analysis.

Thermogravimetric method can be applied for the study of various reactions such as

1. Decomposition reaction of the type

$$A_{(Solid\ phase)} \longrightarrow B_{(Solid\ phase)} + C_{(Gas\ phase)}$$

2. Reaction between two solid substances

$$A_{(Solid\ phase)} + B_{(Solid\ phase)} \longrightarrow C_{(Solid\ phase)} + D_{(Gas\ phase)}$$

3. Reaction between a solid and a gas

$$A_{(Solid\ phase)} + B_{(Gas\ phase)} \longrightarrow C_{(Solid\ phase)}$$

4. The transition of a solid or a liquid substance to a gas

$$A_{(Solid\ phase)} \text{ or } A_{(Liquid\ phase)} \longrightarrow B_{(Gas\ phase)}$$

When the kinetic study is based on the observation of the weight change, two approaches are possible in principle viz., the isothermal (static) and non isothermal (dynamic heating) methods.

Dynamic or Non isothermal methods

The non isothermal method is the determination of the degree of transformation as function of time during a linear increase of temperature compared with static method. Advantage of non isothermal method over isothermal method is that it requires a smaller number of experimental data and the kinetic parameters may be determined from a single thermogravimetric curve for the whole temperature range.

In general there are two approaches for the evaluation of kinetic parameters of thermal decomposition reaction under isothermal conditions [20].

1. A general kinetic study, which is the simple extension of homogeneous kinetics to solid kinetics, usually heterogeneous.

2. A mechanism based study which gives the physicochemical description of the process.

The foundation of calculation of kinetic data from a TG curve is based on the kinetic equation

$$-dx / dt = k\, x^n \qquad (1)$$

where x is the amount of the sample undergoing reaction, n is the order of reaction and k is the specific rate constant. The temperature dependence of the specific rate constant k is expressed by the Arrhenius equation

$$k = A\, e^{-E/RT} \qquad (2)$$

where A is the pre exponential factor, E is the activation energy, R is the Universal gas constant and T is the absolute temperature. The mathematical treatment of kinetic equations makes use of one of the following three methods of evaluation i) differential method ii) integral method iii) approximation method.

The relationship of x to mass loss w is given by the equation:

$$-dx = m_0\, (dw / w\alpha) \qquad (3)$$

Where m_0 is the initial mass of the sample, and $w\alpha$ is the maximum mass loss. By integration of the left hand side of equation (3) from m_0 to x and by the integration of the right hand side of the equation from zero to w the following equation is obtained

$$x = m_0\, (w\alpha - w) / w\alpha \qquad (4)$$

By substitution of equations (4) and (2) in equation (1) and by differentiating the logrithametic form, an expression is obtained, which is one of the differential methods. Integral methods use the integrated form of the equation (1) after the transportation of the mass loss w, in equation (3) and (4).

Integral methods using Coats-Redfern Equation [21-22]

Integral methods are generally considered to be more accurate as they give quite reliable values. The disadvantages are (1) prior determination of n is required and (2) temperature integral has to be approximated. This method considers that in the reaction

$$aA_{(s)} \longrightarrow bB_{(s)} + C_{(g)}$$

The rate of disappearance of A may be expressed as

$$d\alpha / dt = k (1-\alpha)^n \qquad (5)$$

where α is the fraction of A decomposed at a time t, wα is the maximum mass loss, n is the order of reaction and k is the rate constant. By combining equations (2) and (5) rearranging and integrating at a constant heating rate $\Phi = \frac{dT}{dt}$, we obtain

$$\int_0^{\alpha} d\alpha / (1-\alpha)^n = A/\Phi \int_0^{T} \exp(-E/RT)dT \qquad (6)$$

The left hand side of this equation (6) has two different solutions depending on the value of 'n' namely

$$1-(1-\alpha)^{1-n} / (1-n)T^2 \quad \text{for } n \neq 1 \qquad (7)$$

and $$-\log(1-\alpha)/T^2 \quad \text{for n = 1} \tag{8}$$

In both cases, the right hand side of equation (6) has the solution

$$ART^2/\Phi E(1-2RT/E)\exp(-E/RT) \tag{9}$$

The following two equations are obtained after taking logarithms.

For n#1,

$$\log\left[1-(1-\alpha)^{1-n}/T^2(1-n)\right]=\log\left[AR/\Phi E(1-2RT/E)\right]-E/2.303RT \tag{10}$$

and

$$\log[-\log(1-\alpha)/T^2]=\log[AR/\Phi E(1-2RT/E)]-E/2.303RT \quad \text{for n=1} \tag{11}$$

In ordinary thermal decomposition reactions, $\log\left[AR/\Phi E(1-2RT/E)\right]$ is practically constant and plots of $\log\left[1-(1-\alpha)^{1-n}/T^2(1-n)\right]$ vs. 1/T for $n \neq 1$ and $\log[-\log(1-\alpha)/T^2]$ vs. 1/T for n = 1 respectively result in a straight line with slope of -E / 2.303R for correctly chosen value of n. Using this value of 'n' the kinetic parameters were calculated based on the non-mechanistic integral equations.

$$\ln\left[1-(1-\alpha)^{1-n}/(1-n)T^2\right]=\ln\left[AR/\Phi E(1-2RT/E)\right]-E/RT \tag{12}$$

Since $\ln\left[AR/\Phi E(1-2RT/E)\right]$ is sensibly a constant, a plot of left hand side of the above equation (12) against 1/T was drawn, E was calculated from the slope and A from the intercept of the linear plot. The entropy of activation was obtained from the equation.

$$A=\frac{kT_s}{h}\exp\frac{\Delta s}{R}$$

where, k = Boltzman constant

h = Plank's constant

T_s = peak temperature.

Scope of present investigation

In this part, the results of studies on the thermal decomposition of Co(II), Ni(II), Cu(II) and Zn(II) complexes of FATP and Cu(II) and Zn(II) complexes of FAP, FTSC and FSC using TG are presented.

From the TG curves, the temperature regions of stability have been noted. The temperature of inception and decomposition and the temperature of maximum rate of decomposition have been noted. The thermal stability and the decomposition stages of complexes have been discussed.

The non isothermal TG curves have been subjected to mathematical analysis using the integral method of Coats-Redfern[23] and the activation parameters have been evaluated for all the complexes.

CHAPTER 2
MATERIALS, METHODS AND INSTRUMENTS

Materials

Analar grade chemicals supplied by Sigma Aldrich and E-Merck were used for the synthetic purpose. Commercial solvents were distilled by standard methods. Detailed description regarding the reagents and their purity are given in part I.

Methods

Co(II), Ni(II), Cu(II) and Zn(II) complexes of furoin-2-aminothio-phenol(FATP) and Cu(II) and Zn(II) complexes of furoin-2-aminophenol (FAP), furoin thiosemicarbazone (FTSC) and furoin semicarbazone (FSC) were prepared by the methods described in the Part I. The thermogravimetric data was recorded using 2-5 mg of samples at a constant heating rate of 10 or 15°C/min in flowing air or oxygen atmospheres using thermal analyzer. The final products were subjected to X- ray powder diffraction analysis to confirm the final product of decomposition. Computational work was done using personal computer with Microsoft Excel program.

Instruments

Perkin Elmer make Pyris Diamond model thermal analyzer and AXS Bruker Germany make D5005 model X-ray diffractometer was used for this study.

CHAPTER 3
THERMAL DECOMPOSITION KINETICS OF METAL COMPLEXES OF FATP, FAP, FTSC AND FSC

The review of Donia[24] gives the survey of thermal behavior of large number of transition metal complexes and relation between their structural properties and thermal stability. A study of thermal decomposition of Schiff base complexes of Co(II) and Cu(II) has been reported by Bhaskare and More[25]. Wendlandt and co-workers[26-29] and Hill and co-workers[30,31] have studied the thermal properties of metal chelates with different types of complexing agents. Aravindakshan and Muraleedharan have studied the thermal stabilities of metal chelates with azomethine group[32]. Considerable work has been done on the thermal decomposition kinetics of transition metal complexes of Schiff bases and related ligands by Geetha Parameswaran and co-workers[33-36]. Soliman and Linert carried out the thermogravimetric analysis of transition metal chelates of Schiff base, 3-methoxy-salicylidene-2-aminothiophenol and calculated thermodynamic parameters of decomposition[37]. Rodembusch[38] studied the thermogravimetric analysis of four benzoxazole metal complexes, used in organic light emitting diodes and

found that these materials are highly thermostable with melting point above 360°C.

In this chapter, results of thermal decomposition studies on transition metal complexes of FATP, FAP, FTSC and FSC are presented. The kinetic parameters like energy of activation E, pre exponent factor A and entropy of activation ΔS of the decomposition reactions were calculated based on Coats-Redfern kinetic equation.

Treatment of data

Co(II), Ni(II), Cu(II) and Zn(II) complexes of FATP

The instrumental TG curves of complexes were redrawn as weight percentage verses temperature. The TG traces of Co(II), Ni(II), Cu(II) and Zn(II) complexes of FATP are given in figures 2.3.1 to 2.3.4. The temperature ranges, peak temperature, probable assignments and total mass loss from TG curves of Co(II), Ni(II), Cu(II) and Zn(II) complexes of FATP are presented in the tables 2.3.1 to 2.3.4. The kinetic parameters calculated using Coats-Redfern equation is summerised in table 2.3.8.

Cu (II) and Zn(II) complexes of FAP, FTSC and FSC

The TG traces of Cu(II) and Zn(II) complexes of FAP, FTSC and FSC are given in figures 2.3.5 to 2.3.10. The temperature ranges, peak temperature, probable assignments and total mass loss from TG curves of

Cu(II) and Zn(II) complexes of FAP, FTSC and FSC are summerised in the tables 2.3.5 to 2.3.7 respectively. The Kinetic parameters calculated using Coats-Redfern equation are given in table 2.3.8.

Results and discussion

The metal percentage from independent pyrolytic experiments and from thermal studies was found to be agreeable with the calculated values in the case of all studied metal complexes. The thermal data have supported the structure of complexes as $[M(L)(H_2O)_3]$ where M = Co(II), Ni(II), Cu(II) and Zn(II) and L = FATP, FAP, FTSC and FSC. In all the cases the final product of decomposition are identified to be oxides such as Co_3O_4, NiO, CuO and ZnO. The TG traces of complexes of FATP do not show any detectable change up to 100°C when heated, which suggests that there is no water of hydration. At around 150°C, a loss of mass is noted in all the complexes which can be attributed to the loss of coordinated water molecule according to Nikolaev[39].

Two stage decomposition pattern was observed for $[Co(FATP)(H_2O)_3]$. First stage of decomposition stands for the removal of three coordinated water and aminothiophenol part of the FATP ligand moiety. The second stage corresponds to the removal of furoin part of FATP. The overall weight loss from the curve is 79.47% while the theoretical weight loss during the decomposition of complex is 80.37% (Figure 2.3.1).

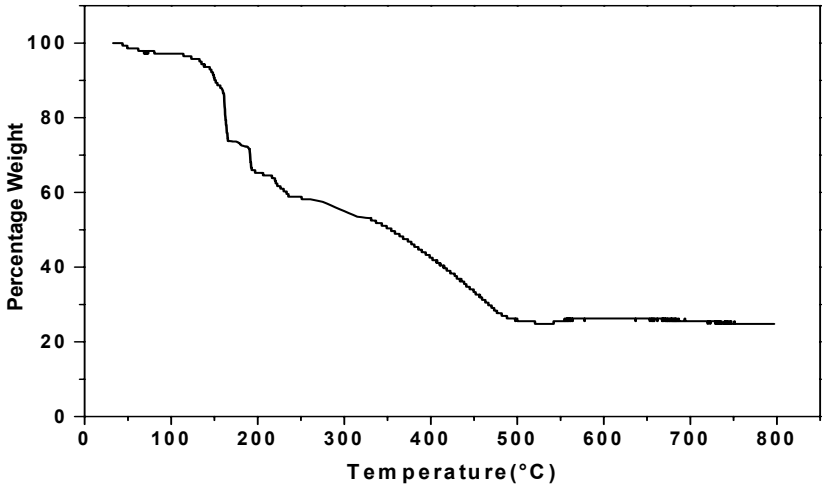

Figure 2. 3. 1 TG trace of Co(II) complex of FATP

Table 2. 3. 1 Thermal decomposition data of Co(II) complex of FATP

Complex	Stage	Temp. range TG (°C)	Peak Temp (°C)	Mass loss from TG (%)	Theoreti-cal mass loss (%)	Probable assignment
[Co(FATP) $(H_2O)_3$]	I	50-300	190	43.97	42.90	Loss of three molecules of water and part of FATP
	II	300-510	460	35.5	37.47	Loss of part of FATP and formation of oxide
				79.47	80.37	[Co (FATP) $(H_2O)_3$] → Co_3O_4

In the case of Ni(II) complex of FATP, three stage decomposition pattern is observed. In the first stage three molecules of water along with the phenol and N part of the FATP were removed. The second stage is attributed to the loss of sulphur and furoin part. The third stage stands for the loss of remaining FATP ligand moiety. The weight loss recorded in the TG, 82.25%, matches with the theoretical weight loss of 81.94%, corresponding to the conversion of $[Ni(FATP)(H_2O)_3]$ to NiO.

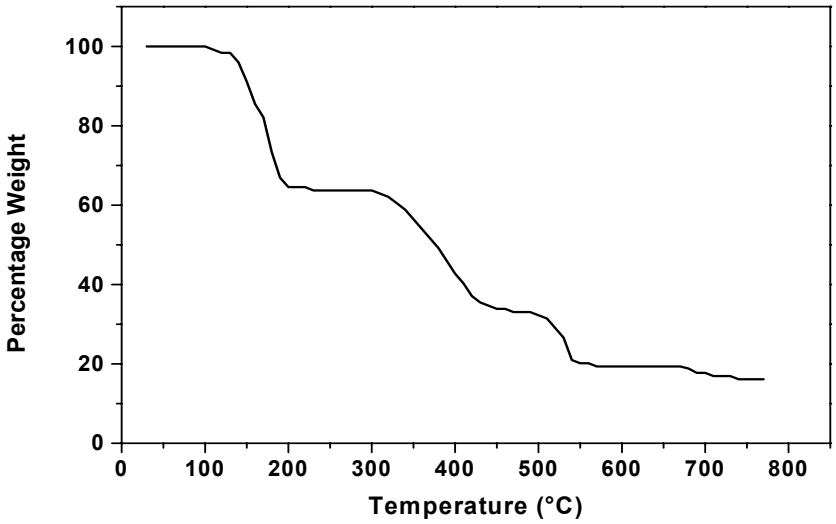

Figure 2. 3. 2 TG trace of Ni(II) complex of FATP

Table 2. 3. 2 Thermal decomposition data of Ni(II) complex of FATP

Complex	Stage	Temp. range TG (°C)	Peak Temp (°C)	Mass loss from TG (%)	Theo-retical mass loss (%)	Probable assignment
[Ni(FATP) $(H_2O)_3$]	I	110-200	180	35.48	35.12	Loss of three molecules of water and FATP part
	II	300-430	390	28.23	27.31	Loss of part of FATP
	III	430-710	540	18.54	19.51	Loss of part of FATP
				82.25	81.94	[Ni(FATP) $(H_2O)_3$]→NiO

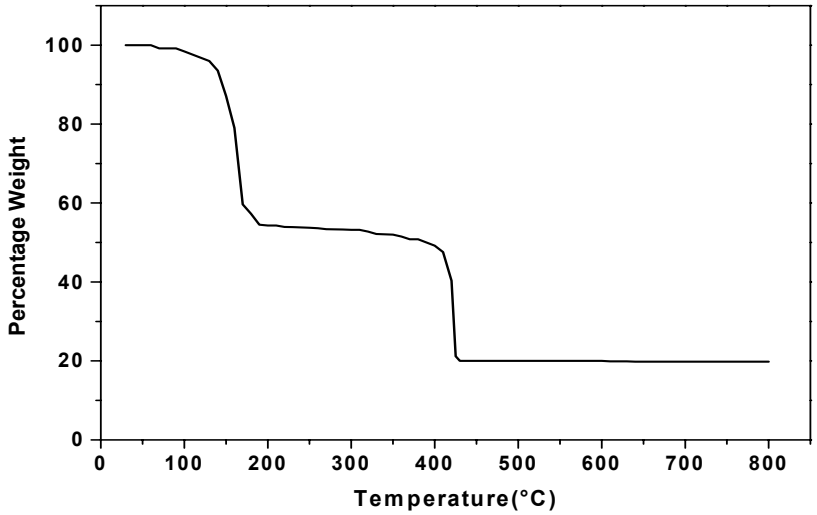

Figure 2. 3. 3 TG trace of Cu(II) complex of FATP

The decomposition pattern obtained for copper complex of FATP has two distinguishable stages. The first decomposition stage represents the loss of three molecules of coordinated water and aminothiophenol part of FATP. The intermediate formed was found to stable up to a temperature of 385°C. The second stage corresponds to the loss of the remaining part of the FATP ligand, i.e. furoin part. The theoretical percentage weight loss agreed well with observed percentage weight loss (Figure 2.3.3).

Table 2. 3. 3 Thermal decomposition data of Cu(II) complex of FATP

Complex	Stage	Temp range (°C)	Peak Temp (°C)	Mass loss from TG (%)	Theor-etical mass loss (%)	Probable assignment
[Cu(FATP)$(H_2O)_3$]	I	70-180	170	42.74	42.40	Loss of three molecules of water and FATP part
	II a	180-400		8.07	38.32	Loss of part of FATP
	II b	400-430	430	28.84		
				36.91		
				79.65	80.72	[Cu(FATP)$(H_2O)_3$]→CuO

Zn(II) complex of FATP also follows three stage decomposition pattern. In the first stage three molecules of water and part of aminothiophenol of FATP were removed. The second stages represent the loss of furoin rings of FATP. In stage three, removal of remaining part of FATP was occurred. The weight loss obtained for the conversion of complex to its metal oxide was 80.85% which is matching with the theoretical value of 80.39%.

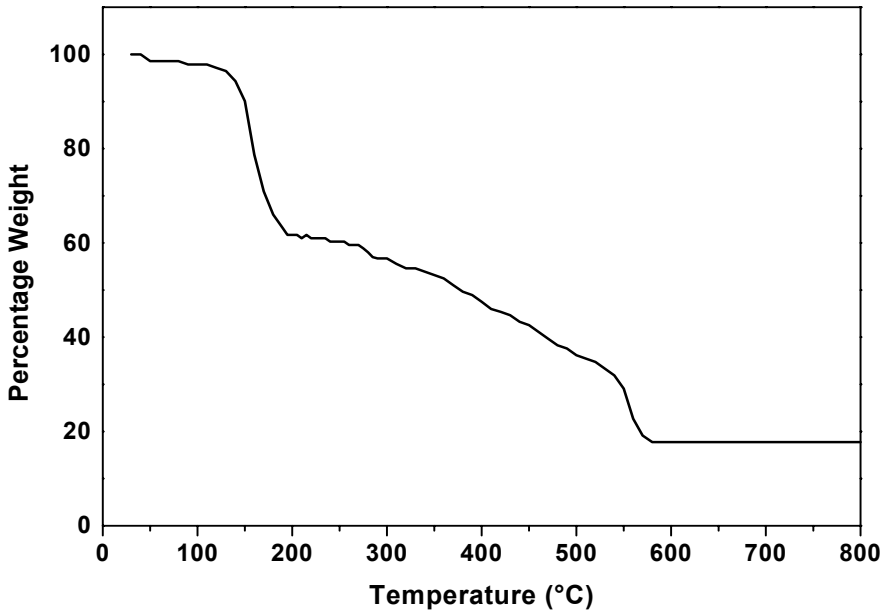

Figure 2. 3. 4 TG trace of Zn(II) complex of FATP

Table 2. 3. 4 Thermal decomposition data of Zn(II) complex of FATP

Complex	Stage	Temp range TG (°C)	Peak Temp (°C)	Mass loss from TG (%)	Theo-retical mass loss (%)	Probable assignment
[Zn(FATP) $(H_2O)_3$]	I	50-200	150	38.3	38.87	Loss of three molecules of water and part of FATP
	II	200-550	290	32.62	32.16	Loss of part of FATP
	III	550-570	550	9.93	9.36	Loss of part of FATP
				80.85	80.39	[Zn(FATP) $(H_2O)_3$] →ZnO

The metal percentage from independent pyrolytic experiments and thermal studies was found to be agreeable with the calculated values in the case of metal complexes of FAP. At around 150°C, a loss of mass is noted in the complexes of FAP which can be attributed to the loss of coordinated water molecule[39].

The decomposition pattern obtained for Cu(II) complex of FAP follows two stages. The first decomposition stage represents the loss of three molecules of coordinated water and part of furoin of FAP. The second stage

corresponds to the loss of remaining part of the FAP ligand. The theoretical percentage weight loss, 80.33% agreed well with observed percentage weight loss of 80.05%.

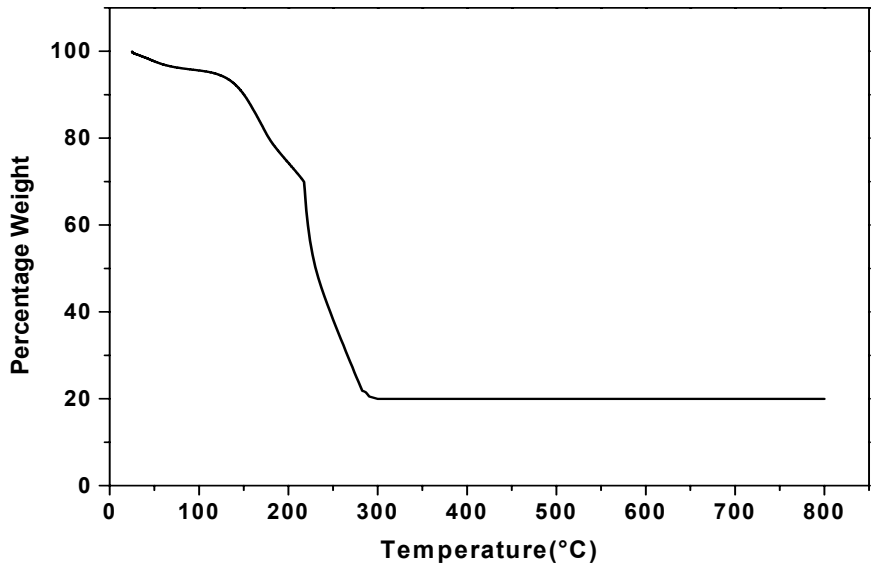

Figure 2. 3. 5 TG trace of Cu(II) complex of FAP

Zn(II) complex of FAP follows two stage decomposition pattern. In the first stage three molecules of water and part of aminophenol of FAP were removed. The second stage is assigned to the loss of furoin part of FAP. The weight loss obtained for the conversion of complex to its metal oxide was 80.89% which is matching with the theoretical value of 80.00% (Figure 2.3.6).

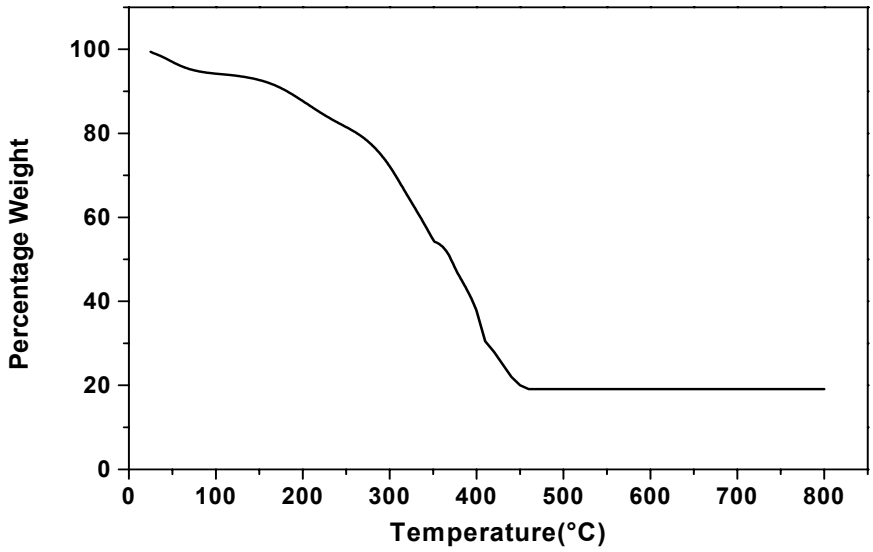

Figure 2. 3. 6 TG trace of Zn(II) complex of FAP

The metal percentages from independent pyrolytic experiments and thermal studies were found to be agreeable with the calculated values. Cu(II) and Zn(II) complexes of the FTSC do not show much weight loss up to 100°C. The loss of weight around 150°C in the Cu(II) and Zn(II) complexes of FTSC represents the loss of coordinated water.

Table 2. 3. 5 Thermal decomposition data of Cu(II) and Zn (II) complexes of FAP

Complex	Stage	Temp. range TG (°C)	Peak Temp (°C)	Mass loss from TG (%)	Theoretical mass loss (%)	Probable assignment
[Cu(FAP) $(H_2O)_3$]	I	30-220	220	31.84	30.49	Loss of three molecule of water and part of FAP
	II	220-300	230	48.21	49.84	Loss of part of FAP
				80.05	80.33	[Cu(FAP)$(H_2O)_3$]→CuO
[Zn(FAP) $(H_2O)_3$]	I	30-340	330	41.65	40.12	Loss of three molecules of water and part of FAP
	II	340-460	410	39.24	39.88	Loss of part of FAP
				80.89	80.00	[Zn(FAP)$(H_2O)_3$]→ ZnO

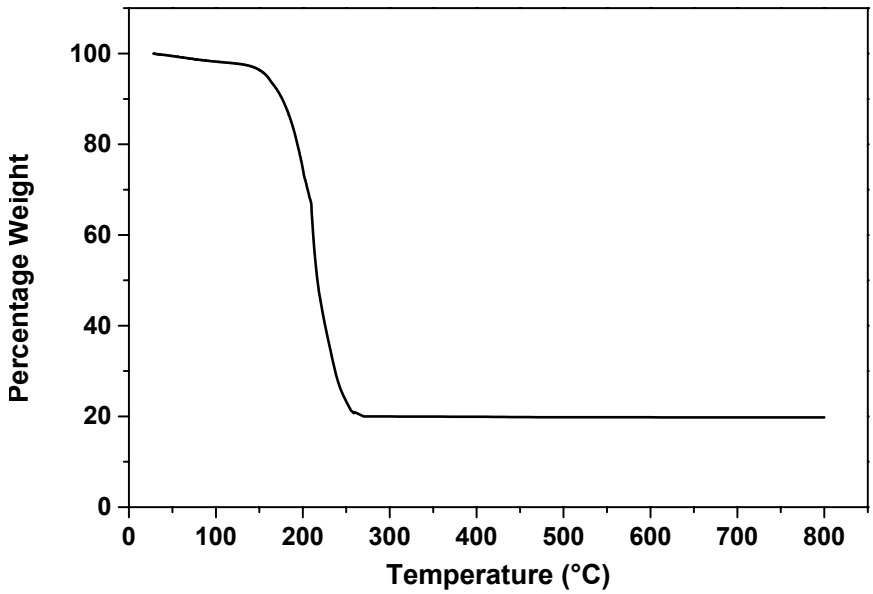

Figure 2. 3. 7 TG trace of Cu(II) complex of FTSC

The decomposition pattern obtained for Cu(II) complex of FTSC follows two major stages. In stage two, major weight loss of 76.12 % was occurred in between the temperature range 140-260°C. The stage two is subdivided into two, first being in the temperature range 140-210°C and second being 210-260°C. In the first part of stage two, coordinated water along with thiosemicarbazone part of FTSC are lost. In the second part, the remaining part of the FTSC ligand moiety is removed forming the CuO. A percentage weight loss of 79.30% was observed for the formation of CuO from $[Cu(FTSC)(H_2O)_3]$ against the theoretical value of 78.92%.

The decomposition of Zn(II) complex of FTSC follows two stages. First stage decomposition stands for the removal of three coordinated water and furoin part of the FTSC ligand. In the second stage the remaining part of the FTSC like thiosemicarbazone part was removed. The total weight loss of 79.42% was recorded against the theoretical weight loss of 78.96% for the formation of ZnO from the complex.

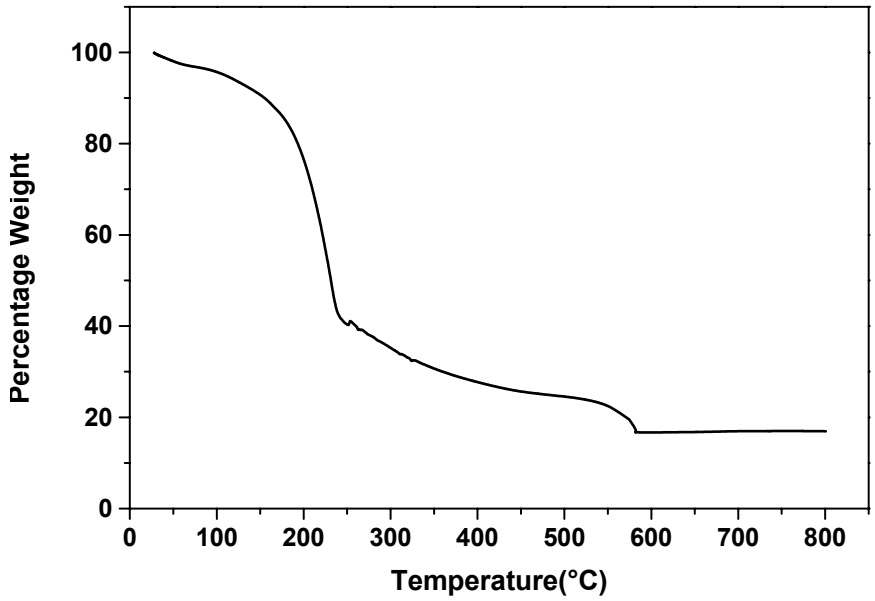

Figure 2. 3. 8 TG trace of Zn(II) complex of FTSC

Table 2. 3. 6 Thermal decomposition data of Cu(II) and Zn(II) complexes of FTSC

Complex	Stage	Temp. range TG (°C)	Peak Temp (°C)	Mass loss from TG (%)	Theoretical mass loss (%)	Probable assignment
$[Cu(FTSC)(H_2O)_3]$	I	30-140	130	2.80	4.73	Loss of one molecule of water
	II a	140-210	200	31.92	32.84	Loss of two molecules of water and part of FTSC
	II b	210-260	220	44.20	41.76	Loss of part of FTSC
				78.92	79.33	$[Cu(FTSC)(H_2O)_3] \rightarrow CuO$
$Zn(FTSC)(H_2O)_3]$	I	30-240	230	54.22	55.69	Loss of three molecule of water and part of FTSC
	II	240-580	240	25.20	23.27	Loss of part of FTSC
				79.42	78.96	$[Zn(FTSC)(H_2O)_3] \rightarrow ZnO$

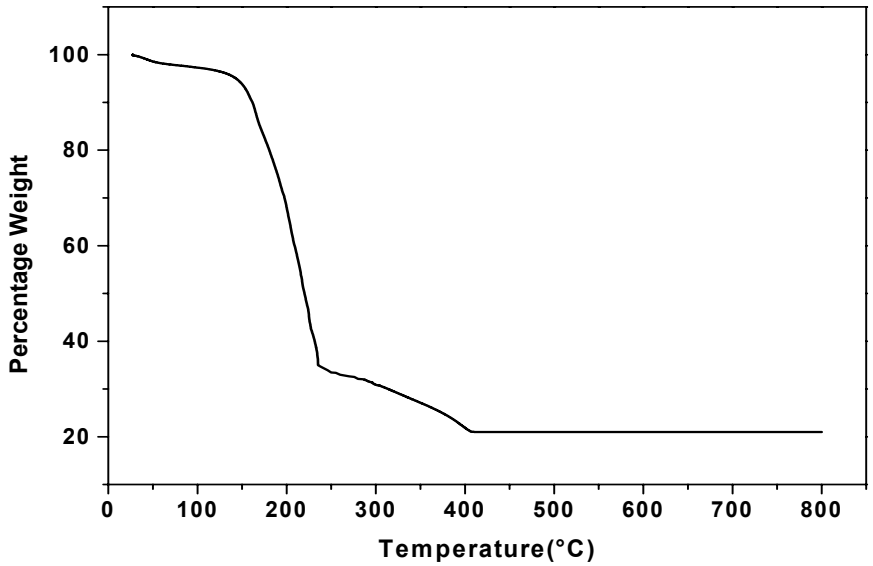

Figure 2. 3. 9 TG trace of Cu(II) complex of FSC

The metal percentage from independent pyrolytic experiments and thermal studies was found to be agreeable with the calculated values in the case of metal complexes of FSC. The final products of decomposition are identified to be oxides. The TG traces obtained for the Cu(II) complex of FSC has three distinct decomposition stages. The coordinated water along with the FSC ligand molecule is removed in the first two stages. In the last stage the remaining part of the ligand is removed and complex is converted in to the oxide i.e. CuO. The overall mass loss from the TG curve is 79.26% while the theoretical loss in mass for the conversion of $[Cu(FSC)(H_2O)_3]$ to CuO is 78.46%.

The TG curve of Zn(II) complex of FSC gives three stage decomposition pattern. The first stage represents the loss of three water molecule and part of semicarbazone. The second stage showing a weight loss of 46.25% corresponding to the loss of two furoin rings. In the last stage the remaining part of ligand is removed finally forming the ZnO. The percentage weight loss obtained from the TG curve matches with the calculated value for the conversion of Zn(II) complex to its oxide.

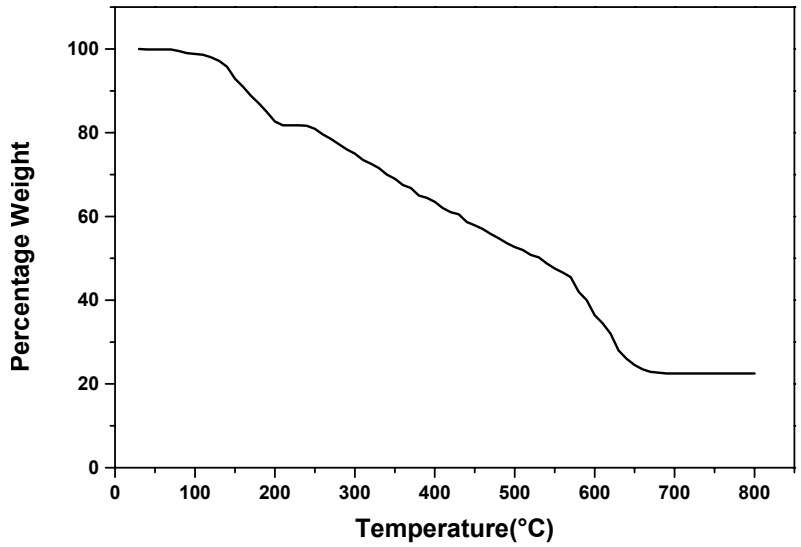

Figure 2. 3. 10 TG trace of Zn(II) complex of FSC

Table 2. 3 .7 Thermal decomposition data of Cu(II) and Zn(II) complexes of FSC

Complex	Stage	Temp. range TG (°C)	Peak Temp (°C)	Mass loss from TG (%)	Theoretical mass loss (%)	Probable assignment
$[Cu(FSC)(H_2O)_3]$	I	30-125	50	3.53	4.94	Loss of one molecule of water
	II	125-235	230	61.74	62.00	Loss of two molecules of water and part of FSC
	III	235-410	400	13.99	11.52	Loss of part of FSC
				79.26	78.46	$Cu(FSC)(H_2O)_3 \rightarrow CuO$
$[Zn(FSC)(H_2O)_3]$	I	30-210	150	18.25	19.11	Loss of three molecule of water and part of FSC
	II	210- 570	330	36.25	36.57	Loss of part of FSC
	III	570-690	610	23.0	22.38	Loss of part of FSC
				77.50	78.06	$Zn(FSC)(H_2O)_3 \rightarrow ZnO$

Decomposition kinetics

The values of activation energy, frequency factor, A, entropy of activation, ΔS and order parameter, n for the thermal decomposition of the Co(II), Ni(II), Cu(II) and Zn(II) complexes of FATP and Cu(II) and Zn(II) complexes of FAP, FTSC and FSC are given in the table 2.3.8.

The activation energies obtained for the decomposition stages of the complexes are comparable to those of coordination compounds of 3d transition metal having similar structure[40,41]. It is found that the higher the thermal stability of the complex, larger the activation energy for decomposition. The negative ΔS values of decomposition stages of the all the complexes show that the complexes are more ordered in the activated state than the reactants and the reactions are slower than normal.

Initial decomposition temperature and inflection temperature have been used to determine the thermal stability of metal chelates. In the present course of studies, based on observations made by earlier workers[41,42] the relative thermal stabilities of the metal chelates of FATP can be given as

$[Ni(FATP)(H_2O)_3]>[Co(FATP)(H_2O)_3]\approx[Cu(FATP)(H_2O)_3]$

$\approx [Zn(FATP)(H_2O)_3]$.

The relative thermal stabilities of the metal chelates of FAP, FTSC and FSC can be given as

$[Cu(L)(H_2O)_3] > [Zn(L)(H_2O)_3]$

where L = FAP, FTSC and FSC.

Table 2. 3. 8 Kinetic parameters for the decomposition of complexes of FATP, FAP, FTSC and FSC

Complex	Stage	E (k Cal/mol)	A (sec^{-1})	ΔS (e.u)	γ	Order (n)
$[Co(FATP)(H_2O)_3]$	II	2.308	4.179×10^{-3}	-112.38	0.95306	2/3
$[Ni(FATP)(H_2O)_3]$	I	16.062	2.148×10^{5}	-98.71	0.98343	1
	II	5.162	8.326×10^{-2}	-106.21	0.94558	1
$[Cu(FATP)(H_2O)_3]$	I	12.939	7.522×10^{2}	-87.34	0.96598	1/3
	II	1.890	9.189×10^{-05}	-119.88	0.79384	1/3
$[Zn(FATP)(H_2O)_3]$	II	0.832	9.274×10^{-05}	-119.42	0.89590	1/3
$[Cu(FAP)(H_2O)_3]$	II	7.853	5.482	-88.22	0.98962	2/3
$[Zn(FAP)(H_2O)_3]$	III	6.998	2.598×10^{-1}	-104.03	0.98904	1/2
$[Cu(FTSC)(H_2O)_3]$	I	3.774	7.601×10^{-03}	-110.05	0.77511	1
	II a	13.28	3.752×10^{2}	-88.88	0.99558	1
$[Zn(FTSC)(H_2O)_3]$	I	3.471	1.379×10^{-2}	-109.24	0.95678	1
	II	1.458	1.066×10^{-4}	-118.96	0.97754	1/3
$[Cu(FSC)(H_2O)_3]$	II	1.232	1.211×10^{-4}	-119.25	0.97990	1/3
$[Zn(FSC)(H_2O)_3]$	I	8.360	6.1964	-96.78	0.98761	1/3

REFERENCES

1. A. M. Donia and H. A. El-Boraey, Transition Met.Chem., 18 (1993) 315.
2. W. W. Wendlandt and J. P. Smith, J. Inorg. Nucl. Chem., 25 (1963) 843.
3. W. W. Wendlandt and L. A. Funes, J. Inorg. Nucl. Chem., 26 (1964) 1879.
4. J. P. Smith and W. W. Wendlandt, J. Inorg. Nucl. Chem., 26 (1964) 1157.
5. W. W. Wendlandt, Tex. J. Sci. 14 (1962) 264.
6. W. W. Wendlandt, J. Inorg. Nucl. Chem., 25 (1963) 545.
7. W. W. Wendlandt and J. P. Smith, Inorg. J. Nucl. Chem., 25 (1963) 985.
8. G. Liptay, Thermochim. Acta., 150 (1989) 93.
9. A. M. Donia and E. M. Ebeid, Thermochim. Acta., 31 (1998) 1.
10. A. M. Donia, Thermochim. Acta., 162 (1989) 335.
11. A. Donia, E. El-Shereafy and M. A. El-Ries, Reactivity of Solids, 8 (1990)1.
12. A. M. Donia and H. A. El-Boraey, Transition Met. Chem., 18 (1992) 303.
13. A. M. Donia, and H. A. El-Boraey, Transition Met. Chem., 18 (1993) 315.
14. R. C. Mackenzic, "Differential Thermal Analysis", Academic Press, London, Vol. I (1970) 17.
15. W. W. Wendlandt, "Thermal Analysis", 3rd Ed., Wiley, New York (1985).

16. C. Duval, “Inorganic Thermogravimetric Analysis” Elsevier, New York (1963).
17. W. J. Smoothers and M.S. Yaochiang, “Handbook of Differential Thermal Analysis”, New York Chemical Publishing Co., New York (1996).
18 D. Schulze, “Differential Thermo Analyzer”, VEB Verlangder Wissenchaften, Berlin (1969).
19. P. D. Garn, “Thermo Analytical Methods of Investigation”, Academic Press, New York (1964).
20. J. Sestak, V. Satava and W. W. Wendlandt, Thermochim. Acta., 7 (1973) 333.
21. J. P. Redfern, “Differential Thermal Analysis”, Academic Press, New York (1970).
22. J. Sestak, Talanta, 13 (1966) 567.
23. A. W. Coats and J. P. Redfern, Nature, London, 68 (1964) 201.
24. A. M. Donia, Thermochim. Acta., 320 (1998) 187–199.
25. C. K. Bhaskare, P. G. More and P. F. Hankare, “Proceedings of the National Symposium on Thermal Analysis”, India (1981).
26. G. D. Ascenzo and W. W. Wendlandt, Anal. Chim. Acta., 50 (1970) 75.
27. F. C. Chang and W. W. Wendlandt, Thermochim. Acta., 2 (1971) 293.
28. G. D. Ascenzo and W. W. Wendlandt, Anal. Chim. Acta., 50(1970) 75.
29. P. L. Perry, C. Vaz and W. W. Wendlandt, Thermochim. Acta. 9 (1974) 76 .
30. C. G. Scency, J. O. Hill and R. J. Magee, Thermochim. Acta., 11 (1975) 301 .
31. C. G. Scency, J. F. Smith, J. O. Hill and R. J Magee, J. Therm. Anal., 9 (1976) 415.

32. K. K. Aravindakshan and K. Muraleedharan, J. Indian. Chem. Soc., 68 (1991) 348.
33. K. Rehina and G. Parameswaran, Asian J. Chem., 7 (1995) 189.
34. V. Indira and G. Parameswaran, Thermo. Chim. Acta., 101 (1986) 145.
35. S. Laly and G. Parameswaran, React. Kinet. Cal. Lett., 43 (1991) 169.
36. N. L. Mary and G. Parameswaran, Thermo Chim. Acta., 185 (1991) 345.
37. A. A. Soliman and W. Linert, Thermochem. Acta., 338 (1999) 67-75.
38. F. S. Rodembusch, F. R. Brand, D. S. Correa, J. C. Pocos, M. Martinelli and V. Stefani, Mater. Chem. Phys., 92 (2005) 389-393.
39. A. V. Nikolaev, V. A. Logvinenko and L. I. Myachina, "Thermal Analysis", Academic Press, New York (1969) 779.
40. S. Vatsala and G. Parameswaran, J. Therm. Anal., 31 (1986) 883.
41. R. S. Naidu and R. R. Naidu, Indian J. Chem., 15A (1997) 65.
42. R. S. Naidu, E. N. Rao, R. Ruby and K. G. Mallikarjun, Thermochim Acta., 131 (1988) 299.

PART III

X-RAY DIFFRACTION STUDIES

CHAPTER 1
INTRODUCTION

X-ray diffraction is a tool for the investigation of the fine structure of matter. This technique had its beginning in Von Laue's discovery in 1912, that, crystals diffract X-rays, the manner of the diffraction revealing the structure of the crystal. The diffraction of X-rays by matter is the basis of this unique scientific tool. X-ray diffraction has provided a wealth of important information to science and industry. This method is adapted due to the simplicity and versatility. Using this technique, a clear cut idea can be obtained about the arrangement and spacing of atoms in crystalline materials[1,2].

X-ray diffraction currently plays an important role in elucidating the structure of metal complexes. X-ray powder methods are based upon the fact that an X-ray diffraction is unique for each crystalline substance. It is the only analytical method that is providing qualitative and quantitative information about the compounds present in a solid sample. For analytical diffraction studies the sample is ground to a fine homogeneous powder. When an X-ray beam traverses the material a significant number of the particle can be oriented in such a way to fulfill Bragg condition for reflection. Diffraction patterns are obtained by automatic scanning. The identification of a species from its diffraction patterns is based upon the position of lines and

their relative intensities. The X-ray powder diffraction method is used now days to determine the lattice type of complexes.

X-ray method used in the determination of the structure of coordination compounds has increased immensely during the last decade. The work on coordination compounds has confirmed the basis of Werner's theory concerning structure of such compounds. In X- ray crystallographic studies graphical methods have been used by Hull and Davey[3], Bjurstrom[4] and Bunn[5] for indexing powder photographs. Hesse[6] and Lipson[7] introduced easier methods for studying crystallographic pattern. Hentry et al.[8] introduced equations for studying powder crystallographs.

X-ray diffraction is the only convenient and hence widely used physical procedure for the complete determination of molecular structure. Crystallographic study of materials depends on the nature of crystals. Studies of crystal faces and their intercepts on crystal axes show that all known crystals can be classified into seven systems. Particular axial lengths and axial angles characterise each system. Depending on these values the crystals are classified as cubic, tetragonal, orthorhombic, trigonal, hexagonal, monoclinic and triclinic. Bhagavantam[9], Hearmon[10], Krishnan[11] and Suryanarayana[12] already report a number of studies on elastic constants of such compounds. By the X-ray crystallographic studies the determination of unit cell dimensions, lattice type of crystal, the interplanar spacing of lattice planes and miller indices of the reflection planes are possible[13-15]. This is

obtained by allowing the X-rays of required wavelengths to fall on the crystal. The interference pattern will be created because of the scattering of these rays from neighbouring atoms produces diffraction. Since this diffraction obeys Bragg's law

$$n\lambda = 2d \sin\theta$$

where, n is an integer, λ is the wave length of the incident light, d is the inter planar distance and θ is the angle of diffraction. The X-ray crystallographic pattern between twice the angles of diffraction (2θ) against intensity of diffraction is very useful for the analysis.

Determination of crystal system

In the study of crystal systems, the relationship between the interplanar space, d and Miller indices h, k, l are used. Crystals belonging to regular or cubic system are built up on three equal axes at right angles. In this case axial lengths a = b = c and axial angles $\alpha = \beta = \gamma = 90°$. In this case the relation d and Miller indices (h, k, l) is given as

$$1/d^2 = (h^2 + k^2 + l^2) / a^2 \quad \text{and}$$

$$d^2 = \lambda^2 / 4 \sin^2\theta$$

$$\sin^2\theta = \lambda^2 (h^2 + k^2 + l^2) / 4a^2 \qquad (1)$$

$(h^2 + k^2 + l^2)$ will be constant and other than 7, 15, 23 etc.

On measuring Bragg angles, the values of $\sin^2\theta$ will be obtained. It is found to be an integral multiple of $\lambda^2 / 4a^2$ which is a constant.

For a tetragonal system all axial angles are 90° where as a = b ≠ c. Because of the change in values of c the above equation (1) will become,

$$\mathrm{Sin}^2\theta = [\lambda^2 (h^2 + k^2) / 4a^2] + \lambda^2 l^2 / 4c^2 \qquad (2)$$

If all the axial lengths are different in each other for the same axial angles, such a crystal system is called orthorhombic and for this, the equation is

$$\mathrm{Sin}^2\theta = [(\lambda^2 h^2) / 4a^2] + [(\lambda^2 k^2) / 4b^2] + [(\lambda^2 l^2) / 4c^2] \qquad (3)$$

$d_{(h\ k\ l)}$ represents the distance between adjacent planes. For an orthorhombic lattice the interplanar distance is given by the equation.

$$1/d^2_{(h\,k\,l)} = (h / a)^2 + (k / b)^2 + (1 / c)^2 \qquad (4)$$

For a cubic lattice, a = b = c

$$\text{Hence, } 1/d^2_{(h\,k\,l)} = (h / a)^2 + (k / a)^2 + (1 / a)^2 = (h^2 + k^2 + l^2) / a^2 \qquad (5)$$

$$d_{(h\,k\,l)} = a / (h^2 + k^2 + l^2)^{1/2} \qquad (6)$$

For a hexagonal system a = b ≠ c and α = β = 90°, γ = 120°, $\mathrm{Sin}^2\theta$ in this case is

$$\mathrm{Sin}^2\theta = \lambda^2 / 3a^2 (h^2 + hk + k^2) + (\lambda^2 l^2 / 4c^2) \qquad (7)$$

For rhombohedral or trigonal system a = b = c, α = β = γ ≠ 90°, for monoclinic system, a = b ≠ c, α = γ = 90°, β ≠ 90° and for triclinic system a ≠ b ≠ c, α ≠ β≠ γ ≠ 90°.

Density and number of molecules per unit cell of the complex have been calculated using the formula

$$D = n M / VN \qquad (8)$$

where D is the density of the complex, n the number of molecules in the unit cell, N is the Avogadro Number, V is volume of unit cell and M is the

molecular mass of the complex. The relative intensity of each peak can be calculated using the equation, 100 (I/I_0), where I is the intensity of diffracted beam and I_0 is the intensity of the incident beam.

The synthesis and crystal structure of the Schiff base complex of Cu(II) complexes have been reported by Doman et al.[16] X-ray powder analysis of complex of Ni(II) with Schiff bases derived from o-vanillin and diamines have been reported[17]. X-ray analysis of Cu(II) complexes of Schiff bases derived from salicylaldehyde and glycine was carried out by Nathmala[18]. Mononuclear and binuclear Cu(II) complexes with Schiff bases were prepared and studied by X-ray powder method[19]. X-ray diffraction structure of two N-salicylidene tryptophanato diaquo Cu(II) complexes (erythro and thero isomers) have been reported by Garcia-Raso et.al[20]. The structure of salicylaldehyde vaniline copper was studied using this method by Li Shuilan[21]. Synthesis and X-ray crystal structure of Schiff bases prepared from salicylaldehyde and diamine acids have been reported by Saleem et al.[22] The structure of N-salicylidine amino acidate complexes of oxovanadium(IV) dissolved in pyridine complexes (glycine and alanine) were detected by X-ray diffraction analysis[23]. In both the tridentate Schiff base ligands occupy equatorial positions and an octahedral geometry was suggested.

The application of X-ray diffraction technique to the determination structure of coordination compounds has increased immensely during the last few years. There are reports on study of different types of crystalline systems

of coordination compounds[24-28]. X-ray diffraction studies of Cd(II) complexes of anthranilic acid and 5-bromo-anthranilic acid derived Schiff bases have been reported[29]. X-ray diffraction studies of Fe(II), Ni(II) and Cu(II) complexes of o-vanillin L-histidine were carried out[30]. The crystal structure determination of metal complexes of amino acid Schiff bases of anthracene carboxaldehyde were carried out by Indiradevi[31]. The crystal and molecular structure of neutral Cu(II) complexes of Schiff bases from 2-aminopyridine and substituted salicylaldehydes were detected by X-ray diffraction method by Casrineiras et al.[32] The structure of β alanine Schiff base complex was detected by X-ray crystallography[33].

Scope of present investigation

In this section attempt has been made to determine the crystal systems of some of the synthesised transition metal complexes of furoin-2-aminothiophenol (FATP), furoin-2-aminophenol (FAP), furoin thiosemi-carbazone (FTSC) and furoin semicarbazone (FSC). The unit cell dimensions a, b, c, number of molecules per unit cell n, and density D has been found out from crystallographic data.

CHAPTER 2
MATERIALS, METHODS AND INSTRUMENTS

Materials and Methods

Analar grade chemicals supplied by Sigma Aldrich and E-Merck were used for the synthetic purpose. Commercial solvents were purified by distillation.

Preparation of Ligands and complexes

The ligands FATP, FAP, FTSC and FSC and their complexes were synthesised by the procedures described in part I. X-ray diffraction patterns of the metal complexes were recorded using AXS Bruker Germany make D5005 model X-ray diffractometer with a vertical goniometer. X-ray generator was operated at 40 KV and 30 mA. Cu K_α (λ =1.54056 A°) radiation was used with Ni filter. The measurements were done for 2θ values from 5° to 70° at a scan rate of 2°/min. The dried powders of metal complexes were compacted into pellets using a hydraulic press and densities were calculated from their mass and volume.

Instruments

The instruments used for this investigation are

1) AXS Bruker Germany make D 5005 model X-ray diffractometer
2) Hydrocraft India make 10T capacity uniaxial press with die set.

CHAPTER 3
X-RAY DIFFRACTION STUDIES OF SELECTED COMPLEXES OF FATP, FAP, FTSC AND FSC

X-ray crystallography is a standard technique for solving crystal structures. During the past century after its discovery, it has gone through continual development in data collection, instrumentation and data reduction methods. In recent years, the advent of synchrotron radiation sources, area detector based data collection instruments and high speed computers has dramatically enhanced the efficiency of crystallographic structural determination. Although single crystal X-ray diffraction is the most powerful and the routinely applied technique for determining crystal structures and an intrinsic limitation of this technique is the requirement to prepare a crystal of sufficient size, quality and stability. When appropriate single crystals cannot be obtained, it is necessary to tackle structure determination using powder diffraction data[34-36]. X-ray powder method is found to be applicable in determining the structure of complexes in solid state. Lipson et al.[6] have proposed useful equations for studying the X-ray powder pattern of each type of crystalline systems.

The detailed crystal structure of some selected metal complexes of FATP, FAP, FTSC and FSC were carried out. Even though powder diffraction pattern between 2θ values of 5° and 70° is recorded for simplicity first few peaks are considered using Lipson equation[6] in some cases. The

nature of crystalline systems and constants A, B, C, (where $A = \lambda^2/4a^2$, $B = \lambda^2/4b^2$, $C = \lambda^2/4c^2$) were found out from which the lattice constants a, b, c, and hence the volume were obtained. The density and number of molecules were found out by using the equation 8 in the chapter 1.

Results and discussion

The X-ray crystallographic pattern of the Ni(II) and Cu(II) complexes of FATP and FAP are shown in the figures 3.3.1 to 3.3.4 and complexes of FSC are shown in the figures 3.3.7 and 3.3.8. The diffraction pattern obtained for the Cu(II) and Zn (II) complexes of FTSC are shown in figures 3.3.5 and 3.3.6 respectively. The complexes, $[Ni(FATP)(H_2O)_3]$, $[Cu(FTSC)(H_2O)_3]$, $[Zn(FTSC)(H_2O)_3]$ and $[Ni(FSC)(H_2O)_3]$ belongs to the orthorhombic crystal system where as $[Cu(FATP)(H_2O)_3]$, $[Cu(FAP)(H_2O)_3]$ and $[Cu(FSC)(H_2O)_3]$ were found to be tetragonal crystal system. The cubic crystal system was obtained for the $[Ni(FAP)(H_2O)_3]$ complex. The values of $Sin^2\theta$ for each peak have been calculated with help of cell parameters and the corresponding h, k, l in all cases are in good agreement with observed values as in tables 3.3.1 to 3.3.8. The lattice constants a, b, c for each unit cell have been found out and are tabulated in tables along with density and number of molecules per unit cell. The calculated density of each complex was in good agreement with that of experimental value found out. This confirms the molecular

structure with an existence of 1:1 stiochiometry between the metal ion and the ligands for all the complexes.

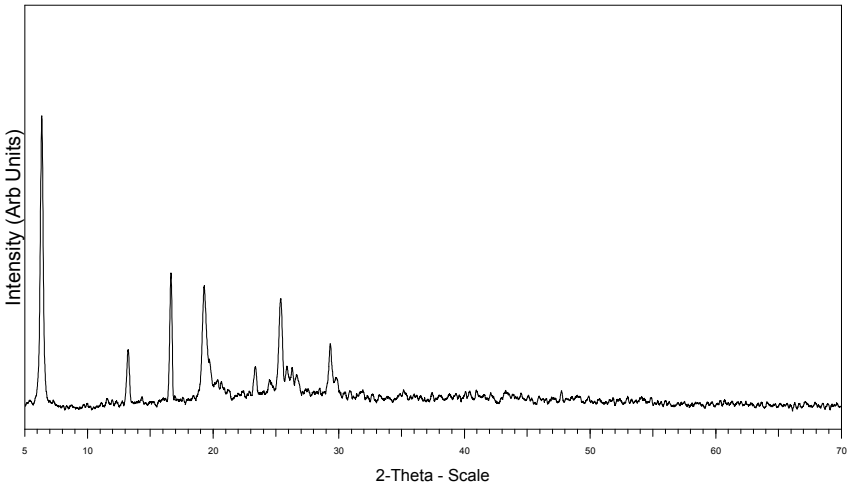

Figure 3. 3. 1 Crystallographic pattern of Ni(II) complex of FATP

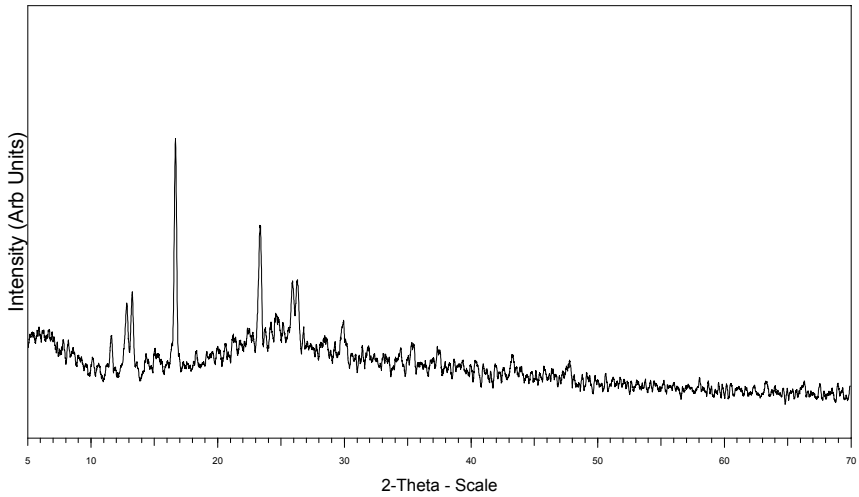

Figure 3. 3. 2 Crystallographic pattern of Cu(II) complex of FATP

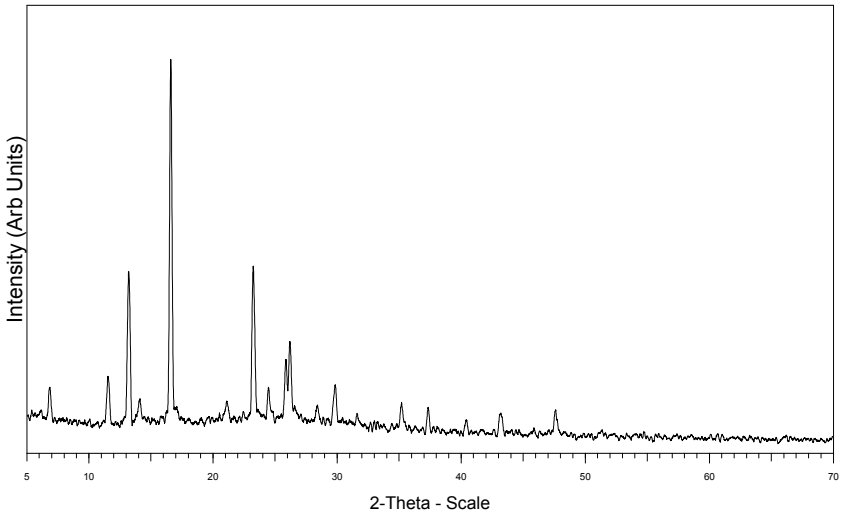

Figure 3. 3. 3 Crystallographic pattern of Ni(II) complex of FAP

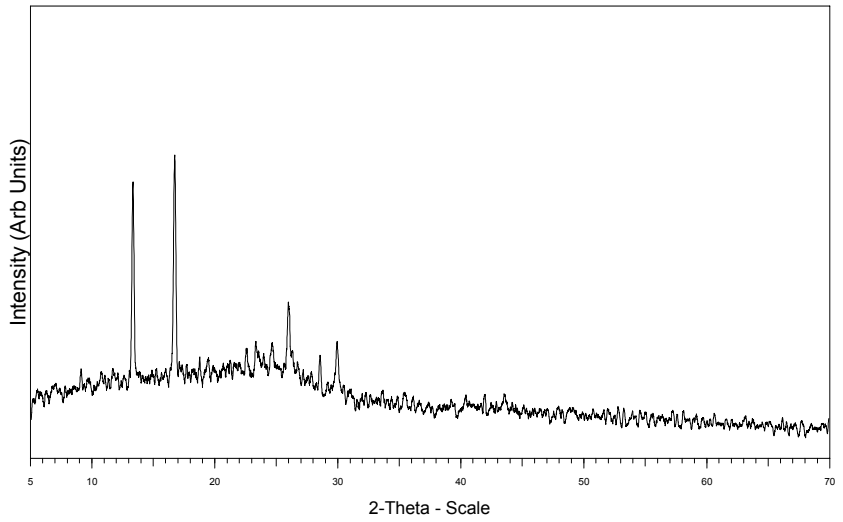

Figure 3. 3. 4 Crystallographic pattern of Cu(II) complex of FAP

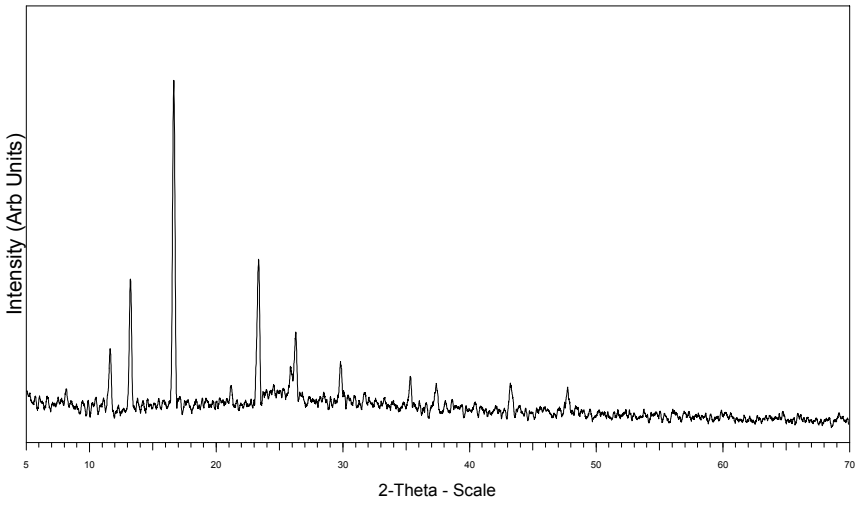

Figure 3. 3. 5 Crystallographic pattern of Cu(II) complex of FTSC

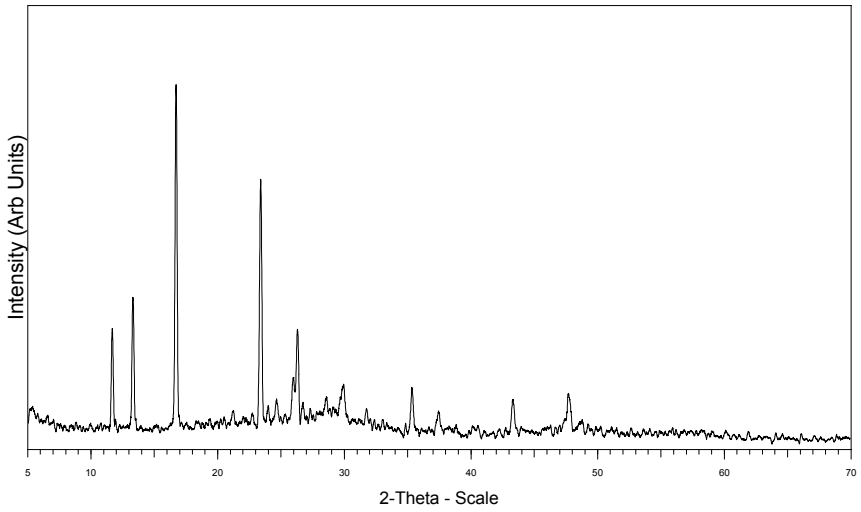

Figure 3. 3. 6 Crystallographic pattern of Zn(II) complex of FTSC

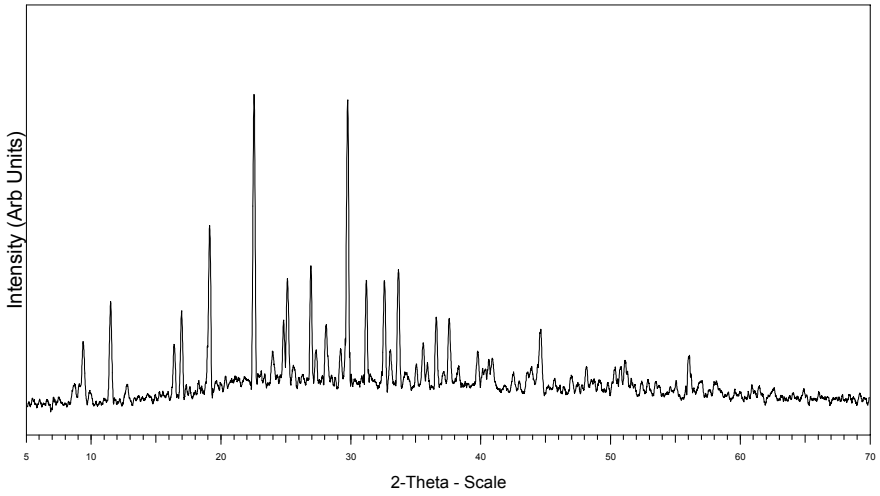

Figure 3. 3. 7 Crystallographic pattern of Ni(II) complex of FSC

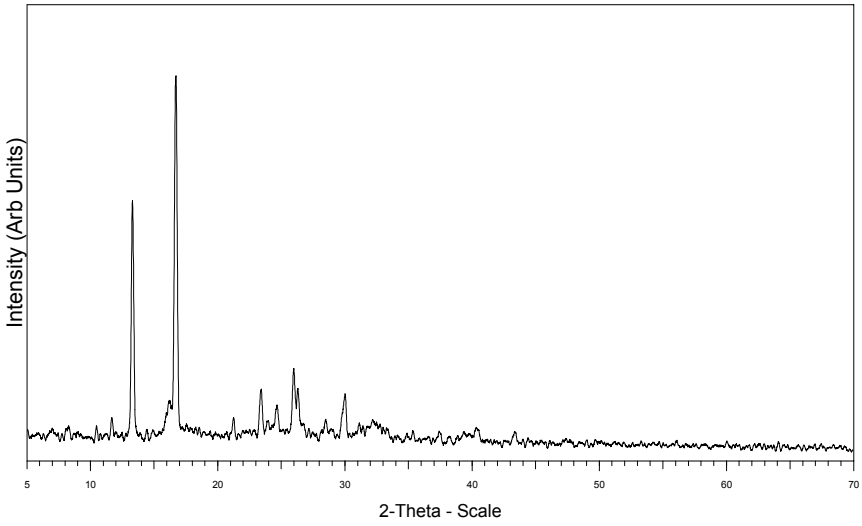

Figure 3. 3. 8 Crystallographic pattern of Cu(II) complex of FSC

Table 3. 3. 1 X-ray data of [Ni(FATP)(H_2O)$_3$]

Crystal system : Orthorhombic system

A = 0.003015, B = 0.001005, C = 0.001508

a = 14.0383 A°, b = 24.3151 A°, c =19.8532 A°

Cell volume, V = 6776.7813 (A°)^3

Density = 1.5069 g/cm^3

No of molecules per unit cell, n = 15

Peak No	2θ°	d spacing A°	Relative intensity	$Sin^2θ$ observed	$Sin^2θ$ calculated	h	k	l
1	6.296	14.026	100	0.00301	0.00301	1	0	0
2	13.191	6.706	25.1	0.01319	0.01306	2	1	0
3	16.606	5.334	49.7	0.02085	0.01909	1	4	0
4	19.257	4.605	45.6	0.02797	0.02814	3	0	0
5	23.336	3.809	19.7	0.04090	0.04071	3	0	3
6	25.357	3.510	41.5	0.04817	0.04825	4	0	0
7	29.307	3.045	27.1	0.06399	0.06332	4	3	2

Table 3. 3. 2 X-ray data of [Cu(FATP)(H_2O)$_3$]

Crystal system : Tetragonal system

A = 0.010124, B = 0.002249

a = b = 7.66154 A°, c = 16.2526 A°

Cell volume, V = 954.0145 (A°)^3

Density = 1.5885 g/cm^3

No of molecules per unit cell, n = 22

Peak No	2θ°	d spacing A°	Relative intensity	$Sin^2θ$ observed	$Sin^2θ$ calculated	h	k	l
1	11.550	7.655	34.1	0.01012	0.01012	1	0	0
2	12.773	6.925	45	0.01237	0.01237	1	0	1
3	16.627	5.327	100	0.02090	0.02024	1	1	0
4	23.327	3.810	70.8	0.04087	0.04049	2	0	0
5	26.270	3.390	52.8	0.05164	0.05062	2	1	0
6	29.990	2.977	38	0.06694	0.06637	1	0	5
7	40.366	2.2326	25.6	0.11903	0.11699	2	2	4

Table 3. 3. 3 X-ray data of $[Ni(FAP)(H_2O)_3]$

Crystal system : Cubic system

A =B = C = 0.003492, a = b = c = 13.045889A°

Cell volume, V = 2220.3249 $(A°)^3$, Density = 1.465 g/cm^3

No of molecules per unit cell, n = 5

Peak No.	2θ°	d spacing A°	Relative intensity	$Sin^2\theta$ observed	$Sin^2\theta$ calculated	h	k	l
1	6.776	13.034	16.6	0.00349	0.00349	1	0	0
2	11.510	7.681	19.2	0.01005	0.01047	1	1	1
3	13.166	6.719	45.6	0.01314	0.01396	2	0	0
4	14.098	6.277	7.4	0.01505	0.01746	2	1	0
5	16.563	5.348	100	0.02074	0.02095	2	1	1
6	21.080	4.211	6.6	0.03346	0.03142	2	1	2
7	23.225	3.827	47.4	0.04051	0.04190	2	2	2
8	24.443	3.639	16.5	0.04481	0.04539	3	0	2
9	25.853	3.443	23.6	0.05130	0.05587	4	0	0
10	28.395	3.141	5.8	0.06015	0.05936	4	0	0
11	29.830	2.993	17.2	0.06624	0.06634	3	1	3
12	35.178	2.549	7.4	0.09131	0.09079	5	1	0
13	37.343	2.406	11.4	0.10248	0.10126	5	2	0
14	40.498	2.226	3.6	0.11978	0.11872	5	3	0

Table 3. 3. 4 X-ray data of [Cu(FAP)(H_2O)$_3$]

Crystal system : Tetragonal system

A = 0.013396, B = 0.001913

a = b = 6.66060 A°, c =17.62232 A°

Cell volume, V = 781.7896 (A°)^3

Density = 1.3416 g/cm^3

No of molecules per unit cell, n = 16

Peak No	2θ°	d spacing A°	Relative intensity	$Sin^2\theta$ observed	$Sin^2\theta$ calculated	h	k	l
1	13.293	6.655	91.1	0.01339	0.01339	1	0	0
2	16.699	5.304	100	0.02108	0.02105	1	0	2
3	25.985	3.426	51.4	0.05054	0.05358	2	0	0
4	28.6	3.118	16.6	0.06100	0.06124	2	0	2
5	29.939	2.982	38.3	0.06672	0.06698	2	1	0

Table 3. 3. 5 X-ray data of [Cu(FTSC)(H_2O)$_3$]

Crystal system : Orthorhombic system

A = 0.010173, B = 0.003391, C = 0.001130

a = 7.64306 A°, b = 13.23819 A°, c = 22.9292 A°

Cell volume, V = 2319.9857 (A°)^3, Density = 1.6342 g/cm^3

No of molecules per unit cell, n = 6

Peak No	2θ°	d spacing A°	Relative intensity	$Sin^2θ$ observed	$Sin^2θ$ calculated	h	k	l
1	11.578	7.637	25.7	0.01017	0.01017	1	0	0
2	13.185	6.710	45.0	0.01318	0.01356	1	1	0
3	16.610	5.333	100	0.02086	0.02034	1	0	3
4	21.142	4.199	15.5	0.03365	0.03165	0	3	1
5	23.316	3.812	50.5	0.04083	0.04069	2	0	0
6	26.257	3.391	30.3	0.05159	0.05086	2	0	3
7	29.819	2.994	22.0	0.06619	0.06556	1	4	1
8	35.332	2.538	18.0	0.09209	0.09269	3	0	1
9	37.383	2.404	16.1	0.10270	0.10512	1	5	3
10	43.265	2.090	16.2	0.13590	0.13565	2	5	3
11	47.768	1.9024	15.1	0.16393	0.16391	4	0	1

Table 3. 3. 6 X-ray data of [Zn(FTSC)(H_2O)$_3$]

Crystal system : Orthorhombic system

A = 0.01027, B = 0.003423, C = 0.001141

a = 7.60718 A°, b = 13.17767 A°, c =22.82117 A°

Cell volume, V = 2287.5353 (A°)^3

Density = 1.665 g/cm^3

No of molecules per unit cell, n = 6

Peak No	2θ°	d spacing A°	Relative intensity	$Sin^2θ$ observed	$Sin^2θ$ calculated	h	k	l
1	11.633	7.601	33	0.01027	0.01027	1	0	0
2	13.268	6.668	41.5	0.01335	0.01369	1	1	1
3	16.678	5.311	100	0.02103	0.02054	1	0	3
4	23.375	3.802	74	0.04103	0.04108	2	0	0
5	26.286	3.388	32.8	0.05170	0.05135	2	0	3
6	29.925	2.983	16.8	0.06666	0.06617	1	4	1
7	35.350	2.537	10.3	0.09218	0.09243	9	0	0
8	37.453	2.399	13.4	0.10307	0.10611	1	5	3
9	43.335	2.086	15.1	0.13632	0.13691	4	5	3
10	47.738	1.904	18.8	0.16379	0.16432	4	0	0

Table 3. 3. 7 X-ray data of $[Ni(FSC)(H_2O)_3]$

Crystal system : Orthorhombic system

A = 0.006618, B = 0.003309, C = 0.001323

a = 9.47591 A°, b = 13.40096 A°, c = 21.18879 A°

Cell volume, V = 2690.6875 $(A°)^3$, Density = 1.3317 g/cm^3

No of molecules per unit cell, n = 6

Peak No	2θ°	d spacing A°	Relative intensity	$Sin^2\theta$ observed	$Sin^2\theta$ calculated	h	k	l
1	9.333	9.468	27.2	0.00661	0.00661	1	0	0
2	11.448	7.723	39.0	0.00994	0.00992	1	1	0
3	16.933	5.232	36.3	0.02167	0.02118	0	0	4
4	19.097	4.643	61.4	0.02751	0.02779	2	0	1
5	22.523	3.944	100	0.03813	0.03838	2	0	3
6	25.103	3.545	45.8	0.04722	0.04765	2	0	4
7	26.91	3.310	49.5	0.05414	0.05427	0	4	1
8	28.076	3.176	32.2	0.05837	0.05758	2	3	0
9	29.206	3.055	25.0	0.63564	0.64201	3	1	1
10	31.189	2.865	45.3	0.07226	0.07280	3	2	0
11	32.585	2.746	45.1	0.07870	0.07810	3	2	2
12	33.046	2.708	24.8	0.08088	0.08074	3	0	4

Table 3. 3. 8 X-ray data of $[Cu(FSC)(H_2O)_3]$

Crystal system : Tetragonal system

A = 0.010270, B = 0.003423

a = b = 6.12629 A°, c =10.61106 A°

Cell volume, V = 398.2492 $(A°)^3$

Density = 1.5197 g/cm^3

No of molecules per unit cell, n = 10

Peak No	2θ°	d spacing A°	Relative intensity	$Sin^2\theta$ observed	$Sin^2\theta$ calculated	h	k	l
1	11.633	7.601	11.1	0.01027	0.01027	1	0	0
2	13.258	6.672	67.5	0.01332	0.01369	1	0	1
3	16.668	5.314	100	0.02100	0.02054	1	1	0
4	21.222	4.183	11.1	0.03390	0.03423	1	1	2
5	23.375	3.802	18.3	0.04103	0.04108	2	0	0
6	24.628	3.612	14.2	0.04548	0.04450	2	0	1
7	26.283	3.388	18.6	0.05169	0.05135	2	1	0
8	29.991	2.977	17.2	0.06694	0.06504	1	0	4

REFERENCES

1. B. D. Cullity, "Elements of X-ray Diffraction", 2nd Edition, Addison-Wesley Publishing Company Inc., London (1978).
2. H. P. Klug and L. E. Alexander, "X-ray Diffraction Procedures for Poly Crystalline and Amorphous Materials", 2nd Edition, John Wiley & Sons, New York (1974).
3. A. W. Hull and W. P. Davey, Phys. Rev., 17(1921) 549.
4. T. Bjurstrom, Phys. Z., 69 (1931) 346.
5. C. W Bunn, "Chemical Crystallographic Physics", Oxford University Press (1945) 133.
6. R. Hesse, Acta Crystallogr., 1(1948) 200.
7. H. Lipson, Acta Crystallogr., 2 (1949) 43.
8. N. F. M. Hentry, H. Lipton and W. A. Wooster, "Interpretation of X-ray Diffraction Photographs" (1951) 81.
9. S. Bhagavantam, Proc. Indian. Acad. Sci., 4b (1955) 72.
10. R. F. S. Hearmon, Phil. Mag., 5 (1956) 323.
11. R. S. Krishnan, "Progress in Crystal Physics" (1958).
12. M. Krishnamurty and M. S. Narayana, "Physics of Solid State", Academic Press, London (1969) 487.
13. L.V. Azaroff and M. J. Buerger, "The Powder Method in X-ray Crystallography", McGraw Hill, New York (1958).
14. R. W. M. D. Eye and E. Wait, "X-ray Powder Photography in Inorganic Chemistry", Academic Press, New York (1960).
15. H. Lipson and H. Steeple, "Interpretation of X-ray Powder Diffraction Pattern", Macmillan, London (1970).

16. T. Doman, N. Williams, D. E. Banks, J. F. Buchen, R. M. Chang, H. Rong, J. W. Robert, Hendrickson and N. David, Inorg. Chem., (1990).
17. Liu Dexin, Li Shulan, Cu Xuegue, Li Xiaoyan, Gaogeng Xuexiao and Huaxuc Xuehao 14,7 (1993) 879-901.
18. Nathmala, Thermo. Chim. Acta., 185 (1) (1991)11-24.
19. S. S. Dodwad, R. S. Dhamwaskar and S. V. Salvi, Asian J. Chem., 7, 2 (1995) 289-295.
20. Garcia–Raso, Angel Feol, J. Jual, Badenas, Ferran and Quiros Miuel, Polyhedron, 15, 24 (1996) 4407- 4413.
21. Li Shuilan, Liu De-xin, Xu, Hai-wei, Yang Zhao-He and Jiegou Huaxue, 16, 20 (1997) 159-163.
22. M. Saleem, M. Mohammed, M. A. Molevalli, B. Nunn and P. O. Paul, Tetrahedron, 54, 21 (1998) 5721-5730.
23. C. Isabel, P. J. Costa, Costadina, T. D. Maria, G. D. Robert and M. Petro, J. Chem. Soc. Dalton Trans., 2 (1994) 149-157.
24. K. K. Mahesh and R. K. Goutam, Asian J. Chem., 4 (1991) 417.
25. P. Chourasia, K. K. Suryesh and A. P. Mihra, Proc. Indian. Acad. Sci., 105, 3 (1993) 173.
26. R. Singh and R. K. Gautam, J. Indian. Chem. Soc., 14 (1987) 631.
27. J. A. Cherayat and C. P. Prabhakaran, Trans. Met. Chem., 15 (1990) 449.
28. S. Caric, D. Petrovic, D. Lazar and V. M. Leovaz and Z. Kristallogr., 148 (1978) 153.
29. K. T. Lali, Ph. D Thesis, Calicut University, Kerala (1994) 206-227.
30. B. Sleema and Geetha Parameswaran, Asian J.Chem., 14 (2002) 961.
31. G. Indiradevi, Ph. D Thesis, Calicut University, Kerala (2002) 144-151.
32. A. Casrineiras, J. A. Castro, M. L. Duran, J. A. Garcia Vazquez, A. Macias, J. Romero, and Sousa A, Polyhedron, 89, 21 (1989) 2543-2549.

33. C. S. Kumar, B. P. Ray, D. P. Samudranil, Chakravarthy and Anemesh, Inorg. Chem., 29 (13) (1990) 2428.
34. K. D. M. Harris, Curr. Opin. Solid. St. M., 6 (2002) 125-130.
35. K. D. M. Harris, M. Tremayne and B. M. Kariuki, Angew . Chem. Int. Ed., 40 (2001) 1626-1651.
36. J. I. Langford and Daniel Louer, Rep. Prog. Phys., 59 (1996) 131-234.

PART IV

CORROSION INHIBITION STUDIES OF SCHIFF BASES ON MILD STEEL

CHAPTER 1
INTRODUCTION

Aggressive acid solutions are extensively used in the industries for manufacturing processes and other applications like acid pickling, acid cleaning, acid de-scaling and oil well cleaning[1]. Metals which are subjected to painting, enameling, galvanizing, electroplating, phosphate coating, cold rolling etc. must have a clean surface free from salt or oxide scaling. To remove unwanted scale such as mill scale rust, the metal is immersed in an acid solution known as acid pickling bath. The most commonly used acids in industrial process are hydrochloric acid, sulphuric acid, nitric acid, hydrofluoric acid, citric acid, formic acid, acetic acid etc. Hydrochloric acid is extensively used in the pickling baths because of its easy economic regeneration from the depleted pickling solution. The use of acids makes the industrial pipe lines and metal vessels to corrode and there by reducing the production and causing economical loss.

Corrosion inhibitor

A corrosion inhibitor is a substance which when added in small quantities to a corroding medium brings about an appreciable reduction of the corrosive action. Corrosion inhibitors are commonly added in small amounts to acids, cooling waters, steam and other environments, either continuously or intermittently to prevent serious corrosion. The selection of suitable inhibitor

depends on the type of acid, its concentration, temperature, flow velocity, the presence of dissolved inorganic or organic substance and type of metallic material exposed to the acid solution.

Corrosion is an electrochemical phenomenon and inhibitors decrease the velocity of electrochemical electrode reactions[2,3]. Depending upon the mechanism of their action corrosion inhibitors are classified as anodic inhibitors, cathodic inhibitors and organic or mixed type inhibitors. Anodic inhibitors are substances, which reduce the anode area by acting on the anodic sites and polarize the anodic reaction and displace the corrosion potential in the positive direction. Chromates, nitrates, tungstate, molybdates are some examples of anodic inhibitors.

Cathodic inhibitors reduce the cathode area by acting on the cathodic sites and polarize the cathode reaction and displace the corrosion potential in the negative direction. They reduce corrosion current and thereby retard the cathodic reaction and suppress corrosion rate. Examples for cathodic inhibitors are phosphates, silicates and borates.

Substances which affect both cathodic and anodic reaction are called mixed inhibitors. In general these are organic compounds, which are also known as organic or adsorption type inhibitors, which absorb on the metal surface and suppress metal dissolution and reduction reaction. Organic inhibitors affect the entire surface of the corroding metal when present in sufficient concentration. Both the anodic and cathodic areas are probably

inhibited but to varying degrees, depending on the potential of the metal, chemical structure of the inhibitor molecule, and the size of the molecule

Schiff bases as corrosion inhibitors in acid solutions – A review

Compounds containing functional groups with hetero atoms, which can donate lone pair of electrons, are found to be very efficient as inhibitors against metal corrosion in many environments. Many N-heterocyclic compounds with polar groups and/or π electrons are also acting as efficient corrosion inhibitors in acidic solutions. Schiff base, an organic compound which has both these features combined in one molecule, will be a potential inhibitor. Schiff bases have been previously reported as effective corrosion inhibitors for steel, copper and aluminum in acid medium like hydrochloric acid, sulphuric acid, acetic acid, formic acid etc.[4-26].

Emregul and Atakol[4] studied the corrosion inhibition efficiency of Schiff base compounds N-(2-hydroxyphenyl)salicyaldimine, N,N'-bis-(salicy-aldehyde)-1,3-diaminopropane, N,N'-bis-(2-hydroxybenzyl)1,3-diaminopro-pane on iron in 1M HCl using weight loss, polarization and electrochemical impedance spectroscopy (EIS) techniques. All these Schiff bases act as good inhibitors and among the three compounds N,N'-bis-(2-hydroxybenzyl) 1,3-diaminopropane showed maximum inhibition efficiency. Sorkhabi et al.[5] determined the inhibition efficiency of pyridinimic Schiff bases, benzilidene-pyrimidine-2-yl-amine, (4-methyl-benzilidene)–pyrimidine-2-yl-amine, (4-

choloro-benzilydene)–pyrimidine-2-yl-amine towards mild steel (MS) in 1M HCl medium by weight loss and electrochemical polarization methods. These results reveal that these compounds act as good corrosion inhibitors even at very low concentrations and adsorption followed Langmuir isotherm.

In terms of molecular parameters, Lukovits[6] explained the variation in the inhibition efficiency of thiosemicarbazide and thiosemicarbazones derivatives using quantitative structure activity relationships (QSAR). It was found that in the studied series of thiosemicarbazide and thiosemicarbazone derivative corrosion inhibition efficiency depends on the E_{HOMO} and the dipole moment, or alternatively, on the minimal electronic excitation energy. Rehim et al.[7] have tested 4-amino antipyrine (AAP) for the corrosion inhibition of MS in 2M HCl using weight loss, potentiodynamic polarization and EIS methods. The results showed that AAP is an inhibitor for MS and the inhibition was assumed to take place via adsorption of the inhibitor molecule on the metal surface.

Quraishi and co-workers[8] investigated the influence of three macro cyclic compounds on corrosion of MS in HCl using weight loss method, potentiodynamic polarization, AC impedance and hydrogen permeation techniques. All the investigated compounds showed significant efficiencies and reduced permeation of hydrogen through MS in HCl. Potentiodynamic polarization results reveal that macrocyclic compounds acted as mixed inhibitors.

The influence of pyridinium chloride (PC) and n-hexa decyl pyridinium chloride (HDPC) on the corrosion of MS in 5N HCl and 5N H_2SO_4 has been studied using weight loss, gasometric, linear polarization, potentiodynamic polarization, and small amplitude cyclic voltametric techniques[9]. It was found that HDPC is more inhibitive than PC and both compounds perform better in H_2SO_4. The corrosion inhibition on SS 400 by Schiff base compounds derived from diamines and o-hydroxy, o-methoxy aromatic aldehyde was investigated by weight loss, electrochemical measurements and surface analysis in various aqueous solutions such as tap water, concentrated tap water and HCl solutions by Shokry[10]. It was found that 93% inhibition efficiency was achieved for N,N′-bis(salicyladehyde)-1,12-diaminododecane and adsorption obeyed Langmuir isotherm.

Dadgarnezhad et al.[11] synthesised new tetradendate Schiff base, bis –(2-hydroxy-1-naphthaldehyde)1, 6-hexadiamine and studied its corrosion inhibition on carbon steel in 1M HCl and 0.5M H_2SO_4 using EIS, polarization curves and weight loss techniques. Potentiodynamic polarization tests showed that this inhibitor act as both cathodic and anodic inhibitor and efficiency of 95% was achieved for a 100 ppm concentration. The inhibitor effect of Schiff base compounds N,N'-bis-(salicylidene)-2-hydroxy-1,3-propanediamine and N,N'-bis-(2-hydroxyacetophenlidene)-2-hydroxy-1,3-propane diimine on MS in 2M HCl medium were studied using weight loss, polarization and impedance methods[12]. The results revealed that the latter

Schiff base showed better inhibition property than the former one and both the inhibitors appear to function through the Langmuir adsorption isotherm.

Sorkhabi et al. [13] have carried out the corrosion inhibition studies on MS in 1M HCl medium using the Schiff bases benzylidine-pyridine-2-yl-amine, (4-benzylidene)-pyridine-2-yl-amine and (4-chloro-benzidiline)-pyridine-2-yl-amine by weight loss measurements and electro chemical methods. Results showed that these compounds were excellent inhibitors and inhibition efficiency increased with increase in inhibitor concentration and varied with the type of functional groups substituted on benzene ring. The polarization curves reveal that compounds are mixed type inhibitors and experimentally obtained adsorption isotherms follow the Langmuir equation.

The inhibition efficiency of Schiff bases, 2-((1E)-2-aza-2-pyrimidine-2-ylvinyl)thiophene, 2-((1Z)-1-aza-2-(2-pyridyl)vinyl)pyrimidine, 2-((1E)-2-aza-2-(1,3-thiazol-2-yl)vinyl)thiophene, 2-((1Z)-1-aza-2(2-thienyl)(vinyl) benzothiazole containing hetero aromatic substituents on carbon steel in 0.1 M HCl, using potentiodynamic polarization and EIS studies have been carried out by Yurt et al.[14] Polarization studies reveal that studied Schiff bases act as anodic inhibitors. The variation of inhibition efficiency mainly depends on the type and nature of the substituents present in the inhibitor molecule and these compounds are adsorbed on the steel surface and the adsorption obeys Temkin's isotherm. Desai et al.[15] studied seven Schiff bases as corrosion inhibitors for MS in HCl solutions by weight loss and electrochemical

methods. Polarization data indicate that all these compounds act as predominantly cathodic inhibitors.

Quraishi and Sardar[16] have synthesised organic compounds like 5-mercapto-3-butyl-4-salicylidine-1,2,4-triazole (MBST), 5-mercapto-3-butyl-4-benzilidineiminio-1,2,4-triazole (MBBT) and 5-mercapto-3-butyl-4-cinna-mylidineimino-1,2,4-triazole(MBCT) and investigated their corrosion inhibition capacity on MS in 1N HCl and 1N H_2SO_4 by weight loss and potentiodynamic polarization techniques. Inhibition efficiency was found to vary with respect to temperature, concentration and immersion time. The adsorption of these compounds on the steel surface for both acids was found to obey Temkin's adsorption isotherm. The potentiodynamic polarization data have shown that compounds studied are mixed type inhibitors.

The inhibition capacity of Schiff bases, 2-hydroxyacetophenone-etansulphonylhydrazone, salicyladehyde-etansulphonylhydrazone, 5-bromo salicyladehyde-etansulphonylhydrazone and 5-chlorosalicylaldehyde-etansul-phonylhydrazone on AA3102 aluminum in 0.1M HCl by means of hydrogen evolution tests and EIS technique have been carried out in 2004[17]. Maximum efficiencies were obtained for third and fourth Schiff bases because they have electronegative atoms like chlorine and bromine as para substituents on phenol ring.

Bansiwal et al.[18] conducted weight loss and thermometric methods to study the inhibition of aluminum corrosion in HCl solution by four Schiff

bases such as 2-anisalidine-pyridine, 2-anisalidine-pyrimidine, 2-salicylidine-pyridine, 2-salicylidine-pyrimidine and have shown that they are effective inhibitors for the corrosion of aluminum in HCl. Desai et al.[19] carried out the corrosion inhibition testing of Schiff bases derived from benzaldehyde, aliphatic and aromatic primary amines on aluminium alloy 51S in HCl. Schiff bases showed fairly good inhibition efficiency and conversion of an amine into its Schiff base improved its inhibitive action.

The corrosion inhibition of copper in 0.5 M HCl by 1,3,4-thiadiazole-2,5-dithiol(bismuthiol) using potentiodynamic polarization technique has been reported[20]. It was found that bismuthiol was chemically adsorbed on the copper surface and follows Langmuir isotherm. Li and co-workers[21] examined inhibiting effect of Schiff base N, N'-O-phenylen-bis(3-methoxy salicyaldenimine) on corrosion of copper in 1.0 M HCl and NaCl solutions using potentiostatic polarization and EIS techniques. The results show a remarkable decrease in the corrosion rate in the presence of Schiff base.

Fouda[22] investigated the inhibition action of semicarbazide, thiosemi-carbazide and diphenylcarbazide towards corrosion of zinc in HCl using weight loss, thermometric and polarization techniques. From the weight loss measurements it was observed that the rate of corrosion depends on the nature of inhibitor and its concentration. The polarization studies reveal that these inhibitors act as mixed type inhibitors. The increase in adsorption is due to electron density at the reactive C=S and C=O groups and N atoms.

Corrosion inhibition of Zinc on HCl using *Nypa Fruticans Wurmb* extract and 1,5 Diphenylcarbazone were tested by Okorosaye et al.[23] using weight loss technique. Maximum inhibition efficiency was obtained at an optimum concentration. The corrosive behaviour of Zinc in HCl solution containing various concentrations of glutaraldehyde, glycine, methionine and their condensation products formed between was examined using chemical and electrochemical methods by Rajappa et al[24]. The condensation product of glutaraldehyde and methionine acted as cathodic inhibitor showing an efficiency of 92.5% and adsorption followed Temkin isotherm.

Hosseini et al.[25] have synthesised and studied corrosion inhibition efficiency of Schiff bases N,N'-ortho-phenylene(salicylaldimine-acetyl acetoneimine) and N,N'-ortho-phenylene(salicylaldimine-2-hydroxy-1-napth aldimine) on MS in 0.5M H_2SO_4 using weight loss, polarization and EIS techniques. These compounds achieved 95% efficiency at a concentration of 400 ppm and identified both compounds as good inhibitors.

Quraishi et al.[26] have investigated the inhibition efficiency of three Schiff bases 1-vanillinthiosemicarbazone, 1-salicyaldehyde thiocarbazone, 1-dimethyl aminobenzaldehyde thiosemicarbazone towards MS in aqueous solutions containing 20% formic and 20% acetic acid media by weight loss and potentiodynamic polarization methods. These compounds acted as mixed inhibitors and shown good inhibition efficiency in formic acid solutions.

Scope of present investigation

Organic compounds are used to control the corrosion of MS in acid solutions. Due to the presence of the -C=N group, an electron cloud on the aromatic ring, the electronegative N,O and S atoms in the molecule, Schiff bases may be good corrosion inhibitors. As part of our study four new Schiff bases have been synthesised. The corrosion inhibition studies of these Schiff bases on MS in HCl are not yet reported. Taking into consideration of above factors, the inhibition efficiency studies of four Schiff bases towards MS in 1M HCl are investigated using weight loss and electrochemical methods. An adsorption isotherm which describes the adsorptive behaviour of a corrosion inhibitor provides important clues to the nature of metal inhibitor interaction for the inhibition process. Assignment of suitable adsorption isotherms for the corrosion inhibition of MS in the presence of Schiff bases is also attempted.

CHAPTER 2
MATERIALS, METHODS AND INSTRUMENTS

The corrosion inhibition efficiency of Schiff bases was determined using weight loss measurements and electrochemical methods like potentiodynamic polarization and electrochemical impedance spectroscopy techniques. The method of determining the weight loss of metal coupons exposed to the corrosive environment using laboratory immersion corrosion testing method is the traditional and most widely used method for *in situ* corrosion monitoring[3,27]. As a classical corrosion test method, the weight loss coupon method has provided a great deal of useful information.

Materials

Preparation of inhibitor solution

Schiff bases FTSC, FATP, FAP and FSC were prepared by the methods described in the Part I and employed for the corrosion inhibition studies. The molecular structures of the Schiff bases FTSC, FSC, FAP and FATP are also given in the Part I. 1M HCl solution is used as the test solution (corrodent) and is prepared from the reagent grade HCl (E-Merck) using deionised water. 0.0001M, 0.0002M, 0.0004M, 0.001M, 0.002M, 0.003M, 0.004M and 0.008M solutions of inhibitor solution were employed for inhibition studies and were prepared by dissolving the required amount of the FTSC, FATP, FAP and FSC in 50 ml of 1M HCl by stirring at room

temperature. 50 ml of 1 M HCl without inhibitor is considered as blank test solution.

Preparation of test specimens

The MS having 99.22% Fe, 0.019% Mn, 0.28% Ni and 0.30% carbon as determined by the chemical analysis using Philips PW 2400 model X-ray fluorescence spectrophotometer were selected as test samples for corrosion studies. These MS sheets were cut into coupons having 1cm x 1cm x 0.1cm size using a LeCo VC-50 diamond wheel cutting machine and polished with different grade emery papers (120, 220, 400, 600, 800, 1500 and 2000 grade) to mirror polish. Then these coupons were washed with methanol, acetone and distilled water, dried and weighed using electronic balance having 0.0001g accuracy. The exposed area of the MS coupons was found out using Vernier calipers.

Methods

In laboratory immersion corrosion testing method, the metal coupons are exposed to the corrosive environment like acid solutions and weight loss of the metal coupons are measured at regular time intervals and corrosion rate is calculated from the weight loss measurements. The inhibition capacity of the inhibitor is calculated from the corrosion rates. In the present investigation, American Society for Testing and Materials (ASTM) G31-72 standard procedure for laboratory immersion corrosion testing published in

the year 1990 was adopted for the determination of weight loss and corrosion rate of MS coupons in HCl[28,29]

The polished MS coupons were immersed in hanging position in 50 ml of test solution taken in stoppered glass bottles with the help of a fishing line at room temperature (30°C). The specimens were taken out in 24 hours interval, cleaned with acetone and water, dried and weighed. The weight loss of these coupons immersed in the 1M HCl was recorded for a consecutive seven days period.

The corrosion rate (CR), expressed in millimeter per year (mmY^{-1}), is calculated using the equation (1)

$$CR(mmY^{-1}) = \left[\frac{(87600)(\text{Weight loss in grams})}{(\text{Area in } cm^2)\ (\text{Time in hours})(\text{Density of coupon in g/cc})} \right] \quad (1)$$

The density of the coupon is substituted with density value of iron i.e. 7.88g/cc. The percentage inhibition efficiency $(\eta W_L\%)$ of a corrosion inhibitor is calculated from the corrosion rate values using the equation (2)

$$(\eta W_L\%) = \left[\frac{(W - W')}{W} x100 \right] \quad (2)$$

where W and W′ is the corrosion rate of the MS coupons in the absence and presence of inhibitor respectively[4]. The surfaces of the MS coupons were examined using Olympus Japan make BX 51 model optical microscope.

Electrochemical methods for corrosion rate measurement

Most corrosion phenomena are of electrochemical nature and consist of reactions on the surface of the corroding metal. Therefore electrochemical test methods can be used to characterise corrosion mechanism and predict corrosion rates. Electrochemical methods are used routinely for the evaluation of the efficiency of corrosion inhibitors[30,31]. The advantages of electrochemical methods are short measurement time and mechanistic information that they provide which help not only in the design of corrosion protection strategies but also in the design of new inhibitors.

When a metal is immersed in a given solution, electrochemical reactions characteristic of the metal solution interface occur at the surface of the metal, assuming the metal to corrode. These reactions create an electrochemical potential called the corrosion potential E_{corr} or open circuit potential at the metal solution interface. At the E_{corr} the rate of oxidation process is equal to rate of reduction. At E_{corr} the system is electronically neutral and said to be at equilibrium. The value of either the anodic or cathodic current at E_{corr} is called corrosion current i_{corr} .

Calculation of corrosion rates requires determination of corrosion currents. The corrosion rate is decided by the current produced in the oxidation and reduction reactions. The amount of current is controlled by the kinetics of the reactions and the diffusion of reactants both towards and away from the electrode. The measurement of corrosion rate is actually equivalent

to the determination of kinetics of the corrosion electrochemical process. The common electrochemical techniques used for the determination of corrosion rates and the characterisation of corrosion systems are potentiodynamic polarization and electrochemical impedance spectroscopy.

Potentiodynamic polarization method

The theoretical model used for the corrosion process assumes that the electrochemical corrosion is an activation controlled process. In activation controlled process, an activation controlled reaction is involved for which the rate of reaction is controlled solely by the rate of the electrochemical charge transfer process at the metal surface.

The Butler-Volmer equation

The fundamental formula describing the kinetics of an electrochemical reaction is the Butler-Volmer equation developed by Butler and Volmer[30,31]. The relationship between current density and potential of anodic and cathodic electrode reactions under charge transfer control is given by the Butler – Volmer equation as shown in the equation (3)

$$i = i_{corr}\left[\exp\left(\frac{\alpha n F}{RT}\eta\right) - \exp\left(\frac{-\beta n' F}{RT}\eta\right)\right] \qquad (3)$$

where η is the over potential defined as the difference between applied potential E and corrosion potential E_{corr} , $\eta = E\text{-}E_{corr}$, i is the measured current density, i_{corr} is the corrosion current density, F is Faraday's constant, R is the

Universal gas constant, T is the absolute temperature, n and n' are the number of electron transferred in the anodic and cathodic reactions, and α and β are coefficients related to the potential drop through the electrochemical double layer[32]. While the Butler-Volmer equation is valid over the full potential range, for practical applications to calculate the electrochemical corrosion current, it has to be simplified for more restricted ranges of potential. The two most commonly used simplified forms of the Butler –Volmer equation are Tafel equation and the Stern–Geary equation**.**

The Tafel Equation and Tafel plots

The Tafel equation was first found empirically by Tafel in 1905[1]. This can be deduced from the equation (3) for sufficiently high values of applied potential. As over potentials, either positive or negative, become larger than about $5x10^{-2}V$, the second or the first term of Butler-Volmer equation becomes negligible, respectively.

For anodic polarization, when $\eta >> RT/\beta n'F$, the following equation are obtained.

$$i = i_{corr}\left[\exp\left(\frac{\alpha nF}{RT}\eta\right)\right] \tag{4}$$

$$\text{i.e. } \eta = -\frac{2.303RT}{\alpha F}\log i_{corr} + \frac{2.303RT}{\alpha F}\log i \tag{5}$$

or , for cathodic polarization, when $-\eta >> RT/\alpha nF$

$$i = i_{corr}\left[\exp\left(\frac{-\beta n' F}{RT}\eta\right)\right] \quad (6)$$

$$\text{i.e}\ , \ -\eta = -\frac{2.303RT}{\beta F}\log i_{corr} + \frac{2.303RT}{\beta F}\log i \quad (7)$$

The equations (5) and (7) have the form of Tafel equation as shown in the equation (8)

$$|\eta| = a + b \log i \quad (8)$$

where a and b are constants, $a = -\frac{2.303RT}{\alpha F}\log i_{corr}$ and $b = \frac{2.303RT}{\alpha F}$ for anodic polarization or $a = -\frac{2.303RT}{\beta F}\log i_{corr}$ and $b = \frac{2.303RT}{\beta F}$ for cathodic polarization.

Hence, simple exponential relationships between current i.e. rate and over potential are obtained, or the over potential can be considered as logarithmically dependent on the current density.

A plot of electrode potential versus the logarithm of current density is called the "Tafel plot" and the resulting straight line the "Tafel line". The slope of a Tafel plot, "b", provides information about the mechanism of the reaction. The intercept "a" at $\eta = 0$ gives the exchange current density i_0 and provides information about the rate constant of the reaction. This type of analysis is referred to as Tafel slope analysis. The percentage inhibition efficiency is calculated using the corrosion current densities using the relation,

$$\eta_{pol}\% = \frac{i_{corr} - i'_{corr}}{i_{corr}} x100 \quad (9)$$

where i_{corr} and i'_{corr} are uninhibited and inhibited corrosion current densities respectively[5,25].

Electrochemical impedance spectroscopy (EIS)

Electrochemical impedance spectroscopy is a powerful technique for the characterisation of electrochemical systems and provides a wealth of kinetic and mechanistic information. For this reason this technique is being applied to an increasing extent to understand corrosion process in solution, to study rate determination, inhibitor performance, coating performance and passive layer characteristics[33-39].

Impedance, Z, is a measure of a circuit's tendency to resist (or impede) the flow of an alternating electrical current. The EIS instrument records the real (resistance) and imaginary (capacitance) components of the impedance response of the system. In EIS measurements, frequency dependent impedance $Z(\omega)$ is obtained by applying a sinusoidal alternating potential signal to test system in a range of frequencies. The expression for $Z(\omega)$ is as follows

$$Z(\omega) = \frac{V(t)}{I(t)} = \frac{V_0 \sin \omega t}{I_0 \sin(\omega t + \theta)} = Z'(\omega) + jZ''(\omega) \quad (10)$$

where ω = frequency, t= time, V(t) = sinusoidal alternating potential signal, V_o Sinωt, I(t) time dependent current response, I_o sin (ωt +θ), and θ = phase angle between V(t) and I(t).

Impedance is given by a complex number with real Z′(ω) and imaginary Z″(ω) component as given in the equation (11)

$$Z(\omega) == Z'(\omega) + jZ''(\omega) \qquad (11)$$

where j =√-1 .

EIS applies very small voltages generally in the range of 5 to 10mV between a specimen and a reference electrode. A typical electrochemical impedance experimental set up consists of an electrochemical cell (the system under investigation), a potentiostat/galvanostat, and a frequency response analyzer (FRA). The FRA applies the sine wave and analyses the response of the system to determine the impedance of the system.

When the impedance is measured at a number of frequencies and is plotted on the Cartesian axes, the resulting plot is called a Nyquist plot some time referred as Cole–Cole plot or a Complex plane plot with Z′(ω) versus Z″(ω) is obtained as shown in the figure 4.2.1. In the figure 4.2.1 R_Ω is the uncompensated resistance between the working electrode and reference electrode or solution resistance, R_p is the polarization resistance at the electrode/solution interface. At high frequencies, the impedance of the system is almost entirely created by the ohmic resistance (solution resistance) R_Ω. The frequency reaches its high limit at the leftmost end of the semicircle,

where the semicircle touches the x axis. The frequency reaches its low limit at the rightmost end of the semicircle.

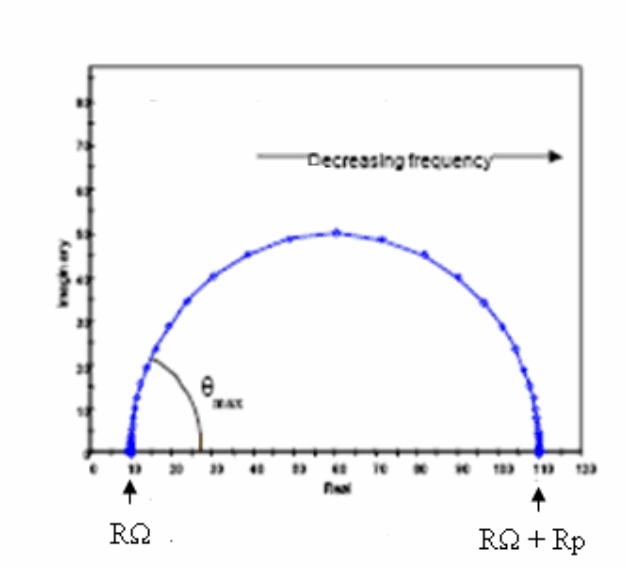

Figure 4. 2. 1 A typical Nyquist plot for a simple corrosion of metal

Polarization resistance is correlated unequivocally to the corrosion current density in the relatively simple corrosion systems characterised by a charge transfer controlled process[40]. Since R_p is inversely proportional to the corrosion current it can be used to calculate the inhibitor efficiency from the relation

$$\eta_{EIS}\% = \frac{R_p - R'_p}{R_p} x100 \qquad (12)$$

where R_p and R'_p denote polarization resistance of electrode with and without inhibitor respectively[4].

Equivalent circuit model

The characterisation of electrochemical systems with impedance spectroscopy requires the interpretation of the data with the help of suitable models. These models can be divided into two broad categories, equivalent circuit model and process model. These models are regressed to experimental data to estimate parameters that can describe the experimental data adequately and can be used to predict the behaviour of the system under various conditions. Electrochemical systems such as coated surfaces or corroding metals often behave like simple electronic circuits. The equivalent circuit is a simple circuit which can be built from electronic parts which behaves exactly in the same manner of an electrochemical system built from electrodes and electrolytes when an alternating current is applied. These models are built with the help of well-known passive elements such as resistors, capacitors, and inductors and distributed elements such as constant phase element and Warburg impedance. These elements can be combined in series and parallel to give complex equivalent circuits and certain physical meaning is then assigned to the various elements of the equivalent circuit[37, 38].

Experimental set up for electrochemical measurements

The electrochemical experiments potentiodynamic and EIS were carried out using a computer controlled Autolab make Metro Ohm PGSTAT 30 model potentiostat/galvanostat having a frequency response analyzer set

up. A three electrode cell consisting of a working electrode, a platinum counter electrode and a saturated calomel electrode (SCE) as a reference electrode were used for the measurements.

The polished MS coupon with an exposed area of 1cm^2 was used as the working electrode. 1M HCl acid was taken as electrolyte. The working electrode was immersed in the test solution for 2 hours prior to the measurements to establish a steady state open circuit potential

The potentiodynamic polarization (Tafel plot method) curves were obtained with a scan rate of 5 mV/Sec in the potential range from -250mV to +250mV relative to the open circuit potential. All the potentials reported versus that of the SCE. Corrosion current density values were obtained by Tafel extrapolation method. The percentage inhibition efficiency is calculated using the corrosion current densities using the relation (9).

The three electrode cell and other setup used for potentiodynamic polarization were used for the EIS measurements along with a Frequency response analyzer. EIS measurements were performed at open circuit potential in the frequency range from 20 kHz to 20 mHz with a 5 mV sine wave as excitation signal.

From impedance measurements, the percentage inhibition efficiency is calculated using the expression (12)

Adsorption isotherm studies

Adsorption plays an important role in the inhibition of metallic corrosion by organic inhibitors. Adsorption isotherms are often shown to demonstrate the performance of organic adsorbent type inhibitors and important in determining the mechanisms of organic electrochemical reactions. Establishment of isotherms that describe the adsorptive behaviour of a corrosion inhibitor is an important part of its study as they can provide important clues to the nature of metal inhibitor interaction. Three types of adsorption isotherms are usually cover all the data relating to adsorption isotherms. The most frequently used adsorption isotherms are Langmuir, Temkin and Frumkin isotherms having the following surface coverage–bulk concentration relationships[1]:

for Langmuir isotherm, $$\frac{\theta}{1-\theta} = KC \qquad (13)$$

for Frumkin isotherm, $$\frac{\theta}{1-\theta} e^{f\theta} = KC \qquad (14)$$

for Temkin isotherm, $$e^{f\theta} = KC \qquad (15)$$

where θ is the degree of surface coverage, C is the inhibitor concentration in the solution and K is the equilibrium constant or the molecular interaction constant, a coefficient expressing interaction between adsorbed and adsorbing molecule. The plots are usually given as $\log\frac{\theta}{1-\theta}$ versus log C for Langmuir

isotherm, $\log \frac{\theta}{C(1-\theta)}$ versus θ for Frumkin isotherm and θ versus log C for Temkin isotherm. The plots which give straight line will be best suitable adsorption isotherm. The values of θ can be calculated from the percentage inhibition efficiency values obtained from weight loss method using the following relation [25].

$$\theta = \frac{\text{Percentage inhibition efficiency}}{100} \tag{16}$$

Calculation of thermodynamic parameters

The values of activation energy for steel corrosion reaction (E_a) were obtained from Arrhenius equation. The activation energy values were calculated from the slopes of the log(corrosion rate) vs 1/T plots[26,42,43]. The equilibrium constant for adsorption process is related to the free energy of adsorption, ΔG_{ads} by the relation

$$\Delta G_{ads} = -RT \ln (55.5 K_{ads}) \tag{17}$$

where R is universal gas constant, T temperature in absolute scale, K is the equilibrium constant for adsorption process and 55.5 concentration of water in the solution[5,41]. The K_{ads} is given by the relation

$$K_{ads} = \frac{\theta}{(1-\theta)C_{inh}} \tag{18}$$

where θ is the degree of coverage on the metal surface and C_{inh} the concentration of inhibitor in mol L^{-1}.

Instruments

The following instruments are used for this study.

1. Philps Netherlands make PW 2400 model X-ray fluorescence (XRF) spectrophotometer
2. LeCo VC -50 USA make diamond wheel cutting machine
3. Olympus Japan make BX 51 model optical microscope
4. Autolab make MetroOhm PGSTAT 30 model Potentiostat/ Galvanostat having a frequency response analyzer set up with computer control.

CHAPTER 3
CORROSION INHIBITION STUDIES OF SCHIFF BASES ON MILD STEEL IN 1M HCl

The results of weight loss experiments and electrochemical analysis carried out to find the corrosion inhibition efficiencies of Schiff bases FTSC, FATP, FAP and FSC on MS in HCl are presented in this chapter.

Weight loss method

The weight loss occurred for the MS coupons immersed in blank, 0.0001M, 0.0002M, 0.0004M, 0.001M, 0.002M, 0.003M, 0.004M and 0.008M inhibitor solutions of Schiff bases FTSC, FATP, FAP and FSC prepared in 1M HCl solution, after 24 hours are given in table 4.3.1. The figure 4.3.1 is the photograph of MS coupons after 48 hours immersion in blank and different concentrations of FTSC inhibitor solutions. It is clear from the photograph that the coupons immersed in the inhibitor solutions were least corroded while the coupon in blank solution was severely corroded. With increase in concentration a film formation on the surface of coupons were observed. The optical microscopic images of the immersed MS coupons for 24 hours in the blank solution and 0.003M solution of FATP are given in the figure 4.3.2. The surface of the MS coupons immersed in the blank solution was completely corroded as visible in the picture 4.3.2 (a). The surface of the MS coupon immersed in the 0.003M FATP solution was

less corroded as observed in the figure 4.3.2(b) showing the inhibition capacity of the inhibitor used. The weight loss recorded in 24 hours interval for MS coupons immersed in the above eight concentrations of inhibitor solutions of FTSC, FATP, FAP, FSC and blank for seven days duration were plotted against immersion time and given in the figures 4.3.3 to 4.3.6.

Table 4. 3. 1 Weight loss occurred for MS in 24 hours time with and without inhibitor

Concentration [M]	Weight loss (mg/cm^2)			
	FTSC	**FATP**	**FAP**	**FSC**
Blank	162.66			
0.0001	35.42	48.47	63.27	158.53
0.0002	20.77	31.86	47.49	154.10
0.0004	8.77	24.07	40.48	149.68
0.001	4.55	12.16	27.43	74.05
0.002	3.48	12.91	20.32	54.53
0.003	2.14	5.39	16.77	39.89
0.004	3.27	3.57	9.76	38.88
0.008	2.36	2.14	5.23	26.36

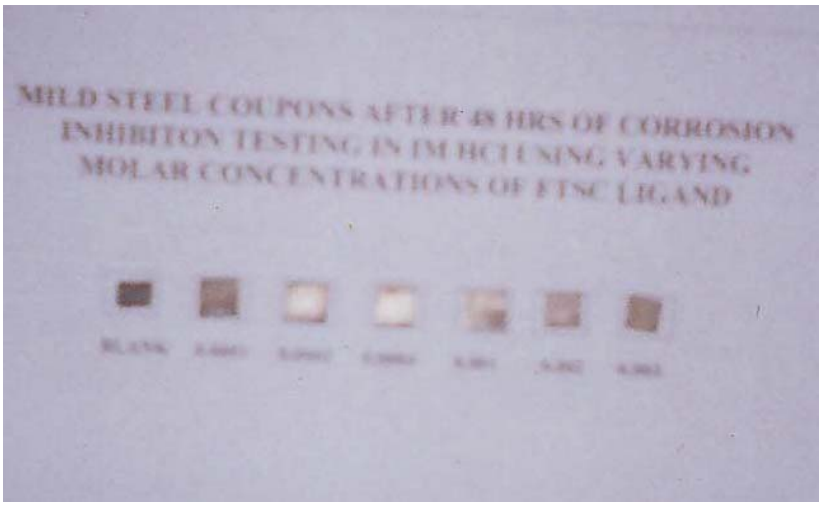

Figure 4. 3. 1 Photograph of MS coupons taken out after 48 hours immersion in blank and FTSC inhibitor solutions. From left to right- blank, 0.0001M, 0.0002M, 0.0004M, 0.001M, 0.002M, 0.003M of FTSC

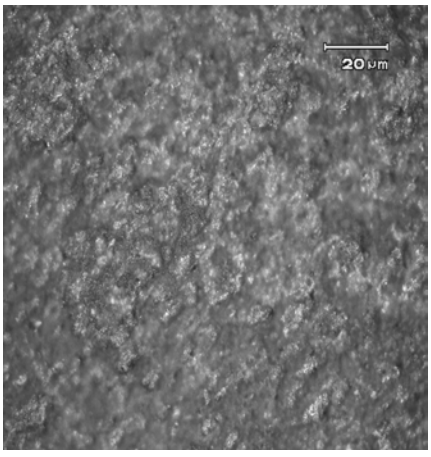

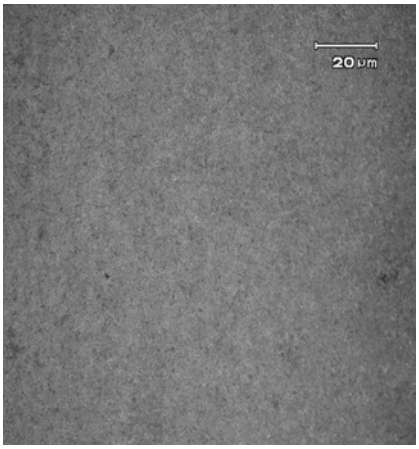

(a) **(b)**

Figure 4. 3. 2 Optical microscope images of MS coupons after 24 hours immersion (a) blank and (b) 0.003 M FATP inhibitor solution

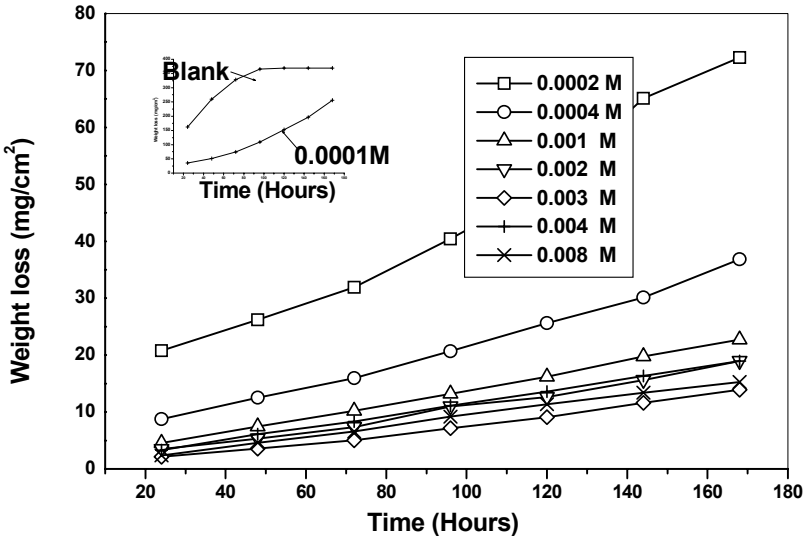

Figure 4. 3. 3 Comparison of weight loss occurred for MS coupons immersed in different concentrations of FTSC and blank for seven days. (The weight loss for the Blank and 0.0001M are given as insert graph)

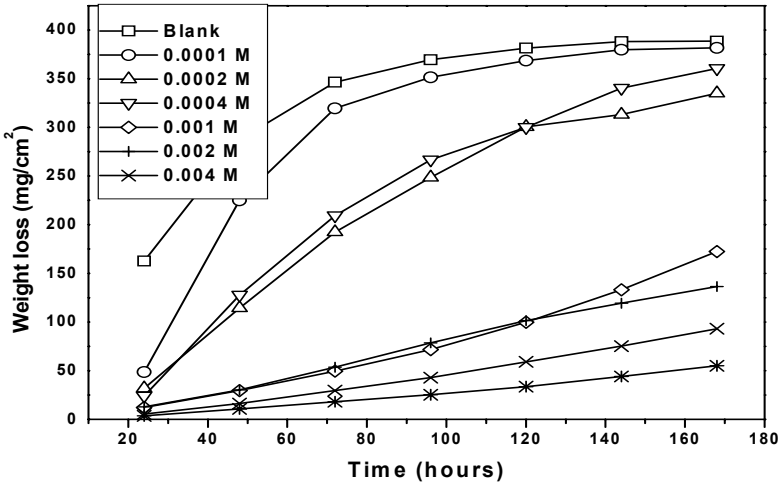

Figure 4. 3. 4 Comparison of weight loss occurred for MS coupons immersed in different concentrations of FATP and blank for seven days

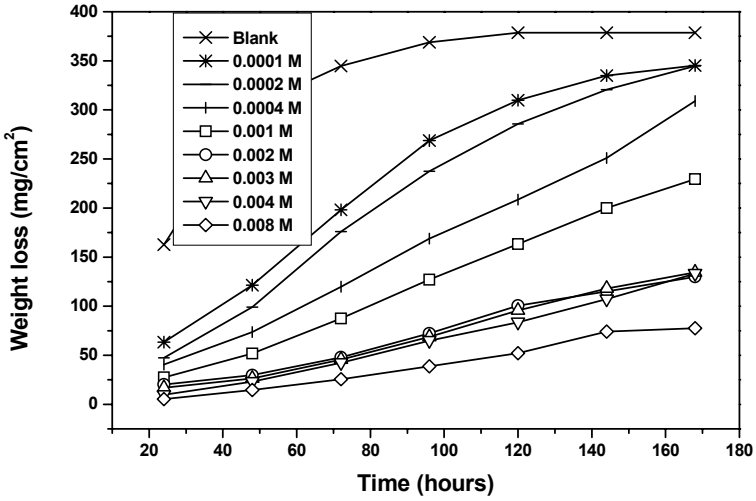

Figure 4. 3. 5 Comparison of weight loss occurred for MS coupons immersed in different concentrations of FAP and blank for seven days

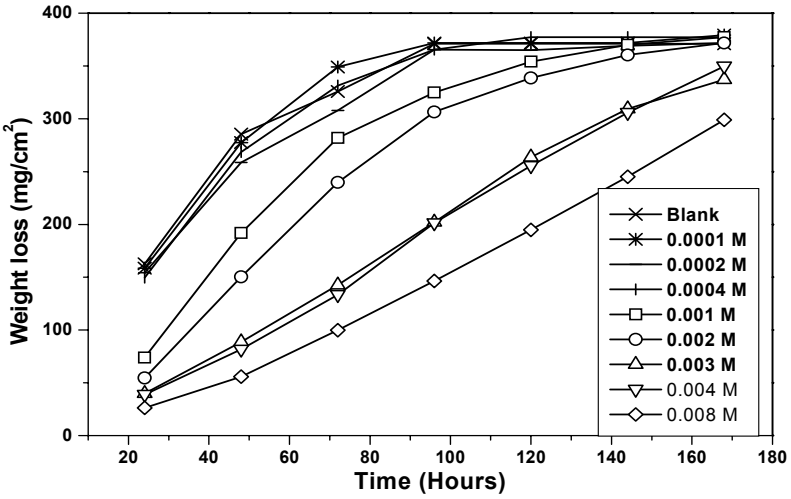

Figure 4. 3. 6 Comparison of weight loss occurred for MS coupons immersed in different concentrations of FSC and blank for seven days

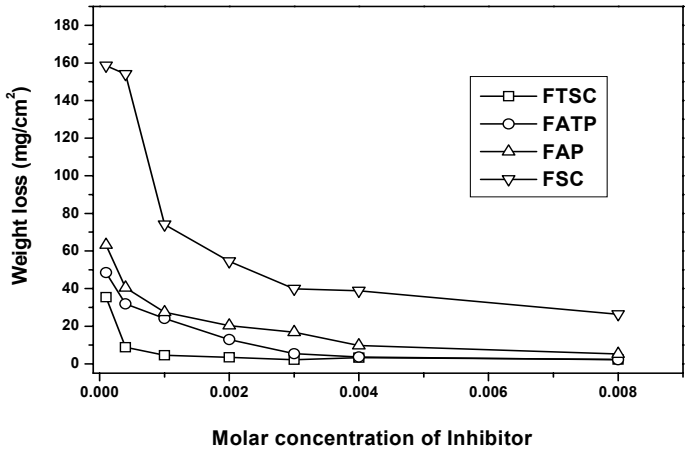

Figure 4. 3. 7 Comparison of weight loss of MS immersed in FTSC, FATP, FAP and FSC inhibitor solutions for 24 hours time.

Minimum weight loss was occurred for the coupons immersed in the inhibitor solution with high concentrations. Similar trends of decreasing the weight loss with increase in inhibitor concentration were noticed for all Schiff base studied. The loss of weight of the coupons in acid solutions was more in the case of FSC and least in the case of FTSC. Among the studied Schiff bases weight loss was decreasing in the order FTSC<FATP<FAP<FSC as shown in the figure 4.3.7. It is clear from figures 4.3.3 to 4.3.6 that, the weight loss of Schiff bases containing systems fall below, with respect to Schiff bases free system indicating the inhibitive properties of the four Schiff bases.

Corrosion rates and percentage inhibition efficiency

The corrosion rates expressed in mm/year of the MS specimens in 1M HCl with and with out the presence of different concentrations are calculated from the weight loss values recorded at room temperature. The corrosion rates of FTSC, FATP, FAP and FSC for the first 24 hours are given in the table 4.3.2.

Table 4. 3. 2 Corrosion rates observed for different concentrations of inhibitors studied for 24 hours

Concentration [M]	Corrosion rate (mm/year)			
	FTSC	**FATP**	**FAP**	**FSC**
Blank	75.35			
0.0001	16.41	22.45	29.31	73.43
0.0002	9.62	14.76	22.0	71.37
0.0004	4.06	11.15	18.75	69.33
0.001	2.10	5.63	12.71	34.30
0.002	1.61	5.98	9.41	25.29
0.003	0.99	2.50	7.77	18.48
0.004	1.52	1.66	4.52	18.00
0.008	1.09	0.99	2.42	12.23

It was observed that the corrosion rate was decreasing with increase in concentration of the Schiff base inhibitor used. The lowest corrosion rates were observed for the higher concentrations of inhibitor solutions. FTSC has shown least corrosion rates among the four Schiff bases studied.

The percentage inhibition efficiencies of the Schiff base inhibitors towards the MS in 1M HCl were found out from the corrosion rates obtained for 24 hours and are given in the table 4.3.3.

Table 4. 3. 3 Corrosion inhibition efficiencies obtained for FTSC, FATP, FAP and FSC inhibitors

Concentration [M]	FTSC η W_L%	FATP η W_L%	FAP η W_L%	FSC η W_L%
0.0001	78.82	70.2	61.00	2.53
0.0002	87.23	80.4	70.80	5.28
0.0004	94.61	85.2	75.11	7.98
0.001	97.21	92.52	83.12	54.47
0.002	97.86	92.06	87.51	66.47
0.003	98.68	96.68	89.69	75.47
0.004	97.98	97.80	94.00	76.00
0.008	98.55	98.68	96.79	83.80

In the case of FTSC an efficiency of ≈95% was achieved for a comparatively lower concentration of 0.0004M equivalent to 106ppm (0.016%) and a maximum efficiency of 98.68% at concentration of 0.003M corresponding to 796ppm (0.0796%). It is also observed that the inhibition efficiency of the FTSC was not further increased after 0.003M. 0.003 M is found to be the optimum concentration for FTSC. In the case of FATP more than 90% efficiency was obtained for 0.001M corresponding to 300ppm (0.03%) and maximum of 98.68% for 0.008M corresponding to 2400 ppm (0.12%). In the case of FAP 90% efficiency attained for a concentration of 0.003M corresponding to 850ppm (0.085%) and a maximum of 96% at 0.008M. Among the four Schiff bases studied the lowest inhibition efficiency was observed in the case of FSC with a maximum efficiency of 83.5% achieved at the highest concentration of 0.008M corresponding to 2286ppm (0.2286%).

To compare the performance of the Schiff bases, the percentage inhibition efficiencies obtained were plotted against the concentrations of inhibitor solutions used and are shown in the figure 4.3.8. It has been found that all these Schiff bases inhibit the corrosion of MS in HCl solution at all concentrations used in this study except in the case of few lower concentrations of FSC. It is also noticed that the inhibition efficiency for all these compounds increase with increase in the concentration of inhibitor.

Among the four Schiff bases studied the FTSC shows maximum inhibition efficiency and follows the order FTSC>FATP>FAP>FSC

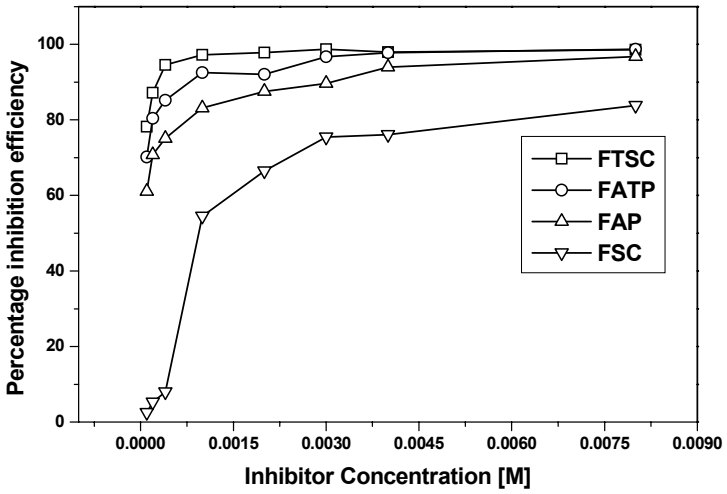

Figure 4. 3. 8 Plot of percentage inhibition efficiencies against the concentration of Schiff bases FTSC, FATP, FAP and FSC.

Effect of Temperature on the performance of Schiff base inhibitors

To study the effect of temperature on the inhibition efficiency, weight loss measurements of MS specimens were carried at three different temperatures 30°C, 40°C and 50°C with 0.003 M inhibitor solution of the Schiff bases FTSC, FATP, FAP and FSC. The weight loss recorded, corrosion rate and percentage inhibition efficiency are given in the table 4.3.4. The percentage inhibition efficiencies obtained for four Schiff bases at different temperatures are plotted and shown in the figure 4.3.9. Inhibition efficiencies found to decrease with increase in temperature.

Table 4. 3. 4 Weight loss, corrosion rate and percentage inhibition efficiency of 0.003M solutions of FTSC, FATP, FAP and FSC at different temperatures

Inhibitor	Temp. (°C)	Weight loss (mg/cm^2)	Corrosion rate (mm/year)	Per. inhibition efficiency ($\eta W_L\%$)
Blank	30	162.66	75.35	-
	40	207.80	96.25	
	50	319.18	147.84	
FTSC	30	2.14	0.99	98.68
	40	7.59	3.51	96.35
	50	13.76	6.37	95.68
FATP	30	5.39	2.50	96.68
	40	16.52	7.65	92.05
	50	31.58	14.63	90.10
FAP	30	16.77	7.77	89.69
	40	28.46	13.18	86.3
	50	58.37	27.04	71.90
FSC	30	39.89	18.48	75.47
	40	72.66	33.65	65.03
	50	162.58	75.31	49.06

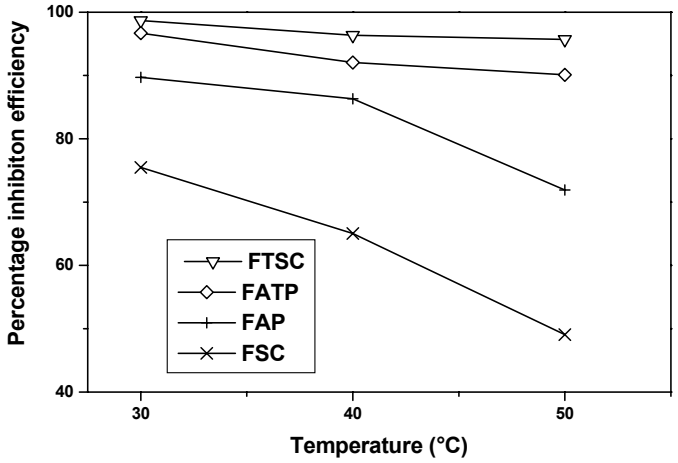

Figure 4. 3. 9 The percentage inhibition efficiency of 0.003M FTSC, FATP, FAP and FSC at different temperatures

Comparison of inhibition efficiency of Schiff base and its parent amine

To compare the inhibition efficiency of the Schiff base furoin thiosemicarbazone and its parent amine, the weight loss measurements of the MS specimens in 1M HCl containing various concentrations of furoin thiosemicarbazone and thiosemicarbazide inhibitor solutions were carried out at room temperature (30°C). The percentage inhibition efficiencies obtained are plotted against concentration and given in the figure 4.3.10. It was found that inhibition efficiency of the Schiff base FTSC was more than the corresponding amine, thiosemicarbazide.

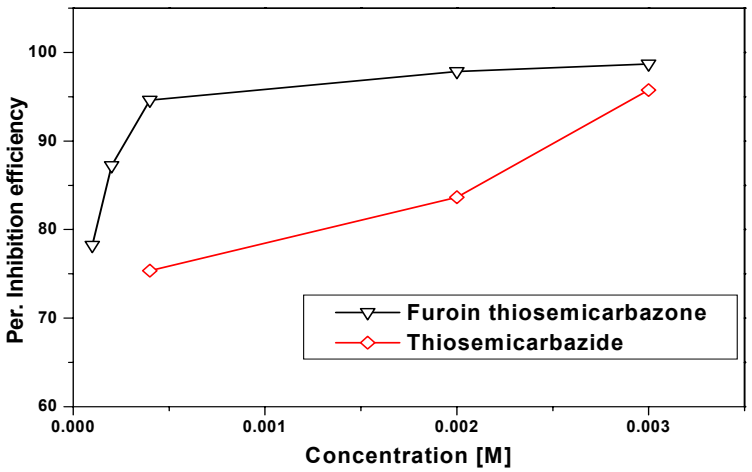

Figure 4. 3. 10 Plot of percentage inhibition efficiency against different concentration of FTSC and thiosemicarbazide

Potentiodynamic polarization studies

Typical Tafel polarization curves obtained for MS in 1M HCl with and without the presence of different concentrations of FTSC are shown in the figure 4.3.11. Various corrosion parameters such as corrosion potential (E_{corr}), corrosion current density (i_{corr}) and percentage inhibition efficiency, (η_{pol} %) are given in table 4.3.5.

It is observed that the presence of Schiff base inhibitor lowers i_{corr} values. The corrosion current obtained for MS coupons tested in the FTSC inhibitor solutions are lower than solution without FTSC i.e. blank. This shows that the presence of FTSC lowers i_{corr} values. A lowest i_{corr} value was observed for a FTSC concentration of 0.002M. The percentage inhibition

efficiency increases with increase in the inhibitor concentrations and a maximum efficiency of 97.68 % was obtained for a low concentration of 0.002M corresponding to 531ppm (0.0053%). The inhibition efficiency was found to remain constant after achieving maximum efficiency at 0.002M. This trend was also noticed in the case of weight loss measurements. It is also observed from the table that there is no significant change in E_{corr} values of inhibited and uninhibited systems.

Table 4. 3. 5 Electrochemical polarization parameters for MS in 1M HCl containing different concentrations of FTSC

Concentration [M]	E_{corr} (V)	i_{corr} (A/cm^2)	Per. inhibition efficiency (η_{pol} %)
Blank	-0.461	4.747×10^{-3}	-
FTSC 0.0001	-0.464	1.373×10^{-3}	71.08
FTSC 0.0002	-0.478	1.42×10^{-3}	70.09
FTSC 0.0004	-0.469	1.44×10^{-3}	69.67
FTSC 0.001	-0.469	9.755×10^{-4}	79.41
FTSC 0.002	-0.476	1.102×10^{-4}	97.68
FTSC 0.003	-0.457	4.361×10^{-4}	90.81
FTSC 0.004	-0.445	4.149×10^{-4}	91.26
FTSC 0.008	-0.476	3.992×10^{-4}	91.59

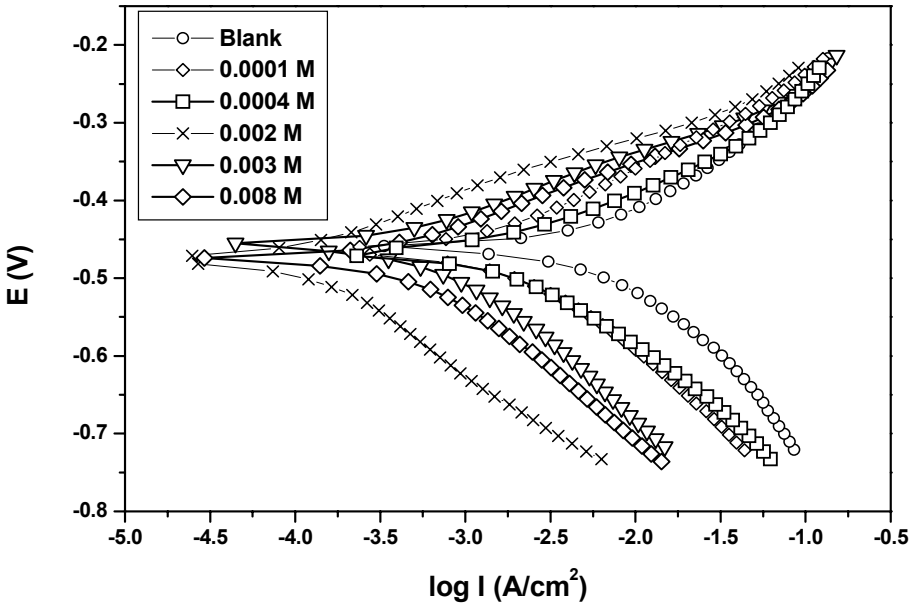

Figure 4. 3. 11 Tafel plots of MS in 1M HCl in presence of different concentrations of FTSC

The potentiodynamic polarization curves obtained for the other three Schiff bases FATP, FAP and FSC for an inhibitor concentration of 0.008M are shown in figure 4.3.12, to 4.3.14 and the electrochemical parameters obtained are summerised in table 4.3.6. The corrosion current densities for the 0.008 M solutions of the four Schiff bases are found to decrease in the order FSC>FATP>FAP>FTSC. The variation of percentage inhibition efficiencies achieved at 0.008 M were found to follow the order FTSC>FAP>FATP>FSC.

Table 4. 3. 6 Electrochemical polarization parameters for MS in 1M HCl containing 0.008 M of FTSC, FATP, FAP and FSC

Concentration of inhibitor [M]	E_{corr} (V)	i_{corr} (A/cm^2)	Per. inhibition efficiency (η_{pol} %)
Blank	-0.461	4.747×10^{-3}	-
FTSC 0.008	-0.476	3.992×10^{-4}	91.59
FATP 0.008	-0.425	1.212×10^{-3}	74.47
FAP 0.008	-0.441	3.953×10^{-4}	90.04
FSC 0.008	-0.456	2.532×10^{-3}	44.13

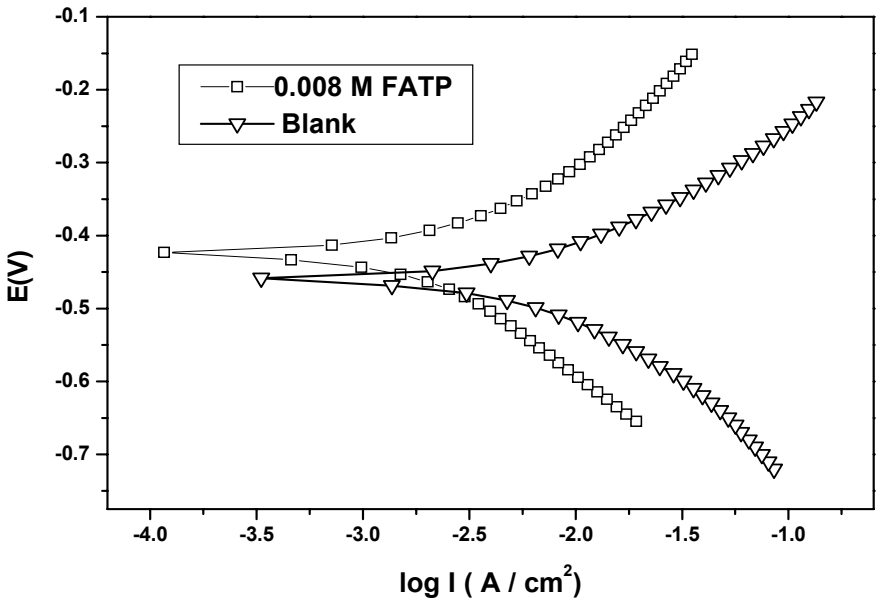

Figure 4. 3. 12 Tafel plots of MS in 1M HCl with and without 0.008 M FATP

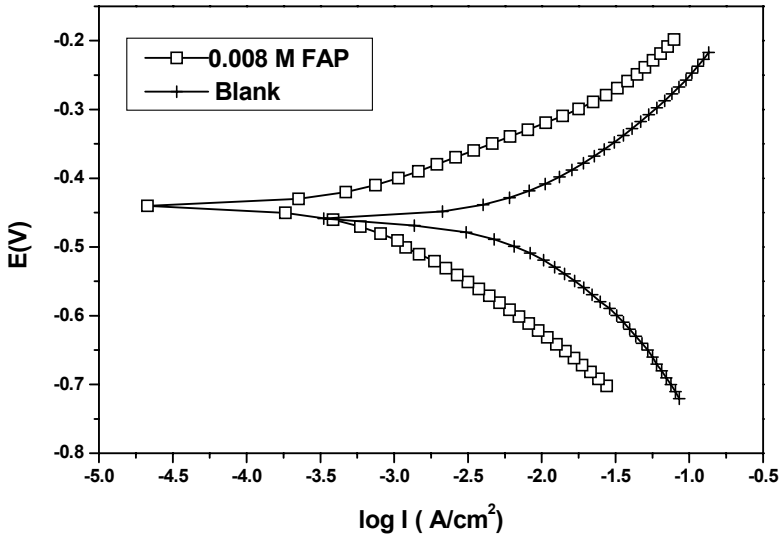

Figure 4. 3. 13 Tafel plots of MS in 1M HCl with and without 0.008 M FAP

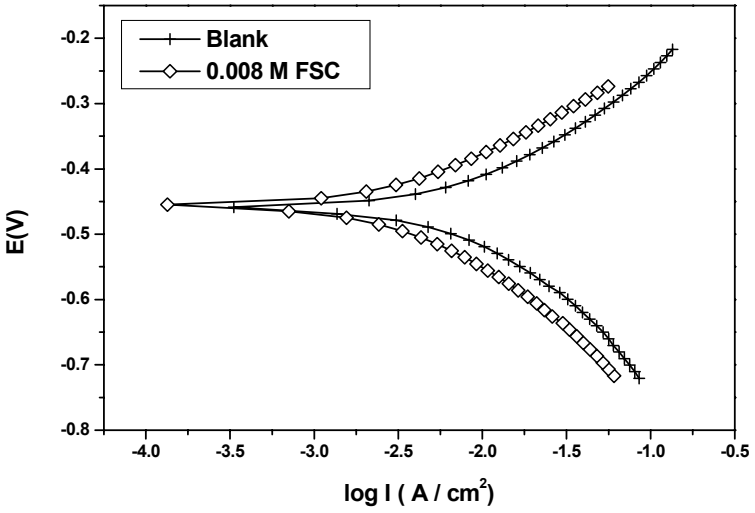

Figure 4. 3. 14 Tafel plots of MS in 1M HCl with and without 0.008 M FSC

Electrochemical impedance spectroscopy

Nyquist plots of MS in 1M HCl in the presence and absence of different concentrations of FTSC are shown in the figure 4.3.15. The impedance parameters like polarization resistance (R_p), solution resistance (R_s), constant phase element or double layer capacitance (CPE), n and percentage inhibition efficiency calculated from the R_p values are given in the table 4.3.7.

Table 4. 3. 7 Impedance parameters and inhibition efficiency for the corrosion of MS with and without different concentrations of FTSC

Con. [M]	R_s (ohm)	R_p (ohm)	CPE ($\mu F/cm^2$)	n	Per. inhibition efficiency (η_{EIS} %)
Blank	0.9523	4.69	279.53	0.8179	
0.0001	0.7904	10.60	164.50	0.8018	55.72
0.0002	1.0470	16.47	157.05	0.7998	71.50
0.0004	1.0846	11.20	129.57	0.8065	58.06
0.001	0.8800	13.65	114.99	0.7790	65.61
0.002	0.9811	146.92	11.48	0.7996	96.80
0.003	0.7947	45.95	69.01	0.8195	89.78
0.004	0.7946	54.13	102.69	0.7984	91.33
0.008	0.9473	53.05	36.75	0.7192	91.15

All the Nyquist plots obtained were semicircle in nature and display a single capacitive loop as seen in the figure 4.3.15. The diameter of the semicircles was increased with increase in inhibitor concentration. The results also show that R_p values were increased with increase in additive concentration. The percentage inhibition efficiencies calculated from the R_p indicate that the inhibition efficiency increases with increase in FTSC concentration. A maximum inhibition efficiency of 96.80% was achieved for the 0.002M FTSC and for further increase in concentration, inhibition efficiency remained almost same as observed in the weight loss and Tafel methods.

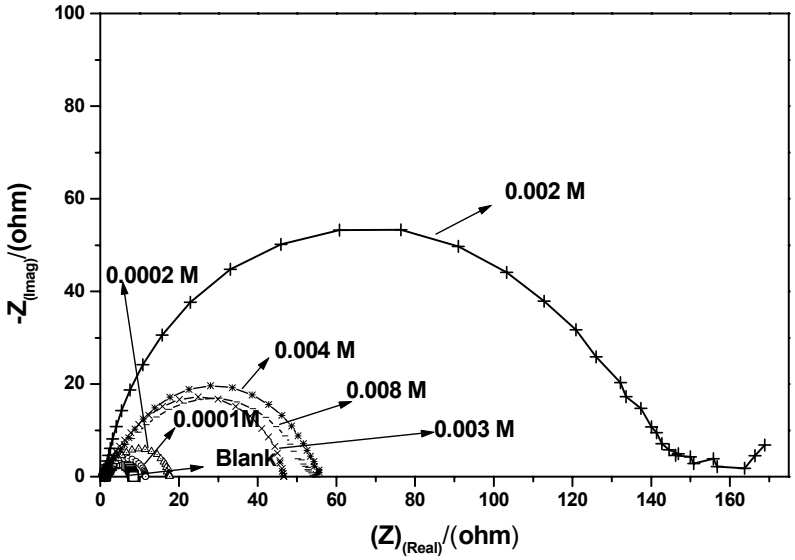

Figure 4. 3. 15 Nyquist plots for MS in 1M HCl in the presence and absence of different concentrations of FTSC

To study the inhibition efficiency of the other three Schiff bases FATP, FAP and FSC, EIS spectrum of the 0.008M solutions of these inhibitors were recorded as earlier. The Nyquist plot of the 0.008 M FTSC, FATP, FAP and FSC are given in the figure 4.3.16. The impedance parameters R_p, R_s, CPE, n and percentage inhibition efficiency, η_{EIS} % are given in the table 4.3.8. As in the case of FTSC, for other three Schiff bases also, the obtained Nyquist plots are semicircle shaped with one single capacitive loop. The diameter of semicircles and R_p values were varied with respect to their inhibition efficiency.

Table 4. 3. 8 Impedance parameters for corrosion of MS in 1M HCl with 0.008M solutions of FTSC, FAP, FATP and FSC.

Inhibitor	R_s (ohm)	R_p (ohm)	CPE ($\mu F/cm^2$)	n	Per. inhibition efficiency (η_{EIS} %)
Blank	0.9523	4.69	279.53	0.8179	-
FTSC	0.9473	53.05	36.75	0.7192	91.15
FATP	0.9668	26.85	46.39	0.6650	82.52
FAP	0.9932	47.15	67.41	0.7383	90.04
FSC	0.8317	8.08	267.86	0.8026	41.90

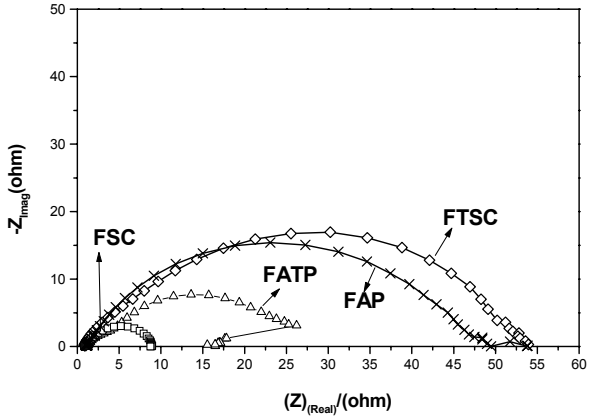

Figure 4. 3. 16 Nyquist plots for MS in 1M HCl in the presence of 0.008M FTSC, FATP, FAP and FSC

Adsorption isotherm studies

In order to understand the mechanism of corrosion inhibition, the adsorption behaviour of the organic adsorbate on the metal surface must be known. The degree of the surface coverage (θ) was evaluated from the weight loss measurement results of MS in 1 M HCl in the presence and absence of the four Schiff bases conducted at 30°C using the equation (16) of chapter 2. The values of surface coverage (θ) for four Schiff bases are given in the table 4.3.9. The data were tested graphically by fitting to various isotherms like Langmuir, Frumkin and Temkin isotherms. The Frumkin and Temkin isotherm did not yield a satisfactory description of the experimental adsorption behaviour. Among the three isotherms assessed Langmuir isotherm found to provide best description of the adsorption behaviour of the

investigated Schiff bases. The plots of $\log\frac{\theta}{1-\theta}$ versus logC give straight lines and shows that the adsorption of studied Schiff base obeys Langmuir adsorption isotherm. The Langmuir isotherm plots of FTSC, FATP, FAP and FSC are shown in the figures 4.3.17 to 4.3.20.

Table 4. 3. 9 The value of θ for the Schiff bases FTSC, FATP, FAP and FSC calculated from weight loss measurement results

Con. [M]	Degree of surface coverage (θ)			
	FTSC	FATP	FAP	FSC
0.0001	0.7822	0.7020	0.6110	0.0255
0.0002	0.8723	0.8040	0.7080	0.0528
0.0004	0.9461	0.8520	0.7512	0.0799
0.001	0.9721	0.9252	0.8313	0.5448
0.002	0.9798	0.9206	0.8751	0.6644
0.003	0.9868	0.9668	0.8969	0.7547
0.004	0.9798	0.9779	0.9400	0.7611
0.008	0.9855	0.9868	0.9679	0.8377

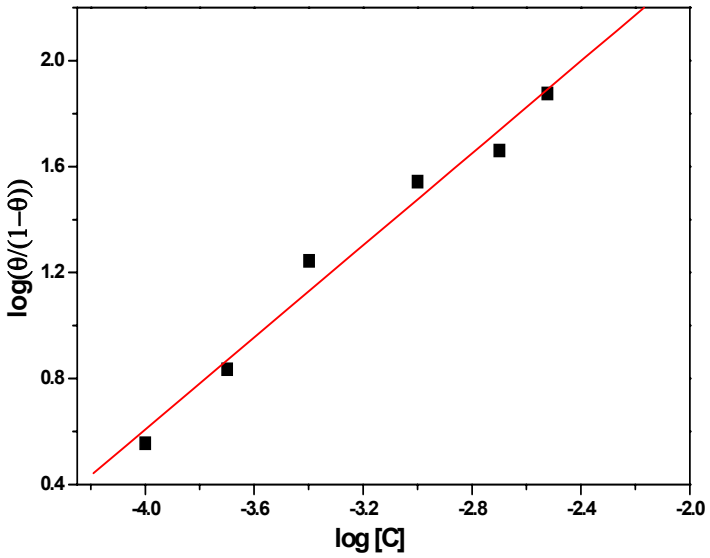

Figure 4. 3. 17 Langmuir adsorption isotherm of FTSC on MS in 1M HCl

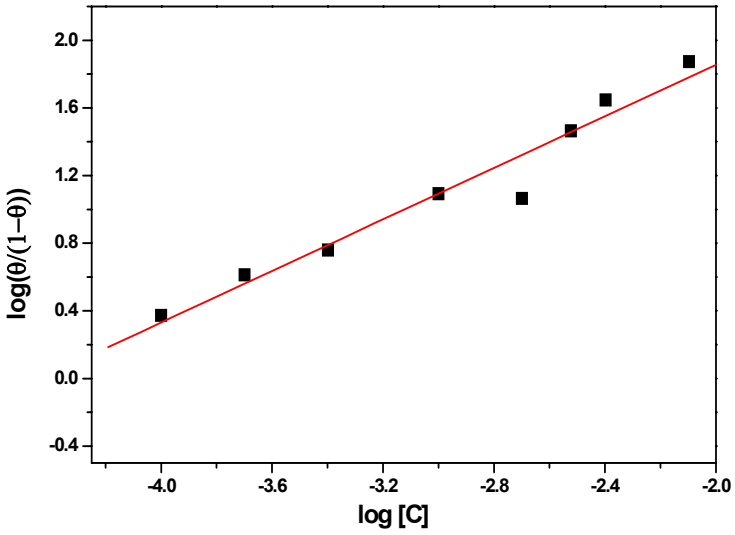

Figure 4. 3. 18 Langmuir adsorption isotherm of FATP on MS in 1M HCl

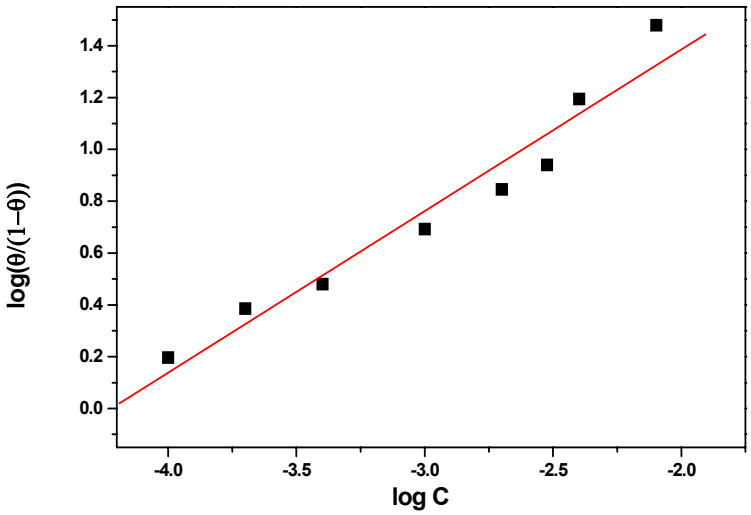

Figure 4. 3. 19 Langmuir adsorption isotherm of FAP on MS in 1M HCl

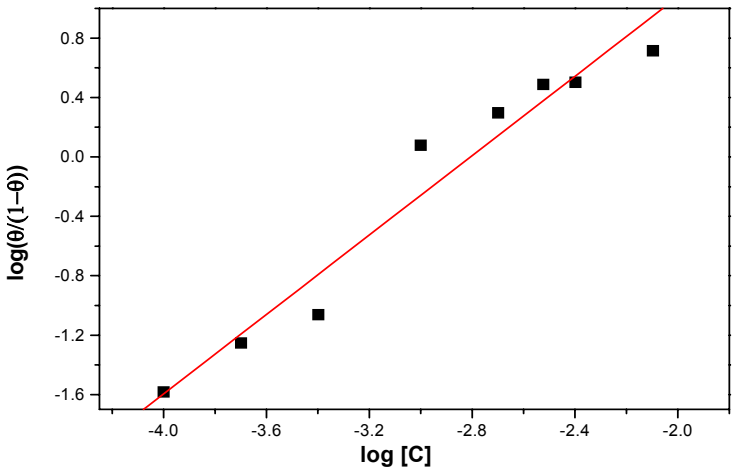

Figure 4. 3. 20 Langmuir adsorption isotherm of FSC on MS in 1M HCl

The activation energy for the corrosion of MS in IM HCl in the presence and absence of 0.003M FTSC, 0.003M FATP, 0.003M FAP and 0.003M FSC solutions are calculated using the Arrhenius equation. The logarithmic values of corrosion rates obtained at temperatures 30°C, 40°C and 50°C for the blank and 0.003 M FTSC, FATP, FAP and FSC are plotted against 1000/T. From the slope of these Arrhenius plots activation energies are calculated**.** The Arrhenius plots of blank, 0.003 M FTSC, 0.003 M FATP, 0.003 M FAP and 0.003 M FSC are shown in the figure 4.3.21. The activation energy for the corrosion of MS in 1M HCl in the presence of 0.003M solutions is given in the table 4.3.10.

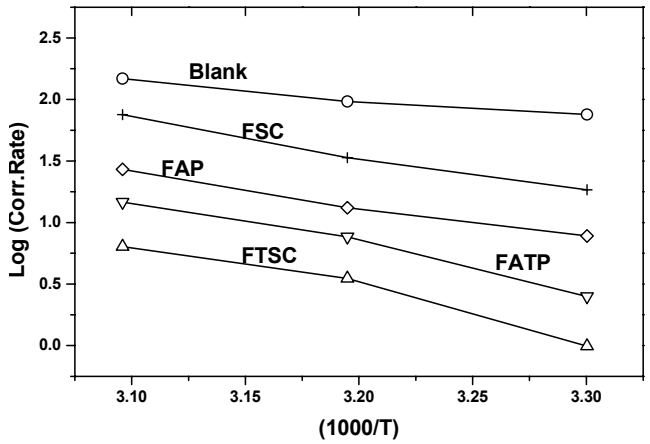

Figure 4. 3. 21 Plots of log corrosion rate vs. 1000/T for blank and 0.003M solutions of FTSC, FATP, FAP and FSC

Table 4. 3. 10 The activation energy and enthalpy of adsorption obtained for the Schiff base inhibitors

Schiff base	E_a($kJmol^{-1}$)	ΔH_{ads} ($kJmol^{-1}$)
Blank	27.28	-
FTSC	76.01	-49.871
FATP	72.07	-47.61
FAP	50.65	-49.52
FSC	57.06	-47.18

The free energy of adsorption (ΔG_{ads}) for the corrosion of MS in 1M HCl in the presence of four Schiff bases was calculated using the relation (17). The free energy of adsorption for the corrosion of MS in 1M HCl for the four Schiff bases is given in the table 4.3.11. The values for free energy of adsorption for the corrosion inhibition are negative.

The Langmuir adsorption isotherm may be expressed by the following equation[13]

$$\log \frac{\theta}{1-\theta} = \log A + \log C - \frac{Q_{ads}}{2.303RT} \qquad (19)$$

The heats of adsorption (Q_{ads}), obtained from the slopes of the linear portion of the log K_{ads} vs 1000/T curves which are equal to –Q/ (2.303 R). In

this case, values of Q_{ads} equal to enthalpy of adsorption (ΔH_{ads}) with good approximation, because pressure is constant. The ΔH_{ads} values obtained for the four Schiff bases FTSC, FATP, FAP and FSC are given in table 4.3.10. Entropy of inhibitor adsorption (ΔS_{ads}) is calculated using the equation[13]

$$\Delta G_{ads} = \Delta H_{ads} - T\Delta S_{ads} \quad (20)$$

The calculated ΔS_{ads} data at different temperature are given in table 4.3.11. It was found that all values are negative.

Table 4. 3. 11 The free energy of adsorption (ΔG_{ads}) and activation energy (E_a) obtained for the corrosion of MS in 1M HCl

Inhibitor	Temperature	ΔS (J/mol K)	ΔG_{ads} ($kJmol^{-1}$)
FTSC	30	-47.03	-35.62
	40	-50.42	-34.08
	50	-46.97	-34.70
FATP	30	-47.40	-33.24
	40	-50.05	-31.94
	50	-47.34	-32.316
FAP	30	-63.77	-30.20
	40	-61.23	-30.36
	50	-63.82	-28.91
FSC	30	-64.68	-27.58
	40	-63.90	-27.18
	50	-64.69	-26.28

The percentage inhibition efficiencies obtained from weight loss, potentiodynamic polarization and EIS method are compared and given in the table 4.3.12. The percentage inhibition efficiencies obtained are showing similar trend of increase in inhibition efficiency with increasing concentration and are close to each other.

Table 4. 3. 12 Percentage inhibition efficiencies obtained for MS in 1M HCl by weight loss, potentiodynamic polarization and EIS method.

Concentration [M]	(ηW_L %)	(η_{pol} %)	(η_{EIS} %)
FTSC 0.0001	78.22	71.08	55.72
FTSC 0.0002	87.23	70.09	71.50
FTSC 0.0004	94.61	69.67	58.06
FTSC 0.001	97.21	79.41	65.61
FTSC 0.002	97.86	97.68	96.80
FTSC 0.003	98.68	90.81	89.78
FTSC 0.004	97.98	91.26	91.33
FTSC 0.008	98.55	91.59	91.15

Discussion

The basic action of an inhibitor is attributed to an increase in over voltage of the hydrogen ion discharge as cathodic reaction of corrosion process or an increase in ohmic resistance of an inhibitor film at the metal electrolyte interface or due to some type of adsorption on the metal surface.[1] The organic inhibitors like Schiff bases generally inhibit the corrosion process through adsorption of the inhibitor on the metal solution interface[44]. The adsorption was considered either as physical adsorption or chemical adsorption. The physical adsorption may be due to the electrostatic attractive forces between ionic charges or dipoles on the adsorbed species and the electric charge on the metal at the metal/solution interface. The forces in electrostatic adsorption are generally weak. The inhibiting species adsorbed on the metal due to electrostatic force can also be desorbed easily. A main feature of the electrostatic adsorption is that the ions are not in direct physical contact with the metal. A layer of water molecule separates the metal from the ions. The physical adsorption process has low activation energy and is relatively independent of temperature[1].

In chemisorption the adsorbed species is in contact with the metal surface. A coordinate type of bond involving electron transfer from inhibitor to the metal is assumed to take place in the process[45]. The chemisorption process is slower than the electrostatic sorption that has higher activation energy. The temperature dependency shows that higher inhibition efficiencies

at higher temperatures. Unlike electrostatic adsorption, it is specific for certain metals and is not completely reversible.

Weight loss method

In this study it has been found that all the four Schiff bases FTSC, FATP, FAP and FSC inhibit the corrosion of MS in HCl at all concentrations of Schiff bases used. It can be seen that inhibition efficiency increases with increase in inhibitor concentration. All the inhibitors reduce the corrosion rate to a significant extent showing higher inhibition efficiencies. The results of the corrosion inhibition studies of four Schiff bases on MS in 1M HCl by weight loss measurements clearly indicates that all studied Schiff bases act as efficient corrosion inhibitors for MS in HCl media as reported in the similar type of Schiff base materials[4,5,12,13] .

It was also observed that the corrosion inhibition efficiency is increasing with increase in Schiff base concentration. The increase in the inhibition efficiencies for MS corrosion in 1M HCl with increasing Schiff base concentration suggests that inhibition is a result of adsorption of inhibitor on the metal surface and these compounds act as adsorption inhibitors[5].

It was observed that corrosion inhibition efficiency of all the four Schiff bases towards MS in 1M HCl was found to decrease with increase of temperature. The decrease in inhibition efficiency with increasing

temperature, suggest a weak adsorption interaction between MS surface and the additives, which is physical in nature[23]. This may due to desorption of some adsorbed molecule from the MS surface with increase of temperature[5,23]. This observation reiterates that type of adsorption is physical in nature because if the adsorption was chemisorption type then the efficiency will be increased with increase in temperature[26]. The inhibition efficiency of the Schiff base, furoin thiosemicarbazone was more than corresponding parent amine thiosemicarbazide. The presence of higher electron density of the -C=N– group which is not present in the parent amine is responsible for the higher inhibition efficiency of the Schiff base than its corresponding amine. Thus conversion of an amine to Schiff base increases its inhibition capacity [5,13,15,46].

Tafel plot analysis

The typical Tafel polarization curves obtained for different concentrations of FTSC and blank shows the change in shape of the cathodic and anodic curves. The corrosion parameters like i_{corr} values of the inhibited systems are lower than the uninhibited systems and i_{corr} values decreases with increase in concentration of FTSC. Thus the inhibition efficiency was increasing with increasing concentration of the Schiff base as reported earlier[4,5,13,15]. Increase in inhibition efficiency with increase of the concentration of the studied Schiff bases shows that inhibition actions are due

to the adsorption on steel surface[13]. It is also observed from the polarization results that there is no significant change in E_{corr} values of inhibited and uninhibited systems. This shows that the addition of studied Schiff bases affected both anodic and cathodic reaction suggesting that the Schiff base FTSC is a mixed type (anodic/cathodic) inhibitor [13,26].

The low values of the corrosion current obtained for the 0.008M solutions of FATP, FAP and FSC compared to the blank values also reveal the ability of these Schiff bases to inhibit the corrosion of MS in 1M HCl as proved by the weight loss method. The results obtained from the potentio-dynamic polarization method are in agreement with weight loss measurement results.

EIS method

The electrochemical impedance results of different concentrations of FTSC in 1M HCl clearly showing semicircle shaped Nyquist plots with increasing radii with increasing concentration of Schiff base FTSC. The appearance of single semi circle in all the cases corresponds to one capacitive loop[14]. It is apparent from these plots that the impendence response of MS in uninhibited HCl has significantly changed after the addition of Schiff bases in to the corrosive solutions. The semicircle shaped Nyquist plots indicate the formation of a barrier on the surface and a charge transfer process mainly controlling the corrosion of MS[17,47]. The polarization resistance R_p values

were found to increase with increasing Schiff base concentrations. The values of the constant phase element (CPE) are found to decrease with increase in concentration. This behaviour is generally seen for system where inhibition is the case and indicates the formation of a surface film by the adsorption of inhibitor on the metal surface[4,12,48]. The nature of CPE can be derived from the values of the n, which is purely resistive when n = 0, capacitive when n = 1 or inductive when n = -1. The values of n obtained for these systems are close to unity which shows that the interface behaves nearly capacitive[25]. The increase in the R_p values with increase in the Schiff base concentration indicates that inhibition is due to the adsorption of Schiff base on the MS [4,12].

In simple case, when corrosion is uniform and corrosion reactions are strictly charge transfer controlled, the electrode impedance Nyquist will be semicircle. This type of impedance behaviour can be explained with the help of a simple and commonly used equivalent circuit diagram as shown in the figure 4.3.22 which is composed of a constant phase element CPE, in parallel with a resistor, $R_{P,}$ which corresponds to a single capacitive loop. The resistor R_s is in series to the CPE and R_p. R_s is the uncompensated resistance between the working electrode and reference electrode or solution resistance, R_p is the polarization resistance at the electrode/solution interface, and CPE is the double layer capacitance at the interface. The double layer capacity is in parallel with the impedance due to the charge transfer reaction. These types of circuit have been used previously to model the iron /acid interface[4, 5,49].

The EIS studies clearly indicate that the Schiff base FTSC is a good corrosion inhibitor for MS in HCl medium. The efficiency of the inhibitor increases with increase in inhibitor concentration. Similar to the FTSC the other three Schiff bases also showing semicircle shaped Nyquist plots with higher radii and R_p values and ascertains their capacity to inhibit the corrosion of MS. The percentage inhibition efficiency calculated from the EIS measurement almost matches with the percentage efficiency obtained from Tafel plot analysis.

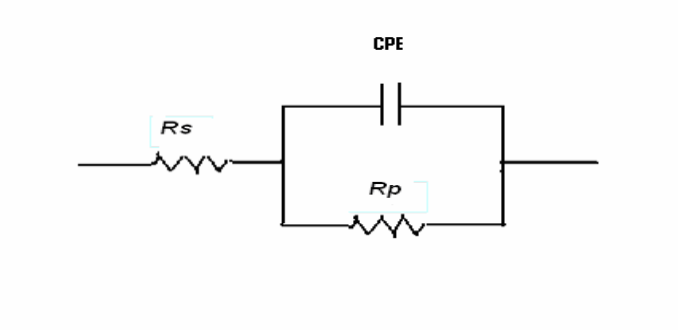

Figure 4. 3. 22 The equivalent circuit for the corrosion behaviour of MS in 1M HCl in the presence of Schiff base inhibitors

Adsorption isotherm studies

The adsorption of Schiff base was found to follow Langmuir adsorption isotherm in all the cases. The inhibiting effects deviate somewhat from the ideal Langmuir adsorption isotherm. It has been postulated in the derivation of the Langmuir equation that the adsorbed molecule do not interact with each other but this is not true in the case of organic molecule having polar atoms or groups which are adsorbed on the cathodic and anodic

sites of the metal surface. Such adsorbed species may interact by mutual repulsion or attraction[18].

Thermodynamic parameters calculated with help of the adsorption isotherm plots also gives indication of the type of adsorption process. The values of free energy of adsorption obtained for the four Schiff bases FTSC, FATP, FAP and FSC for the corrosion of MS in 1M HCl are -35.62, -33.24, -30.20 and -27.58 $kJmol^{-1}$ respectively. The low values of ΔG_{ads} below -40 $kJmol^{-1}$ indicate that adsorption of Schiff base on the MS is physical in nature i.e. physisorption[26,50]. The chemisorption process is mainly characterised by the large interaction potentials, which leads to high heats of adsorption often approaching to the value of chemical bond. The low and negative values of ΔG_{ads} indicate that the spontaneous adsorption of inhibitors on the surface of MS. The negative values of ΔG_{ads} also suggest the strong interaction of the inhibitor molecule on the MS surface[51,52]. The decrease in inhibition efficiency with increasing temperature suggests weak adsorption interaction which is physical in nature.

It is found that the E_a values for inhibited systems are higher than Ea values for the uninhibited systems which propose the conclusion that physical adsorption occurs in the first stage, explains the nature of organic molecule-metal interactions. On the other hand the higher values of activation energy obtained in spite of the lower Ea values of physisorption (30-50$kJmol^{-1}$) may

be due to competitive adsorption of water whose removal from the surface requires some more activation energy [13,22,53].

The negative values of Q_{ads} indicated the adsorption of used inhibitors on the MS surface is exothermic. The negative values also identify that the adsorption is a physisorption process[13]. The obtained values of ΔS are negative indicating that the entropy of inhibitor molecules in the solution phase is higher than solid phase[13].

The reason for the high inhibition efficiencies of these studied Schiff bases towards MS in 1M HCl is due to the presence of azomethine (–C=N-) group, an electron cloud on the aromatic ring and presence of nitrogen, oxygen and sulphur atoms in the molecules. The Schiff bases are strongly adsorbed via the donation of the lone pair of electrons of O atom in the carbonyl group and S atom in the C=S group and N atoms to MS surface. The extent of percentage inhibition depends on the molecular size and electron density on the active groups and atoms[22].

The difference of inhibition efficiencies of the studied Schiff bases towards MS can be explained on the basis of the difference in molecular structure of the Schiff bases and the presence of substituents that increase or decrease electron density of azomethine (-C=N-) group. The higher inhibition efficiency of FTSC compared to the FSC and FATP than FAP may be due to the presence sulphur atom in FTSC and FATP in the place of oxygen atom in FSC and FAP. Adsorption capacity of S is higher than O. Adsorption

capacities of heteroatom present in the organic inhibitor molecules is in the order as reported earlier O<N<S<P[54,55,56,57].

The synthesised four Schiff bases FTSC, FATP, FAP and FSC are acting as good corrosion inhibitors of MS in 1M hydrochloric acid media. Among the four Schiff bases FTSC got maximum efficiency. The inhibition efficiency of the studied Schiff bases decrease in the order FTSC> FATP>FAP>FSC as evidenced from the weight loss measurements. The higher efficiency of the Schiff bases are due to the presence of azomethine group, atoms like sulphur or oxygen, and nitrogen in the Schiff bases molecule. The mechanism of the inhibition process is through the adsorption of the Schiff bases on the MS through physisorption. Thermodynamic parameters calculated and inhibition studies conducted at higher temperature also support the physical adsorption of the Schiff base over the MS. The conversion of an amine into its Schiff base increases the inhibition efficiency. All the Schiff bases are best suited to Langmuir adsorption isotherm behaviour. The results obtained by the weight loss, Tafel method and EIS find better agreement with each other. This shows that the results obtained for the weight loss method are acceptable in all the other cases.

Since all the Schiff bases studied exhibit corrosion inhibiting property on MS in HCl, they can be used as corrosion inhibitors for industrial applications.

REFERENCES

1. V. S. Sastri, "Corrosion Inhibition, Principles and Applications", John Wiley & Sons, New York (1998).
2. "Corrosion Basics an introduction", National Association of Corrosion Engineers, (NACE), Texas (1984) 127-133.
3. H. H. Uhlig, "Corrosion and Corrosion Control", John Wiley and Sons, New York (1985).
4. K. C. Emregul and O. Atakol, Mater. Chem. Phys., 83 (2004) 373–379.
5. H. A. Sorkhabi, B. Shaabani and D. Seifzadeh, Electrochem. Acta., 50 (2005) 3446 -3452.
6. I. Lukovits, A. Shaban and E. Kalman, Electrochem. Acta., 50 (2005) 4128-4133.
7. S. S. A. E. Rehim, M. A. M. Ibrahim and K. F. Khaled, J. Appl. Electrochem., 29, 5 (1999) 593-599.
8. M. A. Quraishi, J. Rawat and M. Ajmal, Corrosion, 54, 12 (1998) 996.
9. T. Vasudevan, B. Muralidharan, S. Muralidharan and S. V. Iyer, Anti-Corros. Method M., 45, 2 (1998) 120-126.
10. H. Shokry, M. Yuasa, I. Sekine, R. M. Issa, H. Y. El-Baradie and G. K. Gomma, Corros. Sci., 40, 12 (1998) 2173-2186.
11. A. Dadgarnezhad, I. Sheikhoaie and F. Baghaei, Anti-Corros. Method M., 51, 4 (2004) 266-271.
12. K. C. Emregul, A. A. Akay and O.Atakol, Mater. Chem. Phys., 93 (2005) 325–329.
13. H. A. Sorkhabi, B. Shaabani and D. Seifzadeh, Appl. Surf. Sci., 239 (2005) 154-164**.**
14. A. Yurt, A. Balaban, S. U. Kandemir, G. Bereket and B. Erk, Mater. Chem. Phys., 85 (2004) 420-426**.**

15. M. N. Desai, M. B. Desai, C. B. Shah and S. M. Desai, Corros. Sci., 26, 10 (1986) 827-837.
16. M. A. Quraishi and R. Sardar, Indian J. Chem. Techn., 11 (2004) 103-107.
17. A. Aytac¸ U. Ozmen and M. Kabasakaloglu, Mater. Chem. Phys., 89 (2005) 176 –181.
18. A. Bansiwal, P. Anthony and S. P. Mathur**,** British Corrosion Journal, 35, 4 (2000) 301-303.
19. M. N. Desai, M. M. Pandya, and G. V. Shah, Indian J. Techn., 19 (1981) 292-294.
20. H. Baeza, M.Guzman, P. Ortega and L.Vera, J. Chil. Chem. Soc., 48, 3 (2003).
21. S. L. Li, H. Y. Ma, S. B. Lei, R. Yu, S. H. Chen and D. X. Liu, Corrosion, 54, 12 (1998).
22. A. S. Fouda, L. H. Madkour, A. A. El-Shafei and S. A. A. El Maksoud, Bull. Korean .Chem. Soc., 16 (1995) 454-458.
23. O. K. Okorosaye and N.C. Oforka., Journal of Applied Sciences & Environmental Management, 8, 1 (2004) 56-61
24. S. K. Rajappa and T. V.Venkatesha, Turk. J. Chem., 27(2003)189-196.
25. M. Hosseini, S. F. L. Mertens, M. Ghorbani and R. M. Arshadi, Mater. Chem. Phys., 78 (2003) 800–808
26. M. A. Quraishi, D. Jamal and M. Luqman, Indian J. Chem. Techn., 9 (2002) 479-483.
27. R. H. Perry, D. W. Green and J. O. Maloney, "Perry's Chemical Engineers Hand Book", International Edition, McGraw-Hill Book Company, Singapore (1984) 23
28. ASTM G-31-72, "Standard Recommended Practice for the Laboratory Immersion Corrosion Testing of Metals", American Society for Testing and Materials (ASTM) Philaldelphia, P.A (1990) 401.

29. G. S. Haynes and R. Baboian, "Laboratory Corrosion Tests and Standards", ASTM Special technical publication, 866, American Society for Testing and Materials, (ASTM) Philadelphia, P A (1990).
30. A. J. Bard and L. R. Faulkner, "Electrochemical Methods, Fundamentals and Applications", Wiley Inter Science Publications, New York (2000).
31. S. W. Dean, R. A. Woodroof and J. S Nicholas, "Electrochemical Methods for Evaluating Corrosion Inhibitors in Strong Acid Systems", in Laboratory corrosion tests and standards, ASTM STP 866, American Society for Testing and Materials, Philadelphia (1985) 228-245.
32. N.G. Thompson and J. H. Payer, "D. C. Electrochemical test methods", National Association Corrosion engineers, Houston, TX (1984).
33. E. Barsoukov and J. R. Macdonald, "Impedance Spectroscopy, Theory, Experiment and Applications", 2nd Ed., Wiley Interscience publications, New York (2005).
34. F. Mansfield, Electrochim. Acta., 35 (1990)1533.
35. M. Kendig, J. Scully, J. Electrochemical Society, 141 (1994) 1823.
36. Mansfeld. F and M. Kendig, "Evaluvation of Protective Coatings with Impedance Measurements", International Congress on Metalic corrosion, 3 (1984) 74-84.
37. G. Reinhard and U. Rammelt. Korrosion, 15 (1984) 175-193.
38. T. Strivens and Taylor. C, Mater. Chem., 7 (1982) 199-222.
39. F. Mansfeld and M. Kendig, Corrosion (1983) 255.
40. M. H. Metikos, R Babic and Z. Grutac, J. Appl. Electrochem., 32 (2002) 35
41. A. A. Sorkhabi, M. R. Majidi and K. Seyyedi, Appl. Surf. Sci., 225 (2004) 176.
42. M. Schorr and J. Yaholom , Corros. Sci., 12 (1972) 867.
43. R. T. Vashi and V. A. Champaneri, Indian J. Chem. Techn., 4 (1997) 180

44. A. Raman and P. Labine, "Reviews on Corrosion Inhibitor Science and Technology" , 1, 11, NACE, Houston, TX (1986) 20.
45. N. Hockerman and R. M. Hurd, Proceedings of International Congress of Metallic Corrosion, London, Butterworths (1962) 166.
46. E. G. Turbina, N. E. Bredikhina, V. V. Pikulev and T. R. Chelyabinsk, Politekh. Inst., 91, 16 (1971).
47. C. Jeyaprabha, S. Sathiyanarayanan, S. Muralidharan and G. Venkatachari, J. Braz. chem.Soc., 17,1 (2006) 61-67.
48. I. L. Rosenfield, "Corrosion Inhibitors", McGraw-Hill, New York (1981).
49. M. El. Azhar, B. Mernari, M. Traisnel, F. Bentiss and M. Lagrenee, Corros. Sci., 43 (2001) 2229.
50. S. Briny, Z. Gruber, R. Basic and M. Metikos-Hukovic, 8th European Symposium on Corrosion inhibition, 1 (1995) 197.
51. M. Elachouri, M.S. Hajji, M. Salem, S. Kertit, J. Aride , R. Coudert and E. Essassi, Corrosion,52 (1996) 103.
52. B. V. Savathri and S. Mayanna, Indian. J. Chem. Techn., 3 (1996) 256**.**
53. Lj. M. Vracar and D. M. Dragic, Corros. Sci., 44 (2002) 1669.
54. J. G. N. Thomas, "Some New Fundamental Aspects in Corrosion Inhibition", 5th European Symposium of Corrosion Inhibitors, Ferra, Italy (1981) 453.
55. B. D. C. Donnelly, T. C. Downie, R. Grzeskowiak, H. R. Hamburg and D. Short, Corros. Sci., 18 (1977) 109.
56. A. B. Tadros and Y. Abdel-Naby, J. Electroanal. Chem., 224 (1988) 443.
57. N. C. Subramanyam, B. S. Sheshadri and S. A. Mayanna, Corros. Science, 34 (1993) 563.

PART V

ELECTRICAL CONDUCTIVITY STUDIES OF SCHIFF BASES AND THEIR TRANSITION METAL COMPLEXES

CHAPTER 1
INTRODUCTION

One of the most important problems of present day chemistry is the creation of new substances and materials possessing a series of valuable properties. Particularly great prospects have been opened up in the synthesis and study of organic compounds having delocalized electrons because of the presence of conjugated bonds in them or the formation of complexes**.** Such compounds have acquired the name, organic semiconductors[1,2]. At the present time organic semiconductors include low molecular weight compound like aromatic dyes and phthalocyanines, polymers with a large number of conjugated bonds, charge transfer complexes, stable free radicals and some biopolymers whose conductivity can be explained by nonionic behaviour[3]. Starting from 1960 large number of report have been published about the chemistry and physics of these materials.

There have been attempts recently to synthesis materials that are intrinsic semiconductors with the guiding principle being that the π – electron system will be highly extended and the charge carrier localization effects weak. The nature of incorporation of metal ion into the organic molecule and its degree of resonance play an important role in the conduction process. The preparation of organic complexes is one of these tries[4].

Inorganic semiconductors stand on the threshold of a bright and exciting future. An organic semiconductor can be synthesised with the properties comparable to those exhibited by inorganic semiconductor materials, such as the development for transistors and the wide array of now existing derivative devices and components of electronics industry[2]. Semiconducting metal complexes constitute one of the most fascinating recent research topics deeply involving both chemists and solid state physicists. Because of the fundamental and technological reasons, considerable interest has been shown in the synthesis and study of organic solids and metal complexes which behave like semiconducting materials [5].

Electrical conductivity studies of organic ligands and their metal complexes - A review

The electrical properties of the organic ligands and their metal complexes have been intensively studied by many of the research groups all over the world. The following review describes the recent studies on the electrical conductivity of organic ligands and their metal complexes.

Aydogdu and co-workers have studied the D.C electrical conductivity of metal complexes of ligands like sodium oxalate (1)[6,7], oxime compounds containing oxolane ring (2)[8], 8,9-bis(hydroxyimino)-4,7,10,13-tetraaza-1,2,15,16-O-dicyclopentylidenehexadecane (3)[9] and observed that all are showing inorganic semiconductor properties. The room temperature

conductivity of Co, Ni and Cu complexes of ligand (1) was found to be 6.43 x 10^{-9}, 3.85 x 10^{-7} and 2.10 x 10^{-6} $ohm^{-1}cm^{-1}$ respectively. The thermal probe measurements of the Cu(II) complex of ligand (2) and Cu(II), Ni(II) and Co(II) complexes of ligand (3) indicated that they have an n-type electrical conductivity. The activation energies of the complexes were also reported.

D.C conductivity of oxovanadium (IV) complexes with quadridentate Schiff base have been investigated by Sarkar[10] and found that the complexes were electrical insulators at room temperature. The semiconducting behaviour of complexes was established by the increase in their conductivity with increase in temperature and explained this in correlation with their chemical structure, which affords an extended conjugation.

Yakuphanoglu[11,12] has reported the room temperature D.C electrical conductivity and activation energy values for the complexes [Co_2 (L)L'V(dioxane)$_2$(NO3)$_2$(NO3)$_2$], (A) and crystalline metal-radical compound, aqua[bis(2-dimethylaminomethyl-4-NIT-phenolato)]copper(II), (B). The observed room temperature conductivity values were 2.57 x 10^{-7} and 1.38 x 10^{-6} $ohm^{-1}cm^{-1}$ with activation energies of 0.46 eV and 0.56 eV. Temperature dependence measurements showed that both compounds were semiconducting in nature and it exhibited two conduction regions suggesting two type of conduction for these regions.

Co(II), Ni(II) and Cu(II) complexes of chloro(phenyl)glyoxime were characterised by D.C electrical conductivity measurements, in the temperature

range 25-250°C by Turkoglu et al. The room temperature conductivity ranged from 10^{-14} to 10^{-6} $ohm^{-1}cm^{-1}$ and increased with rising temperature. The conductivity of complexes, followed the order Co<Ni<Cu and has been attributed to differences in the stability of the complexes[13].

Masoud and co-workers have investigated the D.C conductivity and its temperature dependence of Co, Ni, Cu, and Zn complexes of ligands like 2,4-dinitrosoresorcinol (I)[14], o-substituted arylazo-barbiturate (II)[15], 5-(p-substituted phenylazo)barbituric acid (III)[16], 5-(*o*-substituted phenylazo)-6-amino-2-thiouracils (IV)[17] and 6-(o-substituted phenylazo)-5-aminouracils (V)[17]. These complexes showed semiconducting properties where the metal ion forms a bridge to facilitate the flow of the current with some degree of delocalization in the excited state. In the case of metal complexes of ligand (II), it was found that the copper complexes derived from the -H,-CH_3, and OCH_3 substituted ligand (II) exhibited semiconducting properties at lower temperature and insulator properties at higher temperature. It was also proposed that conductivity is found to depend on the structure of the compounds.

Wahed et.al carried out the electrical characterisation of metal complexes prepared using various ligands such as anthraquinone derivatives (A)[18.19], heterocyclic amines (B) like 8-hydroxyquinoline-5-sulphonic acid and 2-amino-3-hydhydroxy pyridine[20,21], adenine (C)[22], acetylbenzaldehydra-zone and its derivative (D)[23], Coumarin derivatives (E)[24] and phenyl

thiopyridine derivative (F) [25]. The conductivity of ligand, anthraquinone derivatives (A) and its Cr^{3+}, Mn^{2+}, Fe^{3+}, Co^{2+}, Cu^{2+}, Nd^{3+}, Gd^{3+}, Dy^{3+} and Er^{3+} complexes varied from 10^{-9} to 10^{-12} $ohm^{-1}cm^{-1}$. These ligands and their complexes show semiconductivity and the conduction mechanism was interpreted on the basis of hopping theory. Mn(II), Co(II), Ni(II) and Cu(II) complexes of compounds (A) were found to be semiconductors at low temperature but become nearly conductors at higher temperatures. The electrical conductivity of the Zn(II), Cd(II), Hg(II), As(III), Sb(III) and Bi(III) complexes of ligand heterocyclic amine (B) at 303 K was in the range 10^{-9} to 10^{-11} $ohm^{-1}cm^{-1}$. The activation energy of conduction process, the charge carrier concentration and their mobility were also reported. The Mn(II), Co(II), Ni(II), Nd(III), Gd(III) and Yb(III) complexes of ligand 2-amino-3 hydroxy pyridine (B) shows semiconducting nature. The reason for the higher conductivity of complexes was due to the overlapping of d-orbital of metal with π-orbitals of pyridine which increases extend of electron delocalization along the pyridine molecule. The reported electrical conductivity of Mn(II), Fe(II), Co(II), Ni(II) and Cu(II) complexes of ligand adenine (C) were in the range 2×10^{-10} to 3.48×10^{-10} $ohm^{-1}cm^{-1}$ and complexes were found to show semiconducting behaviour. The A.C electrical conductivity of a series of transition metal complexes of acetyl benzaldehydrazone (D) and its derivatives in the frequency range 0.1-20 KHz were measured and their temperature dependence was studied in the

temperature range of 16-80°C. The Arrhenius plots reveal the semi conducting nature of the complexes. In the case of ligand coumarin (E) the conductivity values of complexes were less than the ligand. The electrical conductivity of Co(II), Ni(II) or Cu(II) metal complexes of the composition LM and LM_2 with ligand phenyl thiopyridine derivative (F) were reported in the range 10^{-9}-10^{-10} $ohm^{-1}cm^{-1}$. It is found that the complexing of ligand with transition metals results in the increase of conductivity.

Metal complexes of the Schiff bases derived from reaction of 2-methylbenzopyrrole-3-carboxaldehyde with some aniline derivatives showing slight semiconducting behaviour have been reported[26]. Their conductivity and activation energy were found to depend on molecular structure as well as the ionic radii of the metal ions. Singh measured the electrical conductivity of the complex salts and the heterobimetallic coordination polymers bis(1-ethoxycarbonyl-1-caynoethelene-2,2-dithiolato)cuprate(II) ion[27] and [MM′$(cdc)_2$], [M= Zn(II), Cd(II), Hg(II); M′= Ni(II) or Cu(II); cdc^{2-}=cyanodithioimidocarbonate][28]. All the complexes exhibited semiconducting behaviour.

Nikumbh carried out the electrical conductivity measurements of Cu(II) and Zn(II) malonate, maleate, and succinate complexes and compared with thermal analysis results[29]. The thermal decomposition of manganese (II) oxalate dehydrate and cadmium (II) oxalate monohydrate complexes were also characterised by electrical conductivity measurements under different

atmospheres[30]. The electrical conductivity measurements were found to give additional information on the solid-state reaction as compared to that obtained from conventional thermal techniques. Semiconducting properties of Mn(II), Fe(II), Co(II), Ni(II), Cu(II), Zn(II), Cd(II) and VO(IV) complexes of Schiff base derived from resdiacetophenone and S-benzyldithiocarbazate were studied by Makode. It was found that complexes are semiconducting in nature[31].

Scope of present investigation

The remarkable growth of interest in the physics and chemistry of solid state inorganic metal complexes is reflected by a steady increase in the number of published investigations dealing with various aspects on this subject. The review of the published literature shows that extensive work has been conducted to find out the electrical conductivity of organic ligands and their metal complexes. As part of this research program four new Schiff bases and their transition metal complexes have been synthesised. So it is worth while to investigate the solid state electrical conductivity of the newly synthesised four Schiff bases and some of their transition metal complexes.

CHAPTER 2
MATERIALS, METHODS AND INSTRUMENTS

Materials

Schiff base FATP and its Co(II), Ni(II), Cu(II) and Zn(II) complexes along with the other three Schiff bases FAP, FTSC and FSC and their Cu(II) complexes were subjected to the D.C electrical conductivity studies. The procedure for the preparation of ligands and complexes are described in part I of this thesis.

Methods

Measurement of D.C electrical conductivity

An important property characterising the electrical behaviour of a solid is the electrical conductivity, σ. To study the D.C electrical conductivity of ligands and complexes, these samples were made in the form of pellets of diameter 8-10 mm and thickness of 1-2 mm under a pressure of 3 ton using a hydraulic press at room temperature. The diameter and thickness of the pellets were measured using Vernier calipers. To make electrical contacts, room temperature dryable silver paint was applied on both ends of the pellets and thin copper wires were attached. The dried sample was kept inside a hot and cold chamber having programmable heating and cooling facility. The end of the leads were taken out from the chamber through a small hole and

connected to the terminals of the electrometer. The electrical resistance of the sample was measured using a two probe method with Keithley 6517 A model electrometer by applying a constant D.C voltage of 15 V. The temperature of the chamber was raised slowly from room temperature to 125°C. The resistance values were recorded at 10°C intervals. The D.C electrical conductivity of the sample was calculated using the relation (1) [6,8].

$$\sigma = (1/R)\,(d/A) \qquad (1)$$

where R= resistance in ohm , d = thickness in cm and A = electrode area in cm^2.

Determination of thermal activation energy

According to Arrhenius theory, the dependence of the conductivity of the semiconducting materials on temperature is expressed by the equation (2)[10, 15, 19].

$$\sigma = \sigma^o \exp(-E_a/kT) \qquad (2)$$

where σ^o is pre exponential conductivity, E_a is the activation energy of the conduction process, k is the Boltzmann's constant and T is the absolute temperature.

Generally Arrhenius plots are obtained when logarithmic conductivity values are plotted against the reciprocal of the absolute temperature. By analyzing the shape of $\log \sigma = f(1000/T)$ graphs useful information regarding the process occurring in investigated complexes during the heat treatment can be obtained. If the plot of $\log \sigma$ vs. 1000/T yields a straight line, it shows that

the studied materials have semiconducting behaviour in the studied temperature region. The thermal activation energies for the conduction process of the investigated samples can be determined from the slopes of Arrhenius plots [1, 10, 32].

Calculation of carrier concentration and mobility

To illustrate the suitable model for conduction mechanism of the studied materials, the charge carrier concentration, n, and the mobility, μ, are calculated using the relation (3) and (4) respectively[6, 19].

$$n = 2\left(\frac{2\pi m^{*} kT}{h^{2}}\right)^{\frac{3}{2}} \exp^{\left(\frac{-E_a}{kT}\right)} \quad (3)$$

$$\sigma = ne\mu \quad (4)$$

where m* is the effective mass of the charge carrier which is assumed to be the rest mass of electron, k is Boltzmann's constant, E_a is activation energy of the conduction process, T is absolute temperature and e is the charge of electron. The expression for n is valid when the value of $E_a \geq 3kT$[25, 23]. So n and μ values are only calculated for the samples satisfying the above criteria.

Instruments

The following instruments were used for the electrical conductivity measurement of Schiff bases and complexes

1) Hydrocraft India make hydraulic press with die set
2) Clitech India make hot and cold chamber
3) Keithley make 6517 A model electrometer.

CHAPTER 3
ELECTRICAL CONDUCTIVITY STUDIES OF SCHIFF BASES AND THEIR TRANSITION METAL COMPLEXES

The results of D.C electrical conductivity studies of the synthesised Schiff bases and their selected complexes are described in this chapter. The temperature dependence of semiconductivity is also described. The values of thermal activation energy, carrier concentration and mobility are also presented.

D.C electrical conductivity of FATP and its complexes

The room temperature D.C conductivity (σ_{30}) and activation energies obtained for FATP and its complexes are given in the table 5.3.1. Conductivity values obtained for the Schiff base FATP and its Co(II), Ni(II), Cu(II) and Zn(II) complexes in the temperature range 30-125 °C are given in the table 5.3.2. The plot of the logarithm of conductivity against the reciprocal of the absolute temperature of FATP and Co(II), Ni(II), Cu(II) and Zn(II) metal complexes in the temperature range 30-125°C are presented in the figures 5.3.1 to 5.3.5. The carrier concentration and mobility are given in the table 5.3.5.

The room temperature conductivity (σ_{30}) of FATP was 1.17 x 10^{-12} ohm^{-1} cm^{-1}. The conductivity of FATP was found to increase exponentially

with rise in temperature in the studied temperature region. A maximum value of 4.61 x 10^{-07} $ohm^{-1}cm^{-1}$ was recorded at 125°C. This value is about five orders of magnitude higher than its room temperature value. The Arrhenius plots of FATP explain a positive temperature coefficient of conductivity with conventional semiconducting behaviour of increasing conductivity with increase in temperature (Figure 5.3.1). An activation energy value of 0.83 eV was obtained for the ligand FATP.

Table 5. 3. 1 σ_{30} and activation energy values of FATP and its complexes

Sample	σ_{30} ($\Omega^{-1}cm^{-1}$)	Activation energy E_a (eV)
FATP	1.17 x10^{-12}	0.83
[Co (FATP) $(H_2O)_3$]	4.14 x 10^{-09}	Region A 0.062
		Region B -0.252
[Ni (FATP) $(H_2O)_3$]	3.94 x 10^{-09}	Region A 0.870
		Region B - 0.120
[Cu (FATP) $(H_2O)_3$]	6.48 x10^{-12}	0.260
[Zn (FATP) $(H_2O)_3$]	1.22 x 10^{-09}	Region A 0.160
		Region B -0.110

Table 5. 3. 2 Conductivity values (σ) obtained for the ligand FATP and its complexes

Temp. (°C)	FATP ($\Omega^{-1}cm^{-1}$)	Co(II) Complex ($\Omega^{-1}cm^{-1}$)	Ni(II) Complex ($\Omega^{-1}cm^{-1}$)	Cu(II) Complex ($\Omega^{-1}cm^{-1}$)	Zn(II) Complex ($\Omega^{-1}cm^{-1}$)
30	$1.17x10^{-12}$	$4.14 x10^{-09}$	$3.94 x10^{-10}$	$6.48x10^{-12}$	$1.22 x10^{-09}$
40	$9.92 x 10^{-13}$	$2.51 x10^{-09}$	$6.13 x10^{-10}$	$1.51x10^{-12}$	$1.24 x10^{-09}$
50	$1.43 x 10^{-12}$	$3.73x 10^{-09}$	$8.77 x10^{-10}$	$3.20x10^{-11}$	$1.94 x10^{-09}$
60	$5.98 x10^{-12}$	$4.63 x10^{-09}$	$5.87 x10^{-10}$	$7.05x10^{-11}$	$3.24 x10^{-09}$
70	$2.37x10^{-11}$	$4.27 x10^{-09}$	$4.71 x10^{-10}$	$1.28 x10^{-10}$	$4.73 x10^{-09}$
80	$9.90x10^{-11}$	$5.28 x10^{-09}$	$2.67 x10^{-10}$	$2.31 x10^{-10}$	$6.58 x10^{-09}$
90	$5.24x 10^{-10}$	$5.52 x10^{-09}$	$2.10 x10^{-10}$	$3.86 x10^{-10}$	$7.79 x10^{-09}$
100	$3.68x10^{-09}$	$4.37 x10^{-09}$	$1.79 x10^{-10}$	$5.49 x10^{-10}$	$7.50 x10^{-09}$
110	$5.88x10^{-08}$	$3.32 x10^{-09}$	$1.80 x10^{-10}$	$8.86 x10^{-10}$	$6.04 x10^{-09}$
120	$3.12x10^{-08}$	$1.74 x10^{-09}$	$1.47 x10^{-10}$	$1.36 x10^{-09}$	$5.12 x10^{-09}$
125	$4.61x10^{-07}$	$1.05x10^{-09}$	$1.11 x10^{-10}$	$1.71 x10^{-09}$	$4.52 x10^{-09}$

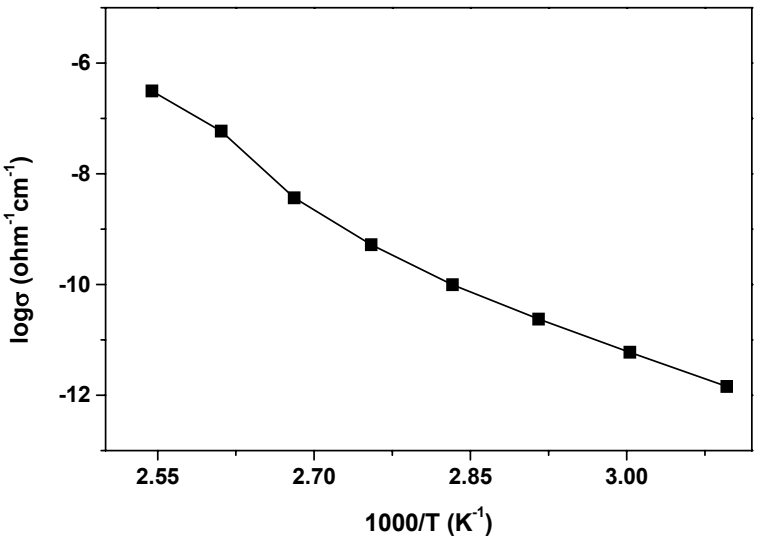

Figure 5. 3. 1 Temperature dependence of electrical conductivity of FATP

The σ_{30} of $[Co(FATP)(H_2O)_3]$ was 4.14 x 10^{-09} $ohm^{-1}cm^{-1}$ which is three orders of magnitude higher than the conductivity of uncomplexed FATP. The temperature dependence curve of $[Co(FATP)(H_2O)_3]$ shows two regions A and B with straight line graphs in each region (Figure 5.3.2). The conductivity was found to increase in region A (from 30 to 90°C) and found to decrease in region B (90 to 125°C). The activation energy value of region A was positive while for the region B it was negative.

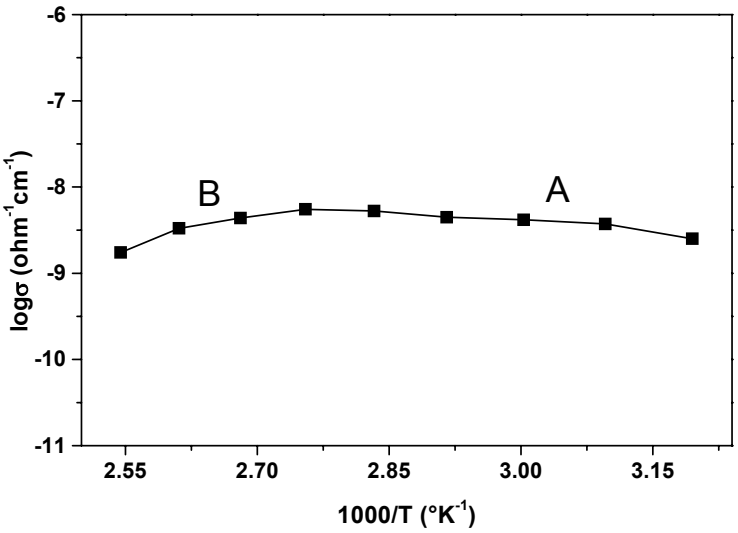

Figure 5. 3 .2 Temperature dependence of electrical conductivity of [Co(FATP)(H_2O)$_3$]

The room temperature conductivity value, 3.94 x 10^{-10} $ohm^{-1}cm^{-1}$, of [Ni(FATP)(H_2O)$_3$] was two orders of magnitude higher than its ligand only value. It is apparent that the complexing of FATP with Ni(II) results in an increased conductivity. The temperature dependence of conductivity curve of Ni(II) complex of FATP exhibit two regions A, B comprising 30 to 50°c and 60 to 125°C respectively (Figure 5.3.3). Region A has positive temperature coefficient of electrical conductivity but the region B has a negative value. Therefore the electrical activation energy of this complex explains positive value in region A, i.e. 0.87 eV, but negative value, -0.12 eV in region B.

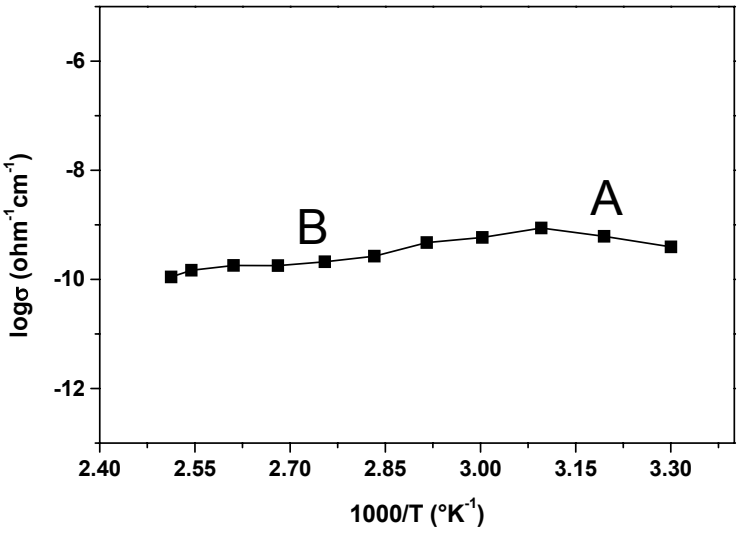

Figure 5. 3. 3 Temperature dependence of electrical conductivity of [Ni(FATP)(H_2O)$_3$]

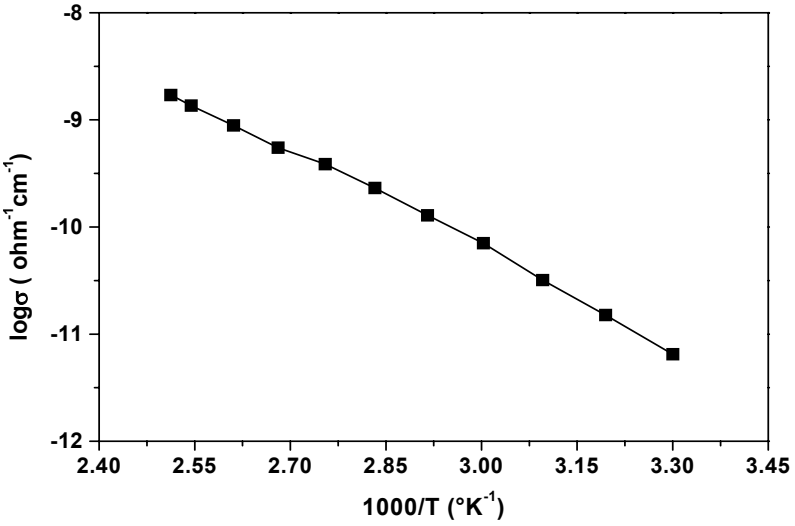

Figure 5. 3. 4 Temperature dependence of electrical conductivity of [Cu(FATP)(H_2O)$_3$]

The electrical conductivity of the Cu(II) complex has positive temperature coefficient. The σ_{30} value, 6.48 x 10^{-12} $ohm^{-1}cm^{-1}$, was changed to 1.71 x 10^{-9} $ohm^{-1}cm^{-1}$ when the temperature changed to 125°C. That is with the increase in temperature, the conductivity increases exponentially. When log σ was plotted against 1000/T, straight line was obtained, which indicates the semiconducting behaviour of the complex (Figure 5.3.4). The conductivity of the ligands does not increase after complexation. A significant reduction in the activation energy value compared to the free ligand was observed.

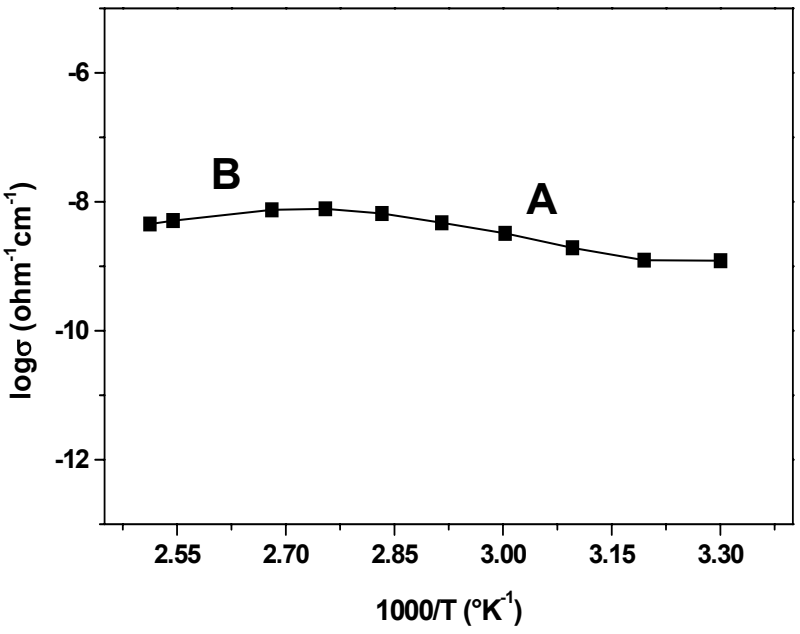

Figure 5. 3. 5 Temperature dependence of electrical conductivity of $[Zn(FATP)(H_2O)_3]$

σ_{30} value obtained, 1.22 x 10^{-09} $ohm^{-1}cm^{-1}$, for the Zn(II) complex was higher than free ligand, FATP's conductivity. The log (σ) vs. 1000/T plot of Zn(II) complex of FATP shows two regions A and B and the conductivity values didn't show an abrupt change with change in temperature (Figure 5.3.5). The region A, between 30°C to 90°C, has positive temperature coefficient with an activation energy value of 0.16 eV. But in the region B, corresponding to 100-125°C, the conductivity values were found to be decreasing.

D.C electrical conductivity of FAP, FTSC, FSC and their Cu(II) complexes

The room temperature conductivity (σ_{30}) and activation energies of the FAP, FTSC and FSC and their Cu(II) complexes are presented in the table 5.3.3. Conductivity values obtained for the Schiff bases FAP, FTSC and FSC and its Cu(II) complexes in the temperature range 30-125°C are given in the table 5.3.4. In the case of FTSC and its copper complex the samples started decomposing above 90°C. So values are recorded only up to 90°C. The plot of the logarithmic conductivity against the reciprocal of the absolute temperature of FAP, FTSC and FSC and its Cu(II) complexes are presented in the figures 5.3.6 to 5.3.8. The calculated values of carrier concentration, n and mobility, μ are presented in the table 5.3.5.

The conductivity of FAP increased with increasing temperature. The room temperature conductivity of 2.46 x 10^{-13} $ohm^{-1}cm^{-1}$ was raised to 4.86 x

10^{-07} $ohm^{-1}cm^{-1}$ when the temperature rose to 125°C. The exponential rise in conductivity and the straight line graph obtained for the Arrhenius plots show the semiconducting nature of FAP (Figure 5.3.6).

Table 5. 3. 3 σ_{30} and activation energy of FAP, FTSC, FSC and their Cu(II) complexes

Sample	σ_{30} ($\Omega^{-1}cm^{-1}$)	Activation Energy (eV)
FAP	2.46 x10^{-13}	0.70
[Cu (FAP) $(H_2O)_3$]	3.35 x 10^{-13}	Region A 0.37
		Region B -0.31
		Region C 0.39
FTSC	1.61x 10^{-11}	0.31
[Cu (FTSC) $(H_2O)_3$]	2.40 x 10^{-12}	-0.002
FSC	8.85x10^{-10}	Region A 0.002
		Region B - 0.61
		Region C 0.02
[Cu(FSC) $(H_2O)_3$]	9.82 x 10^{-8}	Region A -0.19
		Region B -0.38

The temperature dependence curve of Cu(II) complex of FAP shows three regions A, B and C with different slopes. In region A, i.e. from 30 to 70°C, the conductivity values increased slightly and in region B it started decreasing (Figure5.3.6). The conductivity values further increased from 110 to 125°C in region C. The activation energy values obtained were positive in region A and C while it was negative in region B because of the change in slope. A noticeable increment in room temperature conductivity value of FAP was not observed after complexation with Cu(II) .

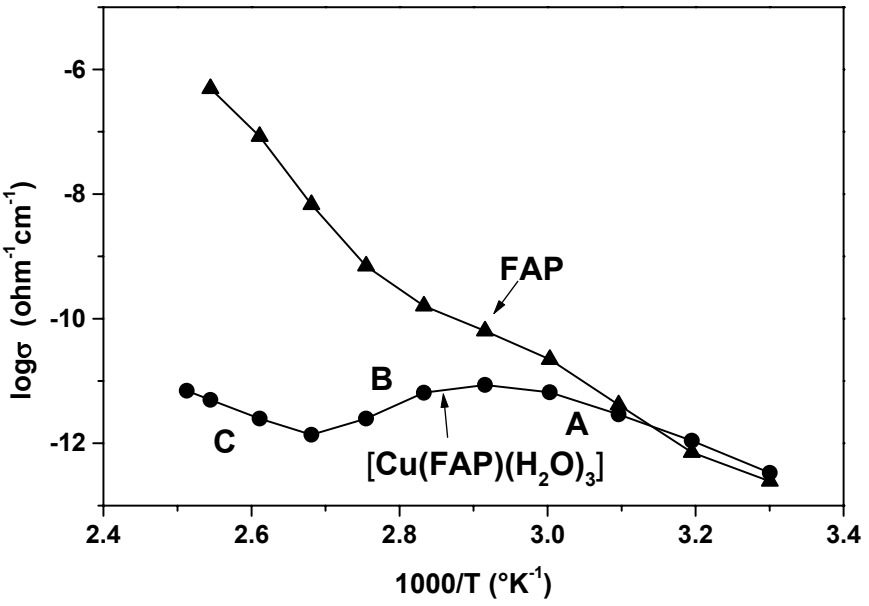

Figure 5. 3. 6 Temperature dependence of electrical conductivity of FAP and [Cu(FAP)(H$_2$O)$_3$]

Table 5. 3. 4 Conductivity values (σ) obtained for FTSC, FAP, FSC and their Cu(II) complexes

Temp. (°C)	FTSC ($\Omega^{-1}cm^{-1}$)	[CU(FTSC) $(H_2O)_3$] ($\Omega^{-1}cm^{-1}$)	FAP ($\Omega^{-1}cm^{-1}$)	[Cu (FAP) $(H_2O)_3$] ($\Omega^{-1}cm^{-1}$)	FSC ($\Omega^{-1}cm^{-1}$)	[Cu (FSC) $(H_2O)_3$] ($\Omega^{-1}cm^{-1}$)
30	$1.61x\ 10^{-11}$	$2.41x10^{-12}$	$2.46\ x\ 10^{-13}$	$3.35x10^{-13}$	$8.86E\ x10^{-10}$	$9.82\ x10^{-08}$
40	$5.10\ x\ 10^{-11}$	$2.42\ x10^{-12}$	$7.15x\ 10^{-13}$	$1.10\ x10^{-12}$	$9.84\ x10^{-10}$	$6.02\ x10^{-08}$
50	$1.81x10^{-10}$	$2.38\ x10^{-12}$	$4.13x\ 10^{-12}$	$2.90\ x10^{-12}$	$1.22\ x10^{-09}$	$3.26\ x10^{-08}$
60	$3.64\ x\ 10^{-10}$	$2.26\ x10^{-12}$	$2.22x10^{-11}$	$6.58\ x10^{-12}$	$8.33\ x10^{-10}$	$2.27\ x10^{-08}$
70	$5.75\ x\ 10^{-10}$	$2.25x\ 10^{-12}$	$6.35x10^{-11}$	$8.64\ x10^{-12}$	$8.50\ x10^{-11}$	$2.27\ x10^{-08}$
80	$4.84\ x\ 10^{-10}$	$2.30x10^{-12}$	$1.60x10^{-10}$	$6.47\ x10^{-12}$	$1.85\ x10^{-11}$	$1.023\ x10^{-08}$
90	$4.56x\ 10^{-09}$	$2.37x10^{-12}$	$7.00x10^{-10}$	$2.49\ x10^{-12}$	$3.71\ x10^{-12}$	$3.17\ x10^{-09}$
100	-	-	$6.80x10^{-09}$	$1.37\ x10^{-12}$	$2.16\ x10^{-12}$	$3.27\ x10^{-09}$
110	-	-	$8.45x10^{-08}$	$2.49\ x10^{-12}$	$2.23\ x10^{-12}$	$1.08\ x10^{-10}$
120	-	-	$4.94x10^{-07}$	$4.98\ x10^{-12}$	$2.32\ x10^{-12}$	$6.56\ x10^{-11}$
125	-	-	$4.86x10^{-07}$	$6.97\ x10^{-12}$	$2.37\ x10^{-12}$	$6.05\ x10^{-11}$

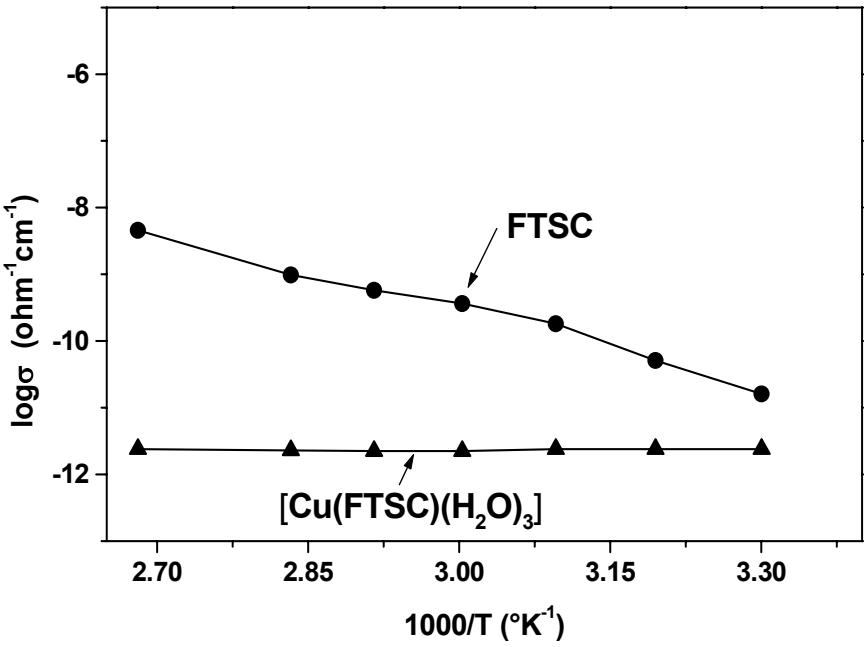

Figure 5.3.7 Temperature dependence of electrical conductivity of FTSC and $[Cu(FTSC)(H_2O)_3]$

The room temperature conductivity of FTSC and its $[Cu(FTSC)(H_2O)_3]$ complex were 1.61 x 10^{-11} and 2.41 x 10^{-12} $ohm^{-1}cm^{-1}$ respectively. It is found that FTSC and Cu(II) complex started decomposing near the melting point of FTSC which is 96°C as described in chapter 5 of Part I of this thesis. The conductivity values of the FTSC were found to increase with increase in temperature. The linear nature of log σ vs. 1000/T plot shows the semiconducting nature of FTSC. But in the case of $[Cu(FTSC)(H_2O)_3]$, the conductivity values does not increased much with respect to the change in the temperature. The conductivity values remain

unchanged from room temperature to 50°C and showed a very small decrease up to 70°C and further increased slightly up to 100°C.

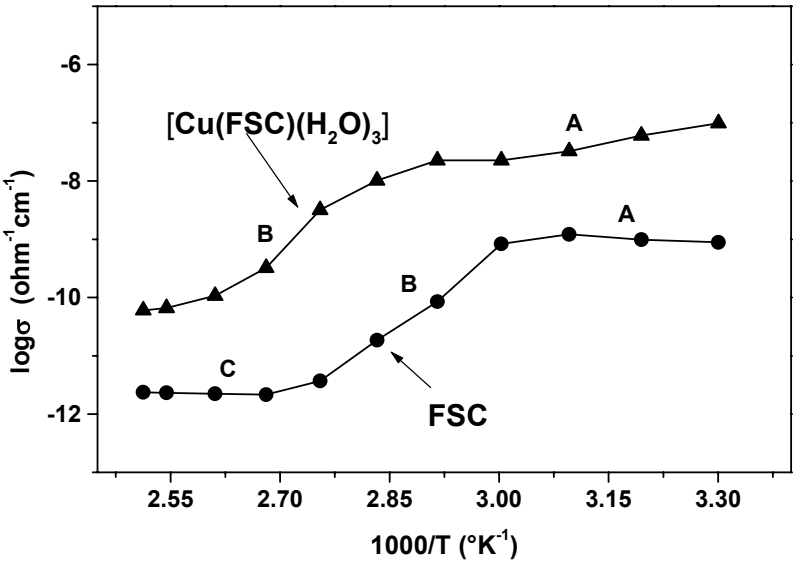

Figure 5.3.8 Temperature dependence of electrical conductivity of FSC and $[Cu(FSC)(H_2O)_3]$

The σ_{30} value of $[Cu(FSC)(H_2O)_3]$ was two orders higher than the ligand FSC's values. The temperature dependence curves of FSC and $[Cu(FSC)(H_2O)_3]$ are almost similar in nature. The log (σ) vs. 1000/T plot of FSC shows three regions A, B and C. The regions A and C are two horizontal plateaus with very little change in conductivity. But in the region C, comprising 60-100°C, an exponential decrease in conductivity with negative temperature coefficient of conductivity was observed. The activation energies obtained for the region A and C are positive and for the region B it is

negative. The temperature dependence curve of $[Cu(FSC)(H_2O)_3]$ shows two regions A and B with negative temperature coefficient of conductivity (Figure 5.3.8). The conductivity values of $[Cu(FSC)(H_2O)_3]$ show a difference of four orders of magnitude between room temperature and 125°C. The activation energies obtained for the two regions have negative values.

Table 5. 3. 5 Calculated carrier concentration and mobility of studied samples

Sample	Carrier Concentration (n) (cm^{-3})	Mobility (μ) ($cm^2V^{-1}S^{-1}$)
FATP	2.12×10^{11}	3.45×10^{-5}
$[Co (FATP) (H_2O)_3]$ - Region A	2.29×10^{24}	1.13×10^{-14}
$[Ni (FATP) (H_2O)_3]$ - Region-A	5.84×10^{10}	4.21×10^{-2}
$[Cu (FATP) (H_2O)_3]$	1.04×10^{21}	3.89×10^{-14}
$[Zn (FATP) (H_2O)_3]$- Region A	4.87×10^{22}	1.56×10^{-13}
FAP	4.36×10^{13}	3.51×10^{-08}
$[Cu (FAP) (H_2O)_3]$- Region A	1.25×10^{19}	1.68×10^{-13}
$[Cu (FAP) (H_2O)_3]$- Region C	6.48×10^{18}	3.22×10^{-13}
FTSC	4.18×10^{20}	6.71×10^{-13}

Based on the results of solid state D.C electrical conductivity studies of Schiff bases and their complexes the following observations and findings are obtained. Since measured room temperature conductivity of the investigated samples were in the range 10^{-09} to 10^{-13} $ohm^{-1}cm^{-1}$, all the samples can be classified into the category of organic semiconductors, which have conductivity in between 10^{-02} to 10^{-14} $ohm^{-1}cm^{-1}$ [1-3,33]. The conductivity reported for similar type of organic ligands and their transition metal complexes are also in the same range[6-26].

Among the studied Schiff base ligands, the σ_{30} value increased in the following order, FAP< FATP< FTSC< FSC. While moving from left to right in the above series the conductivity increased for about one order of magnitude. The conductivity values,(σ_{30}), obtained for these Schiff base molecules are in the range of similar organic compounds[6-26]. The variation in conductivity of the Schiff bases may be attributed to the difference in their conjugation or resonance (the ability of electron to move from one atom of a molecule to another atom of that molecule) which arises due to the difference in chemical structure[18,24].

Earlier workers have pointed out that, the conductivity increase when organic molecules are coordinated with different metal ions[20,24]. An enhancement in conductivity value,(σ_{30}), for about two to three orders of magnitude were observed for Co(II), Ni(II), Zn(II) metal complexes of FATP and Cu(II) complex of FSC than the uncomplexed ligands. This may be due

to the inclusion of transition metal ions in to the π electron delocalization of organic molecule during complexation[21,34].

Among the different transition metal complexes of same ligand FATP, The order of increase of conductivity (σ_{30}) is as follows,

$[Cu(FATP)(H_2O)_3]$ < $[Ni(FATP)(H_2O)_3]$ < $[Co(FATP)(H_2O)_3]$ ≈ $[Zn(FATP)(H_2O)_3]$.

Differences in stabilities of complexes, electronic configuration of central metal ion and the coordination geometry of these complexes are the reasons for this type of behaviour as reported by Turkoglu [13] and Wahed [20]. In our case, the trend seems to be in accordance with natural order of stability of these complexes, Co < Ni< Cu > Zn. Conductivity of copper complex is lower than other complexes indicating its highest stability.

The conductivity,(σ_{30}), of the copper complexes of Schiff bases FATP, FAP, and FTSC remains unchanged or decreased slightly compared to their ligands only value. The order of increase of conductivity was $[Cu(FAP)(H_2O)_3]$ < $[Cu(FATP)(H_2O)_3]$ < $[Cu(FTSC)(H_2O)_3]$ < $[Cu(FSC)(H_2O)_3]$. The decrease of conductivity of the complex than ligand may be due to the interruption of the π orbital sequence which will limit the electron delocalization to small region of Schiff base molecules there by causing a reduction in conduction path[22]. The same order of variation of conductivity of ligands is also followed in the case of complexes. This shows

that organic molecule is playing the major role in the conduction process of copper complexes rather than the metal cation[22,18].

The obtained activation energies are matching with reported values and found that as a result of complexation, activation energy values were lowered. The low values of activation energies are related to electron hopping which is a thermally activated process[8].

The low conductivity of the organic compounds can be explained by the lesser number of carriers present[24, 35]. The increase in conductivity of the metal complexes than the ligands may be due to the production of new charge carriers as evident from the increase in the carrier concentration after complexation[25].

The mobility value gives an idea about the conduction mechanism in organic semiconductors. If the mobility values are higher than $1cm^2\ V^{-1}\ S^{-1}$ the conduction mechanism is described by band model and if it is less than $1cm^2\ V^{-1}\ S^{-1}$ conduction mechanism will be hopping model[6]. The obtained mobility values in the investigated samples are less than $1cm^2\ V^{-1}\ S^{-1}$ so the preferred conduction mechanism may be hopping one.

Among the studied compounds, typical semiconducting behaviour of increasing conductivity with increase in temperature with a positive temperature coefficient of electrical conductivity evidenced by the straight line nature of Arrhenius plots were exhibited only by the samples FATP, FAP, FTSC and [Cu (FATP) $(H_2O)_3$]. The mechanisms of electric conduction

in organic metal complexes which shows positive temperature coefficient of electrical conductivity are explained by the hopping model as proposed by the earlier investigators for similar organic metal complexes [6,7,12,13,22].

The mechanisms of electric conduction by hopping model as reported for similar organic metal complexes are explained as follows. In this model, the electron, or hole, hops from one localized site to next. Whenever it is transferred to another site, the surrounding molecule respond to this perturbation with structural changes and the electron or hole is temporarily trapped in the potential well leading to atomic polarization. The electron resides at this site until it is thermally activated to migrate to another site. Another aspect of this charge hopping mechanism is that the electron or hole tends to associate with local defects, so the activation energy for charge transfer may also include the energy of freeing the hole from its position next to the defect[6,32,36,37].

The temperature dependence plot of $[Cu(FTSC)(H_2O)_3]$ did not show any appreciable change in conductivity with increase in temperature. But in the case of complexes, $[Ni(FATP)(H_2O)_3]$, $[Co(FATP)(H_2O)_3]$, $[Zn(FATP)(H_2O)_3]$, $[Cu(FAP)(H_2O)_3]$, $[Cu(FSC)(H_2O)_3]$ and FSC discontinuation observed in the electrical conductivity-temperature relationships as shown by the two or three segments in the log σ vs. 1000/T plots. The probable reason for the decrease in conductivity with increase in temperature is due to the scattering of carriers by phonons due to lattice

vibrations at these elevated temperatures[7,15,16]. The phenomena of discontinuation observed in the electrical conductivity-temperature relationship showed by two or three segments with variable activation energies are probably due to the presence of different crystallographic or phase transitions[19,22].

Since some of the investigated compounds, FATP, FAP, FTSC and Cu(II) complex of FATP, show characteristic properties of semiconductors, use of these materials for semiconductor applications are proposed.

REFERENCES

1. F Gutmann and L. Lyons, “Organic Semiconductors”, Academic Press, New York (1967).
2. Y. Okamoto and W. Brenner, “Organic Semiconductors”, Reinhold Publishing, Chapman & Hall, London (1964).
3. L. I. Boguslavskii and A. V. Vannikov, “Organic Semiconductors and Biopolymers”, Plenum Press, New York (1970)1-2.
4. W. Jones, “Organic Molecular Solids, Properties and Applications”, CRC Press, Boca Raton, FL (1997) Chap 9.
5. P. Y. Yu and M. Cardona, “Fundamentals of Semiconductors Physics and Material Properties”, Springer, Berlin (1996).
6. Y. Aydogdu, F. Yakuphanoglu, A. Aydogdu, M. Sekerci, C. Alkan and I. Aksoy, Mater. Lett., 54 (2002) 352-358.
7. Y. Aydogdu, F. Yakuphanoglu, F. Dagdelen, M. Sekerci and I Aksoy, Mater. Lett., 57 (2002) 237-241.
8. Y. Aydogdu, F. Yakuphanoglu, A. Aydogdu, E. Tas and A. Cukurovali, Mater. Lett., 57 (2003) 3735-3760.
9. Y. Aydogdu, F. Yakuphanoglu, A. Aydogdu, S. Saydam, M. Sekerci and F. S. Boydag, Synthetic. Met., 122 (2001) 329-335.
10. S. Sarkar, Y. Aydogdu, F. Dagdelen, B. B. Bhaumik and K. Dey, Mater. Chem. Phys., 88 (2004) 357–363.
11. F. Yakuphanoglu, Y. Aydogdu, M. Gomleksiz, M. Sekerci, S. Agan and C. Alkan, Mater. Lett,. 57 (2003) 2219– 2224.
12. Y. Yakuphanoglu, Y. Aydogudu, U. Schatzschneider and E. Rentschler, Solid State Commun., 128 (2003) 63-67.
13. O. Turkoglu, M. Soylak and I. Belenl, Collect. Czech. Chem. Commun. 68 (2003) 1233-1242.

14. M. S. Masoud, B. S. Farag, Y. A. Swan, T. M. Salem and M. M. El Essawy, J. Non-Cryst. Solids, 55 (1983) 209- 213.
15. M. S. Masoud, S. A. El-Enein, and E. El-Shereafy, J. Thermal Analysis, 37 (1991) 365-373.
16. M. S. Masoud, E. A. Khalil and M. E. Kassem, Reactivity of Solids, 2 (1986) 269-276.
17. M. S. Masoud, E. A. Khalil, A. M. Ramadan, Y. M. Gohar and A. Sweyllam, Spectrochimica Acta A**,** 67, 3-4 (2007) 669-677.
18. M. G. A. E. Wahed, S. A. Aly, H. A. Hammad and S. M Metwally, J. Phys. Chem. Solids, 55, 1 (1994) 31-37.
19. M. G. A. E. Wahed, K. A. El Manakhly and A. Amer, J. Mater. Sci. Lett., 15 (1996) 919-921 .
20. M. G. A. E. Wahed, S. M. Metwally, and K. A. El Manakhly, Mater. Chem. Phys. 47 (1997) 62-67.
21. M. G. A. E. Wahed, A. M. Hassan and S. A. Hassan, J. Mater. Sci**.** Lett., 12 (1993) 453-454.
22. M. G. A. E. Wahed and S. M. Metwally, Mater. Chem. Phys., 78 (2002) 299–303.
23. M. G. A. E. Wahed, H. A. Bayoumi and M. I. Mohammed, Bull. Korean Chem. Soc., 24, 9 (2003) 1313-1318.
24. M. G. A. E. Wahed, K. El Manakhly, N. El. Khososy and A. El Farargy, Bull. Korean Chem. Soc. 18, 6 (1997) 594-599.
25. M. G. A. E. Wahed, K. A. El Manakhly, S. M. Metwally, H. A. Hammad and S. A. Aly, Monatshe-Chem., 126 (1995) 663-671.
26. G. B. El Hefnawey, M. M. Ayad and A. E. El Trass, Thermochim. Acta**.,** 198, 2 (1992) 345-355.
27. N. Singh and S. Gupta, Synthetic. Met., 107 (1999) 167-174.
28. N. Singh, A. Prasad and R. K. Sinha, Inorg. Chem. Commun., 9, 10 (2006) 1058-1062.

29. A. K. Nikumbh, S. K. Pardeshi and M. N. Raste, Thermochim. Acta., 374 (2001) 115-128 .
30. A. K. Nikumbh, A. E. Athare and S. K. Pardeshi, Thermochim. Acta., 326 (1999) 187-192.
31. J. T. Makode, S. G. Bhadange and A. S. Aswar, Polish J. Chem., 77 (2003) 855-865.
32. N. F. Mott and E. A. Davis, "Electronic Process in Non-Crystalline Materials", Clarendon Press Oxford (1971).
33. M. G. A. E. Wahed, A. M. Hassan and S. Raaft, Chemistry and Industry, 16 (1990) 263.
34. H. Meier, "Organic Semiconductors, Dark and Photoconductivity of Organic Solids", Verlag Chemie, Weinheim (1974) 161.
35. K. C. Kao and W. Hwang, "Electrical Transportation in Solids", Pregamon Press, Oxford (1981) Chap.1.
36. D. F. Shriver, P. W. Atkins and C. H. Langford, "Inorganic Chemistry", Oxford University Press, Oxford (1996).
37. F. Purcell and C. Kotz, "Inorganic Chemistry", Saunders, Philadelphia, (1977).

SUMMARY

SUMMARY

Schiff bases are an important class of ligands in coordination chemistry and find extensive applications in different spheres. Transition metal complexes with Schiff bases as ligands have been amongst the widely studied coordination compounds. Because of the great synthetic flexibility of Schiff base formation many ligands of diverse structural type can be synthesised. The present study is focused mainly on the metal complexes of Schiff bases derived from furoin. Four new ligands viz furoin-2-aminothiophenol (FATP), furoin-2-aminophenol (FAP), furoin thiosemicarbazone (FTSC), furoin semicarbazone (FSC) and their transition metal chelates have been synthesised and characterised.

The thesis is divided into five parts. Part I deals with the synthesis and characterisation of various complexes derived from Schiff base ligands. Part I comprises of six chapters. The first chapter consists of an introduction and a critical review of the published work on metal complexes of Schiff bases. In the second chapter, materials, methods and instruments used for the various studies are described. Synthesis and characterisation of Co(II), Ni(II), Cu(II) and Zn(II) complexes of FATP are described in the Chapter 3. Structural elucidation of these complexes has been made on the basis of micro analytical, spectral and magnetic data. These data suggest that FATP act as a

dianionic tridendate ligand for the metal ions. All these complexes possess 1:1 metal ligand stoichiometry and they are non-electrolyte in nature. All complexes are found to be paramagnetic except Zn(II) complex which is diamagnetic. Based on the above physicochemical studies, an octahedral structure is suggested for all the four complexes. The synthesis and characterisation of Co(II), Ni(II), Cu(II) and Zn(II) complexes of FAP, FTSC and FSC are described in the Chapters 4, 5 and 6. These complexes are characterised and structural elucidation have been made. All the complexes of FAP, FTSC and FSC possess 1:1 metal ligand stoichiometry and they are non electrolyte in nature. The ligands FAP, FTSC and FSC acted as dianionic tridendate and the geometry of their complexes are found to be octahedral one. Part I ends with reference.

Thermogravimetric investigations of Co(II), Ni(II), Cu(II) and Zn(II) complexes of FATP along with the Cu(II) and Zn(II) complexes of FAP, FTSC and FSC were carried out using TG techniques and results are presented in part II. This part comprises of three chapters. The first Chapter describes introduction and Chapter 2 explains the materials, methods and instruments used for the present study. The thermal decomposition studies of selected ten complexes are discussed in chapter 3. All the TG curves were subjected to kinetic analysis and the kinetic parameters namely energy of activation, Arrhenius frequency factor and entropy of activation for decomposition have been calculated from the TG data using the Coats-

Redfern equation. On the basis of the temperature of inflection and initial decomposition, the relative thermal stabilities of the chelates were determined.

The Co(II) and Cu(II) complexes of FATP follow a two stage decomposition pattern while the Ni(II) and Zn(II) complexes follow a three stage decomposition pattern. The thermal decomposition data are represented in tables 2.3.1 to 2.3.4. The relative thermal stabilities of FATP complexes follow the order, Ni(II)> Co(II) ≈ Cu(II) ≈ Zn(II).

The Cu(II) and Zn(II) complexes of FTSC and FAP follow decomposition in two stages while the complexes of FSC follow a three stage decomposition pattern as summarised in the tables 2.3.5 to 2.3.7. The kinetic parameters calculated for all the complexes are given in table 2.3.8. The relative thermal stabilities of the Cu(II) metal complexes were higher than the Zn(II) complexes of FAP, FTSC and FSC. Part II concludes with reference.

Part III consist of unit cell determination of eight newly synthesised Schiff base complexes using X-ray powder diffraction technique. Chapter 1 and 2 give the introduction, materials and methods employed respectively. In the Chapter 3, the X-ray diffraction studies of Ni(II) and Cu(II) complexes of FATP, FAP, FSC along with the Cu(II) and Zn(II) complexes of FTSC are presented. It was found that Ni(II) complexes of FATP and FSC as well as Cu(II) and Zn(II) complexes of FTSC belong to orthorhombic crystal system. But in the case of Cu (II) complex of FATP, FAP and FSC tetragonal system

is identified. A cubic crystal system is reported for the Ni(II) complex of FAP. The calculated density of each complex was in good agreement with experimental value found out, which confirm the proposed molecular formula and existence of 1:1 stoichiometry between the metal ion and the ligands for all the complexes. References are given at the end of part III.

Studies of corrosion inhibition efficiency of four Schiff bases FTSC, FATP, FAP and FSC towards mild steel in hydrochloric acid are described in Part IV. A critical review of Schiff base based corrosion inhibitors is included in first chapter. A detailed description about the theory and methods used for the corrosion inhibition studies are discussed in Chapter 2. In Chapter 3, the results of the corrosion inhibition efficiency determined using laboratory corrosion immersion technique (weight loss method) and electrochemical methods like potentiodynamic polarization method and electro chemical impedance spectroscopy are presented. Results reveal that all the four Schiff bases act as good corrosion inhibitors, having efficiency of 85% and above towards mild steel in 1M hydrochloric acid solutions. Hence they can be used as corrosion inhibitors for industrial applications. The efficiency of the investigated compounds varied depending upon their chemical structure and constituents present in them. The adsorption isotherm analysis and thermodynamic parameters calculated indicate that the Schiff bases inhibit corrosion through the physical adsorption process and follow

Langmuir adsorption isotherm. Relevant references are given at the end of Part IV.

The Part V of this thesis deals with electrical characterisation of the prepared Schiff bases and their selected metal complexes using D.C electrical conductivity measurements. The Chapter 1 of this part contains introduction and review of literature related to the electrical conductivity studies of metal complexes and Chapter 2 explains the material and methods adopted. The results of D.C. electrical conductivity of Co(II), Ni(II), Cu(II) and Zn(II) complexes of FATP, Cu(II) complexes of the FAP, FTSC, FSC and four Schiff bases are presented in the Chapter 3. The conductivity values obtained for the investigated samples show that these materials can be classified into the category of organic semiconductors. Among the studied materials few of them show typical semiconductor behaviour of increasing conductivity with increasing temperature in the studied temperature region which suggest another potential application of these studied compounds. The probable mechanism of electrical conduction in these materials is also discussed. Part V concludes with references.